Copyright

by

Karl Richard Pennings

1999

# Lateral Load Distribution on Transverse Floor Beams in Steel Plate Girder Bridges

**by**

**Karl Richard Pennings, B.S.C.E.**

**Thesis**

Presented to the Faculty of the Graduate School of

The University of Texas at Austin

in Partial Fulfillment

of the Requirements

for the Degree of

**Master of Science in Engineering**

**The University of Texas at Austin**

**May, 1999**

# Lateral Load Distribution on Transverse Floor Beams in Steel Plate Girder Bridges

**Approved by**
**Supervising Committee:**

**Supervisor: Karl H. Frank**

**Sharon L. Wood**

# Dedication

*This work is dedicated to my parents for their tremendous support throughout the years. They have always been behind me 100% and have offered their encouraging words to keep me going in the tough times.*

# Acknowledgements

This research was made possible through funding provided by the Texas Department of Transportation. I would like to thank everyone involved at TxDOT for their assistance and for enabling this research to be conducted. I would also like to thank Dr. Karl H. Frank for the guidance and support he has offered throughout my time at The University of Texas, and Dr. Sharon L. Wood for being my second reader.

I would like to thank everyone in Austin who made my two years here enjoyable. Special thanks to my good friends Matt Rechtein, Brian Chen, Brent Stephens, and Brian Tinkey for the time spent studying together and the time in between. Thanks to Mike Lopez and Mark Waggoner for making the late nights in the computer lab a little more enjoyable. Thanks to everyone at Ferguson Lab for always being willing to help. Thanks to all my professors for being so down to earth. Thanks to Charles Bowen, David McIlrath, David Jauregui, Norm Grady, Photis Matsis, Scott Barney, Blanca Velázquez, Dilip Maniar, and Sanghoon Lee for helping with bridge testing, rating, and analysis.

I would like to thank my family for their love for each other and their love for God. I thank my parents for their love, guidance, and support. Most of all, I would like to thank God for freeing me from sin and death and allowing me to have everlasting life through the death and resurrection of His Son, Jesus Christ.

"I can do everything through him who gives me strength" – Philippians 4:13

May 7, 1999

# Abstract

## Lateral Load Distribution on Transverse Floor Beams in Steel Plate Girder Bridges

Karl Richard Pennings, M. S. E.

The University of Texas at Austin, 1999

Supervisor: Karl H. Frank

Many twin plate girder bridges have been recently rated inadequate for their current design loads. The controlling members that determine the bridge rating is often the transverse floor beams. The current provisions assume no lateral load distribution on the floor beams. This research focused on determining how the load is actually distributed. Using the SAP2000 finite element program, different floor system models were studied. The floor beam moments found by finite element modeling were 5-20% lower than the moments predicted by the current provisions due to load distribution and the moment carried by the concrete slab. An experimental test was also run on a similar floor system and the moments on the floor beam for this test were even lower than the moments predicted using finite element modeling showing that the finite element results are conservative as well. The goal of the research is to more accurately determine the moments in the floor beams, leading to a more rational rating of the bridge.

# Table of Contents

List of Tables ..... xi

List of Figures ..... xiii

**CHAPTER 1: INTRODUCTION** **1**

1.1. Purpose of Research ..... 1

1.2. Floor System Geometry ..... 1

1.3. Load Path ..... 2

1.4. Load Distribution Models ..... 3

1.4.1. Direct Load Model ..... 4

1.4.2. Lever Rule Model ..... 5

1.4.3. Lateral Load Distribution Model ..... 5

1.4.4. Comparison of Lateral Load Distribution Methods ..... 6

1.5. Loading Geometry ..... 7

1.6. Topics Covered ..... 9

**CHAPTER 2: FINITE ELEMENT MODELING** **10**

2.1. Finite Element Program Selection ..... 10

2.2. Modeling the Floor System ..... 10

2.3. Modeling the Truck Load ..... 12

2.4. Model Size ..... 14

2.4.1. Small Model ..... 14

2.4.2. Large Model ..... 16

2.5. Influence Surfaces ..... 20

**CHAPTER 3: RESULTS OF FINITE ELEMENT ANALYSIS 24**

3.1. Bridge Database ..... 24

3.2. Small Model Results ..... 28

3.2.1. Truck Position ..... 30

3.2.2. Lever Rule ..... 31

3.2.3. Floor Beam Spacing ..... 31

3.2.4. Stringer Spacing ..... 35

3.2.5. Girder moment of Inertia ..... 36

3.2.6. Floor Beam Moment of Inertia ..... 38

3.3. Large Model Results ..... 39

3.3.1. Number of Floor Beams ..... 41

3.3.2. Floor Beam Moment of Inertia ..... 42

3.3.3. Floor Beam Spacing ..... 43

3.3.4. Girder Moment of inertia ..... 44

3.3.5. Stringer Spacing ..... 45

3.4. Summary of Finite Element Results ..... 47

3.4.1. HS-20 Load Case ..... 47

3.4.2. H-20 Load Case ..... 48

**CHAPTER 4: RESULTS OF EXPERIMENTAL TEST 52**

4.1. Llano Bridge Floor System Geometry ..... 52

4.2. Location of Strain Gages ..... 55

4.3. Truck Load ..... 57

4.4. Finite Element Model Results ..... 60

4.5. Experimental Results ..... 65

4.6. Comparison of Results ..... 69

4.7. Second Experimental Test ..... 75

4.7.1. Repeatability of Test ..... 75

4.7.2. Floor Beam Moment Diagram ..... 77

4.8. Conclusions from the Experimental Test ..... 81

**CHAPTER 5: DETERMINING FLOOR BEAM REQUIREMENTS 83**

5.1. Limit State Design ..... 83

5.2. Required Moment ..... 83

5.2.1. Load & Resistance Factor Design ..... 84

5.2.2. Load Factor Design ..... 85

5.3. Allowable Moment ..... 85

5.4. Bridge Rating Example ..... 86

5.4.1. Rating for LRFD and LFD ..... 87

5.4.1.1 Allowable Moment ..... 87

5.4.1.2. Required Moment ..... 88

5.4.2. Rating Using Allowable Stress Design ..... 91

5.4.3. Rating Using the Lever Rule ..... 93

5.4.4. Rating Using Finite Element Results ..... 95

5.5. Bridge Ratings with H-20 Loading ..... 96

5.6. Bridge Rating Using HS-20 Loading ..... 99

**CHAPTER 6: CONCLUSIONS 102**

6.1. Purpose of Research ..... 102

6.2. Overview of Findings ..... 102

6.2.1. Current Analysis Methods Are Over-Conservative ..... 102

6.2.2. Suggested Changes in Load Distribution Methods ..... 103

6.2.3. Comparison of Experimental and Analytical Results ..... 103

6.3. Practical Results of Research ..... 104

Appendix A: Bridge Cross Sections ..... 105

Appendix B: Load Run Descriptions for 1st Llano Test ..... 110

Appendix C: Selected Neutral Axis Calculations for 1st Llano Test ..... 111

Appendix D: Comparison of Top to Bottom Flange Strains in 1st Llano Test ... 114

Appendix E: Comparison of 2nd Floor Beam to 1st Floor Beam Strains ..... 115

Appendix F: Results from Load Runs in First Llano Test ..... 116

Appendix G: Comparison of Maximum Moments From 1st Llano Test ..... 127

Appendix H: Moment Diagrams of 2nd Floor Beam in 2nd Llano Bridge Test 131

References ..... 133

Vita ..... 134

## List of Tables

Table 1.1 Percent Increase in Mid-Span Floor Beam Moment Caused by Decreasing Truck Spacing from 4 to 3 feet ..... 9
Table 3.1 Bridge Database with Floor System Properties ..... 25
Table 3.2 Frame member properties ..... 27
Table 3.3 Small Model Results ..... 29
Table 3.4 Floor beam Spacing Effects for HS-20 Loading ..... 32
Table 3.5 Small Model Results with Wheels on Floor Beam Only ..... 33
Table 3.6 Small Model Results with Wheels away from Floor Beam Only ..... 33
Table 3.7 Effect of Floor Beam Stiffness ..... 38
Table 3.8 Summary of Finite Element Results ..... 40
Table 3.9 Effect of Increasing the Number of Floor Beams ..... 41
Table 3.10 Effect of Increasing the Size of Floor Beams ..... 43
Table 3.11 Effect of Decreasing the Floor Beam Spacing ..... 43
Table 3.12 Effect of Increasing Girder Stiffness ..... 44
Table 3.13 Effect of Decreasing the Stringer Spacing ..... 46
Table 3.14 Summary of Effects of Various Parameters on HS-20 Loading ..... 48
Table 3.15 Effect of Floor Beam Moment of Inertia on H-20 Load Case ..... 50
Table 4.1 Truck Loads ..... 58
Table 4.2 Comparison of Moments Caused by Different Truck Types ..... 60
Table 4.3 Comparison of Finite Element Models ..... 63
Table 4.4 Comparison of Analytical and Experiment Results ..... 73
Table 4.5 Comparing Truck Weights From Both Tests ..... 76
Table 4.6 Maximum Moment Comparison for Side by Side Load Case ..... 76
Table 4.7 Maximum Moment Comparison for Single Truck in Center ..... 77
Table 5.1 Properties of Floor Beam Sections ..... 87
Table 5.2 Calculation of Required Moment ..... 91
Table 5.3 TxDOT Table to Compute Allowable Stress for Inventory Rating ..... 92
Table 5.4 Calculation of Required Moment Using Lever Rule ..... 95
Table 5.5 Calculation of Required Moment Using Equation 5.9 ..... 96

Table 5.6 Over-Strength Factors for the 12 Cross Sections for H-20 Trucks Using LRFD and LFD Specifications ..... 97
Table 5.7 Over-Strength Factors with 33 ksi Steel using H-20 Trucks ..... 98
Table 5.8 Over-Strength Factors for ASD using H-20 Trucks ..... 99
Table 5.9 Over-Strength for HS-20 Loading, 36 ksi Steel ..... 100
Table 5.10 ASD Over-Strength Factors for HS-20 Loading ..... 101

# List of Figures

Figure 1.1 Plan View of Bridge Floor System ..... 2
Figure 1.2 Different Possible Load Paths of the Floor System ..... 3
Figure 1.3 Direct Load Model for Load Distribution ..... 4
Figure 1.4 Lever Rule Model for Load Distribution ..... 5
Figure 1.5 Transverse Load Distribution Model ..... 6
Figure 1.6 Comparison of Lateral Load Distribution Models ..... 7
Figure 1.7 Spacing of Maximum Load (2 HS-20 trucks) ..... 8
Figure 2.1 Actual Bridge Cross Section ..... 12
Figure 2.2 SAP2000 Idealized Cross Section ..... 12
Figure 2.3 Longitudinal Position of Trucks Producing Maximum Moment ..... 13
Figure 2.4 Symmetric Transverse Position of Trucks ..... 14
Figure 2.5 Transverse Position of Trucks to Produce Maximum Moment ..... 14
Figure 2.6 Small Floor System Model ..... 16
Figure 2.7 Large Model Length ..... 17
Figure 2.8 Large Floor System Model ..... 18
Figure 2.9 Constraint Method of Analyzing Cracked Section ..... 19
Figure 2.10 Weak Shell Method of Analyzing Cracked Section ..... 20
Figure 2.11 Influence Surface for Floor Beam Mid-span Moment ..... 21
Figure 2.12 Influence Surface Comparing SAP Model to Direct Load Model ..... 23
Figure 3.1 Influence Surface Comparison of Different Floor Beam Spacing ..... 35
Figure 3.2 Influence Surface Comparison of Different Stringer Spacing ..... 36
Figure 3.3 Influence Surface Comparison of Different Size Girders ..... 37
Figure 3.4 Influence Surface Comparison of Different Floor Beam Sizes ..... 39
Figure 3.5 Influence Surface Comparison for Large Model Stringer Spacing ..... 47
Figure 3.6 Longitudinal Position of H-20 Truck ..... 49
Figure 3.7 Correlation of Floor Beam Stiffness to Moment Reduction ..... 51
Figure 4.1 Historic Truss Bridge in Llano, TX ..... 52
Figure 4.2 Plan View with Strain Gage Locations ..... 54
Figure 4.3 Connection of 2nd Floor Beam to Truss ..... 55

Figure 4.4 Location of Gages on Floor Beams ..... 56
Figure 4.5 TxDOT Truck Geometry ..... 57
Figure 4.6 TxDOT loading vehicle ..... 57
Figure 4.7 Llano Bridge 4-span Finite Element Model ..... 61
Figure 4.8 Comparison of Llano Small Model with Plate-Girder Model ..... 62
Figure 4.9 Comparison of 2 and 4 Span Cracked Slab Models ..... 64
Figure 4.10 Comparison of 2 and 4 Span Continuous Slab Models ..... 65
Figure 4.11 Results from 1st Floor Beam for Side by Side Load Case ..... 66
Figure 4.12 Results from 2nd Floor Beam Gages for Side by Side Load Case .... 67
Figure 4.13 Floor Beam to Truss Connections ..... 68
Figure 4.14 Neutral Axis Calculation for Second Floor Beam ..... 69
Figure 4.15 Comparison of 2nd Floor Beam Moments ..... 70
Figure 4.16 Two Trucks out of Alignment in Run 2 ..... 71
Figure 4.17 Cracked Slab over Floor Beam ..... 72
Figure 4.18 Location of Gages in Both Load Tests ..... 78
Figure 4.19 Moment Diagram for 2nd Floor Beam, Center Run, Truck A..... 79
Figure 4.20 Moment Diagram Without Restraint for Center Run, Truck A ..... 81
Figure 5.1 Cross Section of Trinity River Bridge ..... 87
Figure 5.2 H-20 Truck Moment Calculation Using Direct Load ..... 89
Figure 5.3 H-20 Lane Loading Moment Using Direct Load..... 90

# CHAPTER 1

# INTRODUCTION

## 1.1. Purpose of Research

Many twin plate girder bridges have been recently rated inadequate for their current design loads. The controlling members that determine the bridge rating for this bridge type are often the transverse floor beams. One option to deal with this problem would be to demolish these bridges and build replacements. A second option would involve retrofitting the floor beams to increase their capacity. However, neither may be the most cost-effective way to deal with the problem. Rather than removing from service or retrofitting bridges that might be functioning satisfactorily, it was deemed appropriate to the study the transverse floor beams in a bit more detail. The purpose of this investigation is to determine a better estimate of the actual forces on a transverse floor beam caused by truck loads on the floor system and to compare these forces with the current method for predicting the forces on the floor beams. The goal is to come up with a specification that would allow one to more accurately predict the expected moment in these floor beams.

## 1.2. Floor System Geometry

The floor system in consideration is a floor beam-stringer system supported by twin plate girders. The plate girders, running the length of the

bridge on the outside support the transverse floor beams, which in turn support the stringers. All bridges studied have a 6.5-inch concrete slab resting on the stringers. Figure 1.1 shows the basic floor system geometry and terminology that will be used in this report. Only floor systems containing two stringers and two design lanes were considered. A survey of TxDOT bridges revealed that this was the common system used in early long-span steel girder bridges. The main interest of this research is the maximum moment in the transverse floor beams, simply referred to as floor beams for the duration of this report.

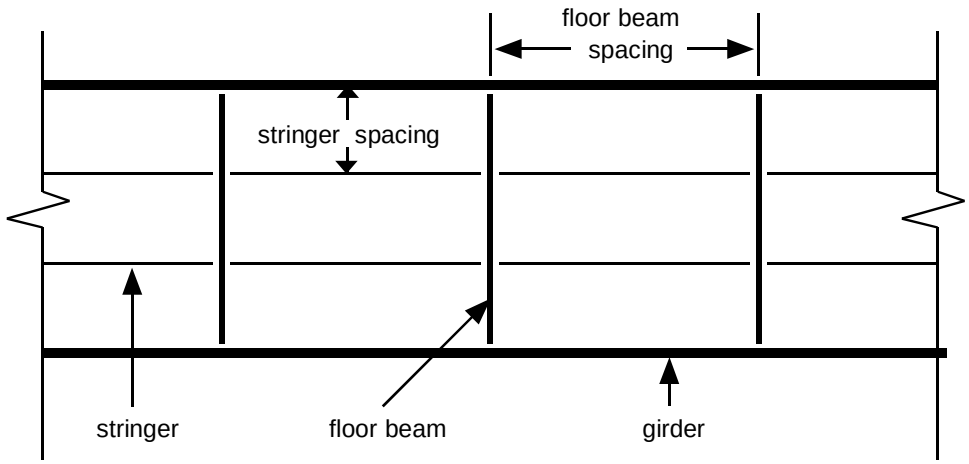


**Figure 1.1 Plan View of Bridge Floor System**

## 1.3. Load Path

An understanding of the load path of the system is necessary to understanding the moment in the floor beam. The two different possible basic load paths for this floor system geometry are shown in Figure 1.2. The only difference in the two load paths is that in the first example there is no load going

directly from the concrete slab to the floor beam. The entire load is transferred from the slab to the floor beam through the stringer connections. That is because there is no contact between the slab and the floor beam. The only link is through the stringers. However, when the slab is in contact with the floor beam, it is possible for some of the load to go directly from the slab to the floor beam. This is an important difference because it can significantly affect the shape of the moment diagram of the floor beam.

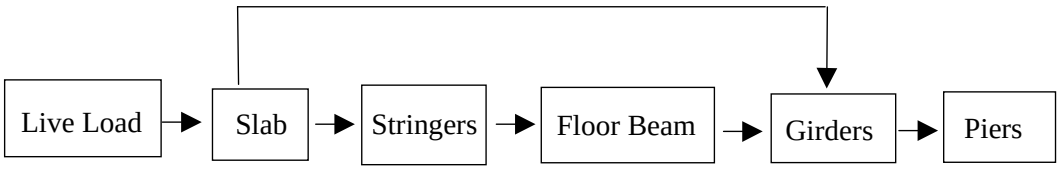


Load Path with No Contact between Slab and Floor Beam

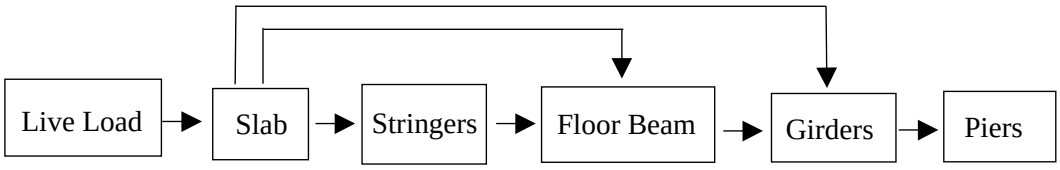


Load Path When Slab is in Contact with Floor Beam

**Figure 1.2 Different Possible Load Paths of the Floor System**

## 1.4. Load Distribution Models

An important part of the research is to understand how a point load is distributed to the floor beams. This is important because the lateral load distribution has a significant effect on the magnitude of the floor beam moment.

Three different load distribution models are outlined in the following section. Note that the first two models, the direct load and lever rule assume simply supported girders and no moment carried by the slab.

### 1.4.1. DIRECT LOAD MODEL

The approach adopted by AASHTO and TxDOT is a structural system that distributes load longitudinally onto the adjacent floor beams using statics. However, the load is not distributed laterally at all. A point load in the middle of the bridge is treated as a point load on each of the adjacent floor beams. Figure 1.3 shows the direct load method of distributing forces. This method has the advantage of being very simple to apply. The direct load approach would also be a conservative estimate for the load on the floor beam since a point load will produce the maximum moment. This is a disadvantage in this case, because it is the goal of this research to try to get a better estimate of the load actually on the floor beam.

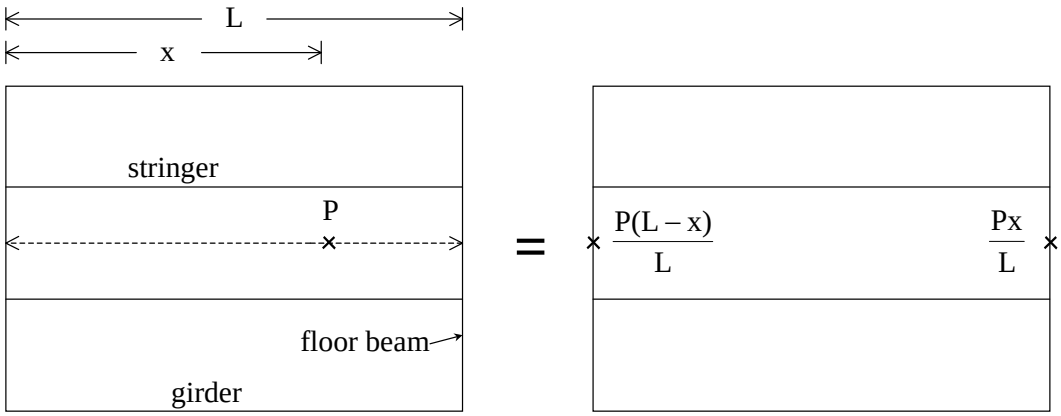


**Figure 1.3 Direct Load Model for Load Distribution**

### 1.4.2. LEVER RULE MODEL

Another method, the lever rule, shown in Figure 1.4, transmits the entire load from the slab to the floor beams through the stringers. It treats the slab as simply supported between the stringers and statically distributes the load to each stringer. Instead of resulting in one point load, it results in two point loads on each floor beam at the location of the stringers. This method is also simple to analyze and is a better model of the intended load path, in which the load is transferred from the slab to the floor beam through the stringers. It is also less conservative than the direct load model. If there is no contact between the floor beam and the slab, it was discovered that the lever rule is a good model of the floor system.

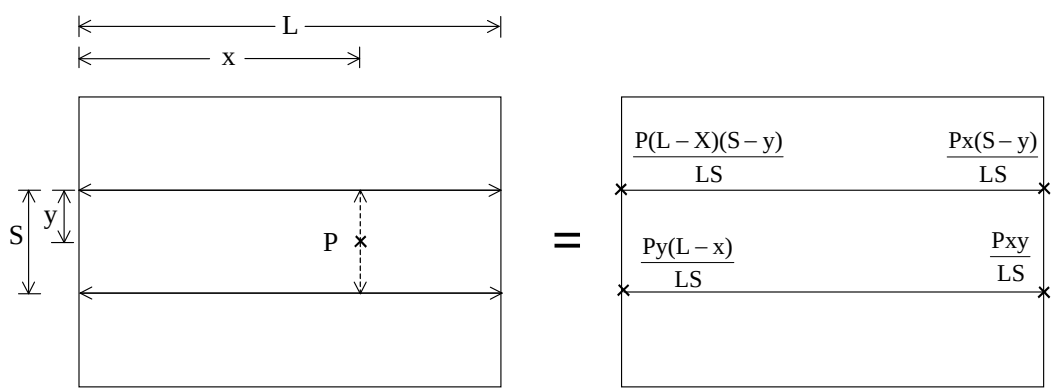


**Figure 1.4 Lever Rule Model for Load Distribution**

### 1.4.3. LATERAL LOAD DISTRIBUTION MODEL

Assuming contact between the floor beam and slab, an example of how the load is more likely distributed is shown in Figure 1.5. Some of the load goes to the stringers and then is transmitted to the floor beams while some of the load

is transmitted from the slab to the floor beams. However this load is not transmitted as a point load, but as a distributed load. This distributed load on the floor beam would lead to a lower maximum moment in the floor beam. It is difficult to determine how the load is distributed transversely because it depends on a number of factors such as the spacing of the system and the stiffness of the members. To gain a better understanding of the load distribution and the resulting floor beam moment, a finite element analysis was done on the bridge floor system.

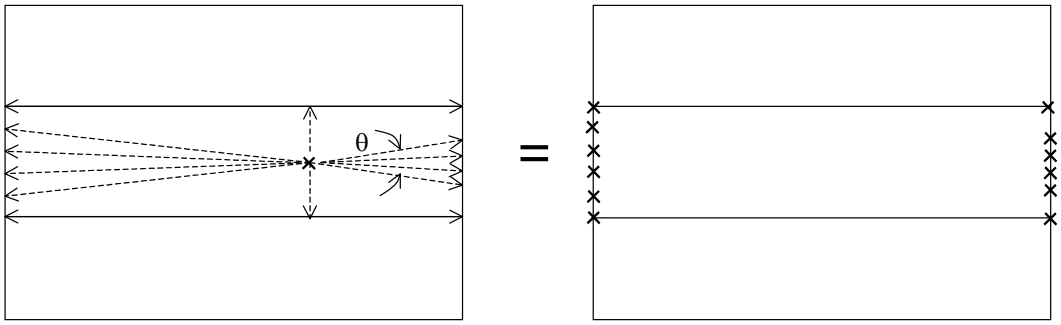


**Figure 1.5 Transverse Load Distribution Model**

### 1.4.4. COMPARISON OF LATERAL LOAD DISTRIBUTION METHODS

Figure 1.6 shows the moment diagram for the floor beam caused by the different distribution methods. A 2-kip load placed in the center of the simple span shown in Figures 1.3-1.5 causes the moment diagrams shown in the figure. The distributed model assumes a distribution of the load of $\theta = 30$ degrees. The model labeled $\alpha = ½$ has half of the load following the lateral distribution method and half of the load following the lever rule path. This is for a floor system with a 22-foot floor beam spacing and 8-foot stringer spacing. The plot indicates that the

lever rule for this single point load results in a 33% reduction from the direct load model.

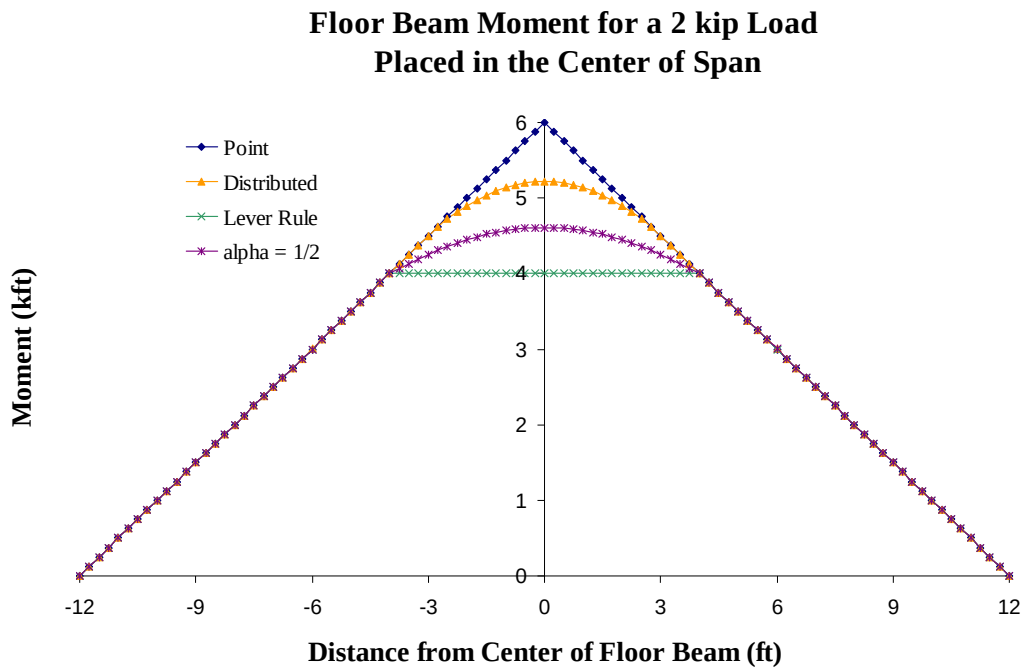


**Figure 1.6 Comparison of Lateral Load Distribution Models**

## 1.5. Loading Geometry

The load placement for bridge rating and for our analysis will consist of either two HS-20 or H-20 trucks placed side by side four feet apart as per AASHTO guidelines. The HS-20 loading, shown in Figure 1.7, consists of two 4 kip wheel loads on the front axle and two 16 kip wheel loads on both rear axles. The total weight of this dual truck load is 144 kips. Wheels are spaced 6 feet apart transversely. The front axle is 14 feet from the first rear axle and the rear axles can be spaced anywhere from 14 feet to 30 feet apart. The shorter 14-foot spacing will be used for the rear axle because it results in the highest floor beam

moment. The H-20 loading is exactly the same as the HS-20 loading without the rear axle. The total weight of two H-20 trucks is 80 kips. Lane loading, having a much smaller impact on the floor beam moment was not modeled in the finite element method. For more detail on lane loading see Chapter 5.

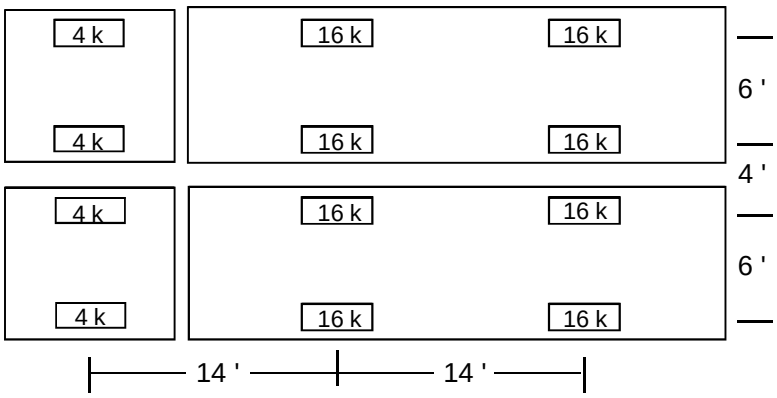


**Figure 1.7 Spacing of Maximum Load (2 HS-20 trucks)**

In 1978, TxDOT adopted a three-foot spacing between trucks according to the Manual for Maintenance Inspection of Bridges published by AASHTO.[2] In 1983, however, the spacing was returned by AASHTO to four feet where it remains today.[3] However, in TxDOT's example calculations from the 1988 Bridge Rating Manual, a three-foot spacing between the trucks is still being used.[4] This shorter spacing can lead to a significantly higher moment in the floor beams as shown in Table 1.1. The percent increase due to the narrower stringer spacing is independent of the floor beam spacing.

**Table 1.1 Percent Increase in Mid-Span Floor Beam Moment Caused by Decreasing Truck Spacing from 4 to 3 feet**

| Stringer Spacing (ft) | % Increase in Floor Beam Moment |
|---|---|
| 6 | 12.5 |
| 7 | 9.1 |
| 7.33 | 8.3 |
| 7.5 | 8.0 |
| 8 | 7.1 |

## 1.6. Topics Covered

To determine the forces on the floor beams finite element analyses of various bridge geometries were conducted. The finite element modeling techniques are discussed in the next chapter and the results of the analyses are shown in Chapter 3. Results from a finite element model are then compared with data from an actual bridge test in Chapter 4. In Chapter 5, an example calculation is shown for a bridge that currently is rated inadequate and compared with the recommended method of calculating floor beam moment. Conclusions are presented in Chapter 6.

# CHAPTER 2

# FINITE ELEMENT MODELING

## 2.1. Finite Element Program Selection

To understand the lateral load distribution on the transverse floor beams, the floor system was analyzed using finite elements. The goal of using the finite element modeling was to develop a more reasonable estimate for the moment in the transverse floor beams. One finite element program that was considered is BRUFEM (Bridge Rating Using Finite Element Modeling), a program developed by the Florida Department of Transportation to rate simple highway bridges. BRUFEM allowed the modeling parameters to be changed easily. However, the limitations imposed by this program on the geometry of the floor system made it a poor choice for modeling the floor system. A general-purpose finite element program, SAP2000, was chosen.[1] SAP allowed the variety of floor beam-stringer geometries to be modeled. The only limitation was that the concrete slab could not be modeled as acting compositely with the stringers.

## 2.2. Modeling the Floor System

The floor system analyzed was a twin-girder steel bridge. These girders support the transverse floor beams, which in turn support the stringers. All bridges analyzed have a 6.5-inch concrete slab resting on the stringers. Figure 1.1

shows the basic floor system geometry and terminology that will be used in this report.

Using SAP2000, the stringers, floor beams and girders were modeled using frame elements, line elements with given cross sectional properties, and the slab was modeled using shell elements with a given thickness. The concrete slab, which overhangs the girder by two feet, was divided into one-foot by one-foot elements, wherever possible. The frame elements were also usually divided into one-foot lengths. The exception to using one-foot elements occurred only when it was required by the loading geometry. Since the concentrated wheel loads had to be placed at the joints located at the intersection of the shell elements, this resulted in some narrower shell elements in certain floor system geometries. The smallest spacing was a shell element width of 3 inches resulting in an aspect ratio of 4 to 1.

All elements were assumed to have the same centroid, which was not the case. In actual bridges, the four centroids are offset as shown in Figure 2.1. The modeling, though, is consistent with the assumption that the slab and supporting elements are not acting compositely. When the system acts in a non-composite manner, the supporting elements and slab act independent of each with the curvature of the slab unaffected by the curvature of the steel members. Figure 2.2 shows the idealized cross section used in the finite element analyses. This assumption of non-composite action is reasonable since no shear studs are specified to connect the slab to the supporting steel elements. Even if there were

some composite action, the assumption of non-composite action should lead to a conservative estimate of the distribution of moments to the floor beams.

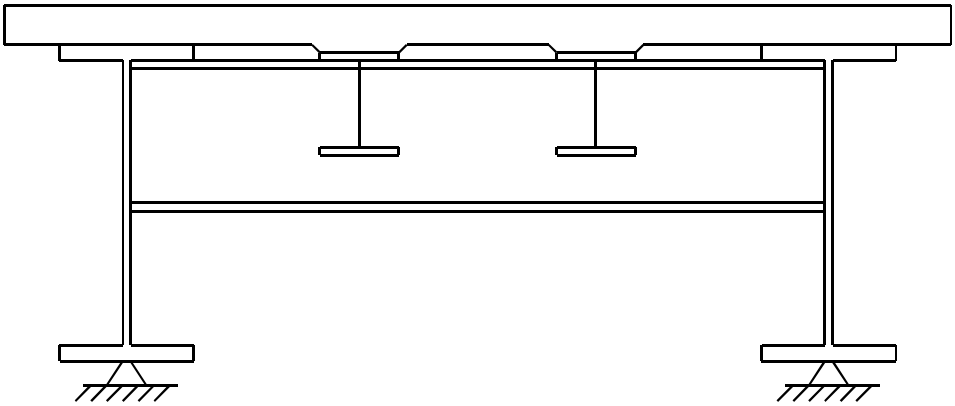

**Figure 2.1 Actual Bridge Cross Section**

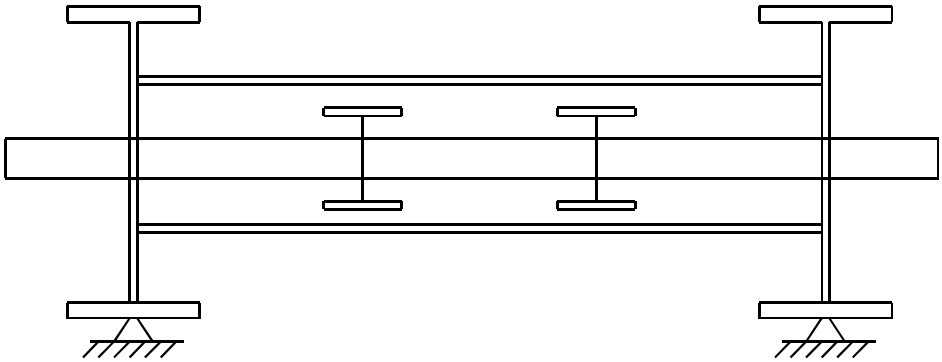

**Figure 2.2 SAP2000 Idealized Cross Section**

## 2.3. Modeling the Truck Load

The truck load placed on each bridge model consists of two HS-20 trucks placed side by side 4 feet apart as per AASHTO guidelines shown in Figure 1.7.

The maximum floor beam moment will occur with middle axle directly over the floor beam with both other axles 14 feet away as shown in Figure 2.3. As mentioned earlier, an inconvenience that arises when trying to apply loads in SAP is that the loads must be applied at the intersection of shell elements.

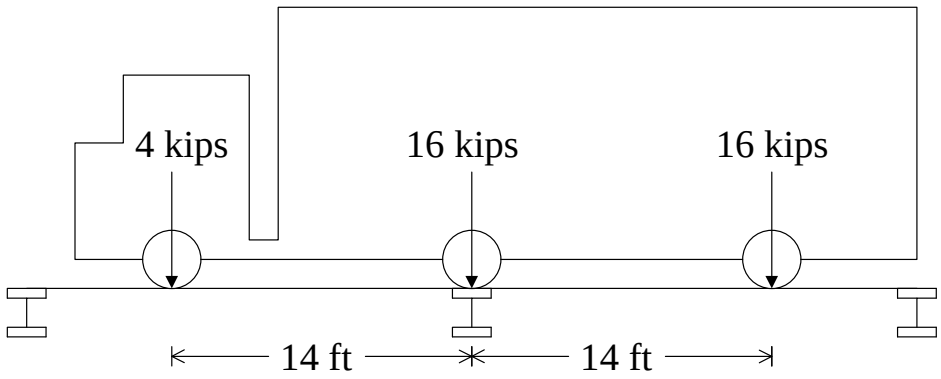


**Figure 2.3 Longitudinal Position of Trucks Producing Maximum Moment**

Transverse placement of the truck load was another issue in finite element modeling. The symmetric position, shown in Figure 2.4 places the two trucks side by side, each two feet away from the center of the bridge. The position that yields the maximum moment using the direct load model is two trucks placed side by side one foot from the symmetrical position, shown in Figure 2.5. This produces a slightly larger floor beam moment than placing the trucks in the symmetric position in the direct load model. Both of these truck positions were analyzed using finite element modeling and the results are discussed in Chapter 3.

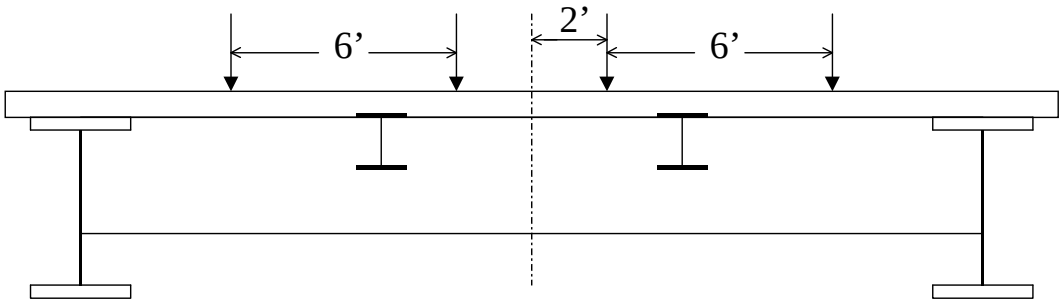


**Figure 2.4 Symmetric Transverse Position of Trucks**

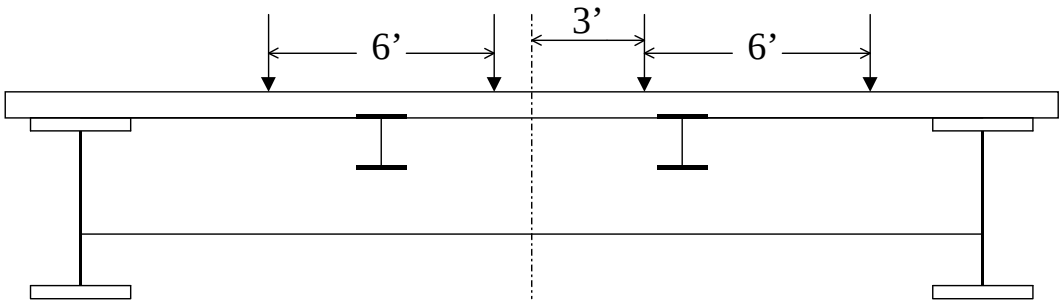


**Figure 2.5 Transverse Position of Trucks to Produce Maximum Moment**

## 2.4. Model Size

### 2.4.1. SMALL MODEL

There are several ways to model the bridge floor systems. The simplest model, referred to as the small model, consists of two floor beams, supported at each end with a single span between two floor beams. This model is shown in Figure 2.6. Although the model actually consists of line and shell elements, for clarity the cross-sections of the elements are also shown. There is a simply

supported boundary condition at the end of each girder. The floor beam identified is the floor beam of interest.

The vertical arrows represent the load due to two HS-20 trucks that produces the maximum moment in the center of the floor beam. This load occurs when the middle axle of each truck is directly over the floor beam and the other axles are 14 feet to either side. However, using the small model it is necessary to use symmetry to apply loads. To use symmetry it is assumed that floor beam spacing, stringer spacing, and stringer size are the same on either side of the floor beam. Instead of applying the 16 kip load from the rear axle and the 4 kip load from the front axle on opposite sides of the floor beam the two are added together to produce a 20 kip load on one side of the floor beam. The advantage of using this small model is that it is quicker to run, much easier to input, and has fewer variables. To understand the effect of the exterior girder stiffness, the outside girders were modeled two different ways in the small model. They were modeled as much larger sections than the stringers (DSG), as shown in Figure 2.6, and as the same section as the stringers (SSG). Due to the small length of the model, however, the small model does not capture the effect of the stiffness of the exterior girders. This is discussed in more detail in Chapter 3.

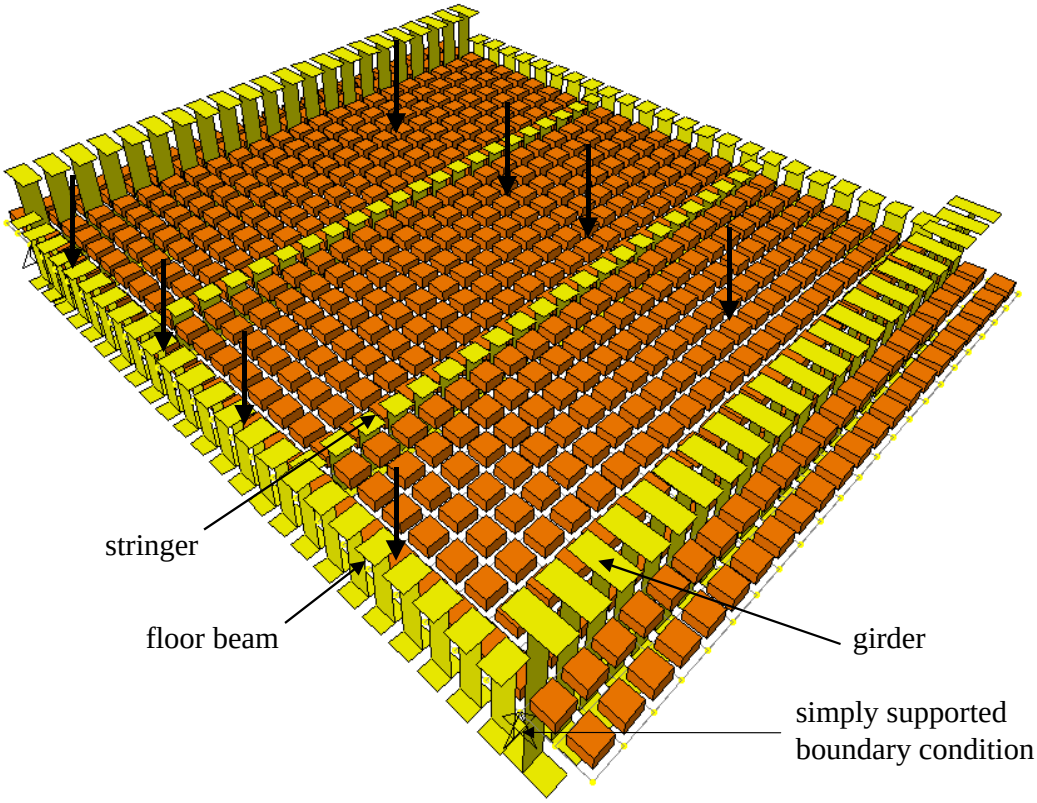


**Figure 2.6 Small Floor System Model**

### 2.4.2. LARGE MODEL

A larger, more complex model that is closer to the actual geometry of the structure was used to study the influence of the girders upon the lateral load distribution. This model consists of more than two floor beams with much longer exterior girders. Actual bridge geometries were used to generate these models. The largest span length of the bridge from support to support determines the length of the model. The girders are continuous over the length of the entire bridge with the distance spanned between inflection points of about 70 to 80% of

the span length. The continuous bridge was modeled as a single span of the bridge with a span length of 80% of the distance between piers as shown in Figure 2.7.

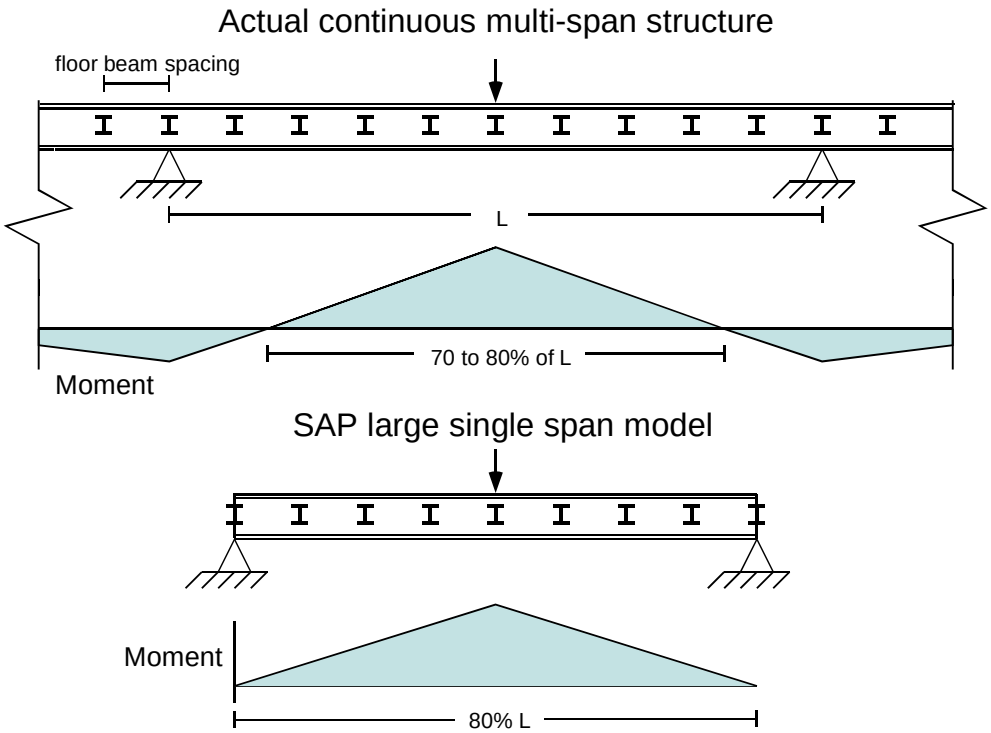


**Figure 2.7 Large Model Length**

The number of floor beams contained in the model determines the length of the model. The model shown in Figure 2.8 is an example of a large model containing 7 floor beams. The stringers and floor beams have rotational releases for both torsion and moment at their ends. The girders are continuous over the span of the entire model with simply supported boundary conditions at each end. The floor beam of interest is also identified in the figure.

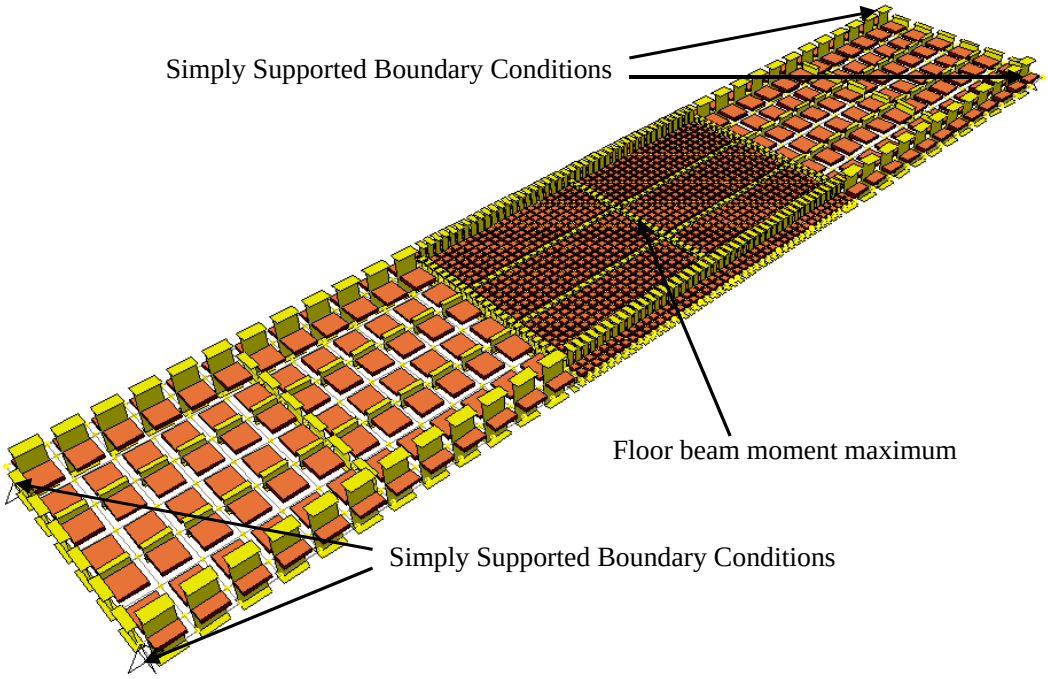


**Figure 2.8 Large Floor System Model**

The mesh farther away from the floor beam is less refined than the sections closer to the center floor beam. Typical mesh sizes away from the center floor beam are 3 to 4 feet. This is to reduce the analysis time without losing accuracy since the elements closer to the floor beam will have a much greater effect on the accuracy of the model.

The modeling of the slab at the floor beams is an important consideration in the large model. It can either be modeled as continuous or simply supported over the floor beam. The slab is effectively simply supported by the floor beams if it modeled as cracked over the floor beam. The influence of slab continuity up the floor beam moment was studied. The default setting in SAP would be to model the slab as continuous over the floor beams. To model the slab as cracked

over the floor beams using SAP requires quite a bit more effort because the program does not provide an option for releasing shell elements.

Two methods that can were considered in this research. Both methods utilize a slab that ends before intersecting the floor beam. The first method is to constrain the nodes on either side the floor beam node in every direction but rotation as shown in Figure 2.9. This causes the slab to behave as if it was cracked over the floor beam. Both portions of the slab are free to rotate with respect to each other but they are forced to have the same vertical and horizontal displacements. The second method, shown in Figure 2.10, is to fill the small gap between the slab and floor beam with a shell element that has a very small stiffness. Reducing the elastic modulus reduced the stiffness.

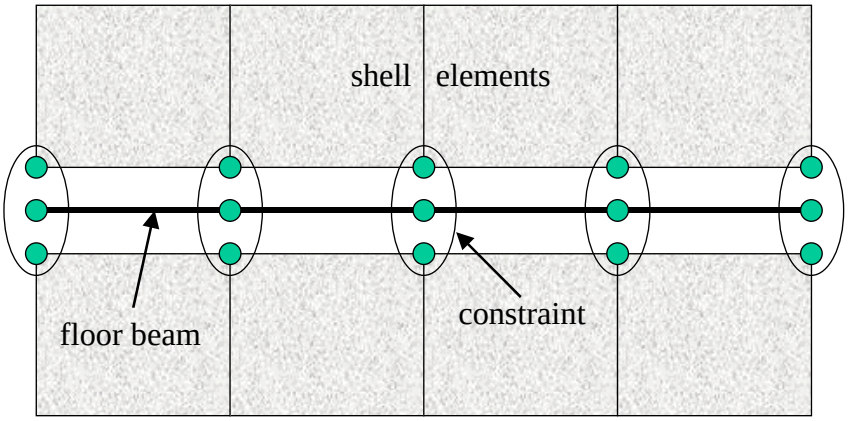


**Figure 2.9 Constraint Method of Analyzing Cracked Section**

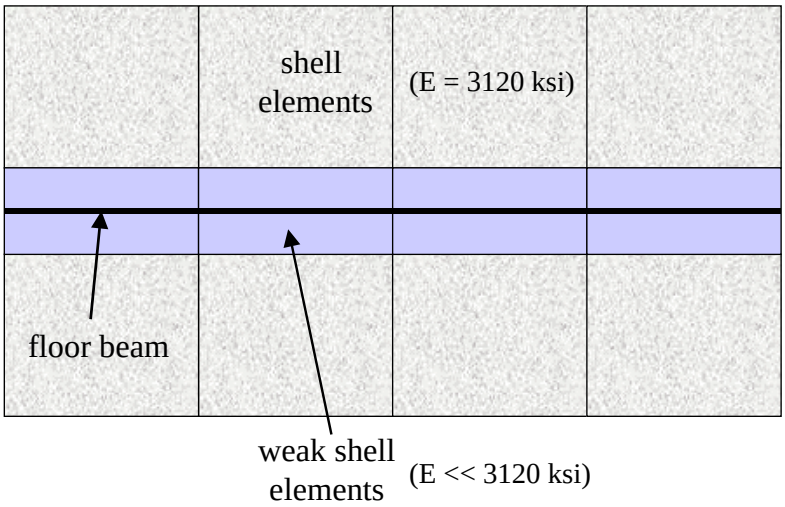


**Figure 2.10 Weak Shell Method of Analyzing Cracked Section**

Using constraints to model a crack over the floor beam is an inefficient method because each set of three nodes must be selected and then separately constrained. However, in the weak shell method the shell elements can all be selected and assigned a different modulus of elasticity very easily. The two methods were compared and shown to give similar results, so the weak shell method was used in the finite element models discussed in the remainder of the thesis.

## 2.5. Influence Surfaces

An influence surface is a useful tool for evaluating finite element models. An influence surface indicates what effect a 1 kip load placed at any location on the floor system will have upon a selected stress resultant. For our analysis, the mid-span moment in the floor beam was selected. To develop an influence

surface for a model, rotational releases for both torsion and moment are placed on each side of the floor beam mid-span. Then equal and opposite moments are also placed on each side of the mid-span of the floor beam. The displaced shape of this structure is in the same shape as the influence surface. It must then be normalized by multiplying the ordinate by the moment due to a one kip load placed directly on the floor beam at mid-span divided by the displacement at mid-span of the floor beam. An example of an influence surface is shown in Figure 2.11. The example shown is from a small span model with 22-foot floor beam spacing and 8-foot stringer spacing. It is evident from the influence surface that a load placed directly on the center of the floor beam will produce the maximum moment at that location. The white rectangles in the figure show the position of the truck wheels on the influence surface for the symmetric loading case.

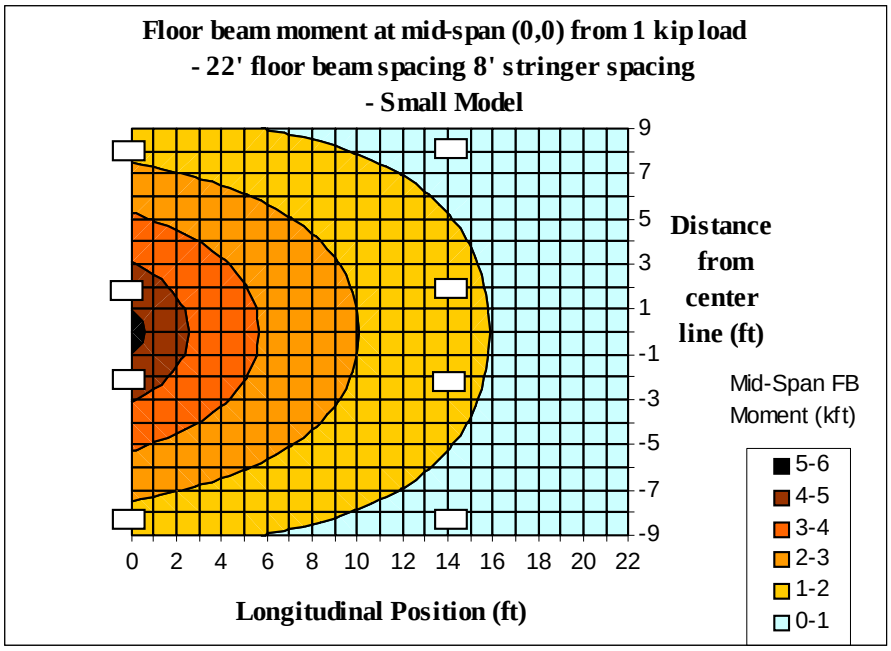


**Figure 2.11 Influence Surface for Floor Beam Mid-span Moment**

Influence surfaces are useful because they show just what effect each wheel of each truck has on the moment and can easily show the differences between models. An influence surface can be used to predict the moments due to any loading case, although only for the moment at one specific location (in this case at the mid-span of the floor beam). Using influence surfaces, it was possible to predict mid-span moments within 0.1% of the value given by directly positioning the load on the floor system of the SAP model.

The most effective use of influence surfaces, though, is to generate surfaces that normalize the moment generated in a finite element model at each location by the moment generated at the same location using the direct load model discussed in Chapter 1. An example of an influence surface showing the normalized moment is shown in Figure 2.12. These surfaces simplify visual comparison of different models to understand which wheel loads cause the differences in models. This can help explain the characteristics or variables in each model that are responsible for the change in floor beam moment. To further simplify this comparison, the width of all influence surfaces consisted of the center 18 feet of the model. This is because the furthest wheel loads in the symmetric load case occur 8 feet on either side of the center line, while the trucks in the maximum moment load case occur 9 feet away on one side and 7 feet on the other. The shaded contour plot shows the moment generated in the finite element model as a percentage of the direct load moment.

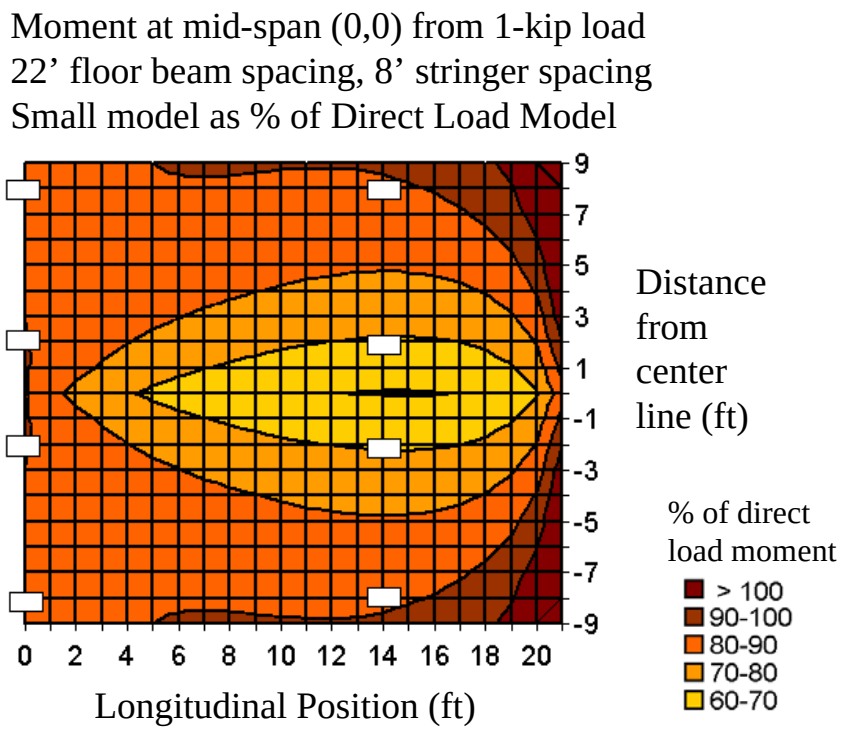


**Figure 2.12 Influence Surface Comparing SAP Model to Direct Load Model**

# CHAPTER 3

# RESULTS OF FINITE ELEMENT ANALYSIS

## 3.1. Bridge Database

In order to limit the study it was necessary to identify the bridges in Texas that use this floor system. With these bridges identified, it was possible to place limits on the parameters to be studied in the finite element analysis. The type of floor system being analyzed on this project is a floor system that occurs in long span bridges built in the 1940s and 1950s. This floor system contains two continuous girders that span the length of the bridge with two intermediate stringers supported by the transverse floor beams as shown in Figure 1.1. Table 3.1 shows some of the bridges analyzed with their floor system properties. The cross sections of these bridges are shown in Appendix A.

Total length for each bridge is defined as the length of the section of the bridge that fits the floor system criteria. For example, if the approach span is a different section than the main span, it is not included in the total length. The span length is the largest span length of the section between supports. As can be seen, the total length of each bridge ranges from 300 feet to almost 800 feet with the longest spans between 60 and 180 feet. Three of the bridges (5, 7, and 9) have two different cross-sections used over the length of the bridge. The second cross section for each structure is 5a, 7a, and 9a respectively. They were included as separate models in the finite element analysis. Floor beam spacing ranges from

15 to 22 feet and stringer spacing ranges from just under 7 feet to 8 feet. This is a fairly small range of values, especially the stringer spacing. About half of the bridges were designed for the H-20 loading and about half were designed for HS-20.

**Table 3.1 Bridge Database with Floor System Properties**

| # | Facility Carried | Feature Intersected | Design Truck | Span Length (ft) | total length (ft) | floor beam spacing (ft) | stringer spacing (ft) |
|---|---|---|---|---|---|---|---|
| 1 | SH 159 | BRAZOS RI | H-20 | 180 | 662 | 15 | 8 |
| 2 | FM 723 | BRAZOS RI | H-15 | 150 | 542 | 15 | 7.33 |
| 3 | SH95 | COLORADO RIVER | H-20 | 160 | 782 | 20 | 7.5 |
| 4 | RM 1674 | N LLANO RIVER | HS-20 | 154 | 528 | 22 | 7.33 |
| 5 | RM 1674 | N LLANO RIVER | HS-20 | 99.25 | 330 | 19.85 | 7.33 |
| 5a | RM 1674 | N LLANO RIVER | HS-20 | 130 | 330 | 18.57 | 7.33 |
| 6 | SH 37 | RED RIVER | H-20 | 180 | 662 | 15 | 7.33 |
| 7 | US 59 | SABINE RIVER | H-20 | 99.3 | 330 | 19.85 | 8 |
| 7a | US 59 | SABINE RIVER | H-20 | 130 | 330 | 18.57 | 8 |
| 8 | US 59 (S) | TRINITY RIVER | H-20 | 154 | 530 | 22 | 8 |
| 9 | 310 | TRINITY RIVER | HS-20 | 60 | 300 | 20 | 6.92 |
| 9a | 310 | TRINITY RIVER | HS-20 | 152 | 380 | 19 | 6.92 |
| MIN | | | H-15 | 60 | 300 | 15 | 6.92 |
| MAX | | | HS-20 | 180 | 782 | 22 | 8 |

All of the bridges have a 6.5-inch thick slab. However, each bridge has different stringers, floor beams, and girders comprising the load carrying system. Those properties are shown in Table 3.2. All of the sections used are the older sections that have different properties compared with the current sections from the LRFD manual and SAP2000 database. In the SAP analysis, however, the current sections were used since there is very little difference in the properties. Member stiffness, an important variable in this study, is defined as the product of the moment of inertia and modulus of elasticity divided by the length. Since the

modulus of elasticity of steel is constant, relative stiffness can be defined as the moment of inertia for models with a constant length.

The stringers range from a 16WF40 section to a 21WF73 section. The 21WF73 section has approximately 3 times the moment of inertia of the 16WF40 section. The floor beams have around 3 to 4 times the moment of inertia of the stringers with the values ranging from 2100 $in^4$ to 4470 $in^4$. Most of the bridges have plate girders with variable depth. A variable depth plate girder model would have been possible to input into SAP, but probably not worth the time and effort. The plate girders are modeled using a constant depth equal to the minimum depth over the length of the span, using the web and flange thickness at that location. From a preliminary analysis it was determined that this will give a conservative estimate for mid-span floor beam moment, because the stiffer the exterior girders are, the more of the load will be attracted to the outside of the bridge and away from the center. This additional load carried by the exterior girders will result in a smaller mid-span floor beam moment. The plate girders range from 4 to 8 feet in height with a moment of inertia that is anywhere from 15 to 150 times that of the stringer moment of inertia.

**Table 3.2 Frame member properties**

| # | Stringer | | Floor Beam | | Plate Girder | |
|---|---|---|---|---|---|---|
| | Type | Moment of Inertia ($in^4$) | type | Moment of Inertia ($in^4$) | Height (in) | Moment of Inertia ($in^4$) |
| 1 | 18WF50 | 800 | 27WF94 | 3270 | 96 | 130957 |
| 2 | 16WF40 | 520 | 24WF76 | 2100 | 48 | 22667 |
| 3 | 18WF55 | 890 | 27WF94 | 3270 | 96 | 126156 |
| 4 | 21WF68 | 1480 | 27WF98 | 3450 | 60 | 42492 |
| 5 | 21WF63 | 1340 | 27WF98 | 3450 | 66.5 | 44149 |
| 5a | 21WF59 | 1250 | 27WF98 | 3450 | 66.5 | 60813 |
| 6 | 18WF50 | 800 | 27WF94 | 3270 | 96 | 130957 |
| 7 | 21WF68 | 1480 | 30WF108 | 4470 | 66.5 | 44149 |
| 7a | 21WF63 | 1340 | 30WF108 | 4470 | 66.5 | 60813 |
| 8 | 21WF73 | 1600 | 30WF108 | 4470 | 60 | 42492 |
| 9 | 21WF62 | 1330 | 27WF94 | 3270 | 50 | 21465 |
| 9a | 21WF62 | 1330 | 27WF94 | 3270 | 50 | 21465 |
| MIN | 16WF40 | 520 | 24WF76 | 2100 | 48 | 21465 |
| MAX | 21WF73 | 1600 | 30WF108 | 4470 | 96 | 130957 |

The goal of this study was to identify parameters that might effect the maximum moment in the floor beam and determine which parameters had the greatest effect on the finite element models. Some of the parameters studied include stringer spacing, floor beam spacing, span length, and the relative stiffness of the girders, floor beams, stringers, and slab. These parameters were studied using both the large model and the small model. The lateral load distribution of the different models is compared using the direct load moment to normalize the values. All values are then given as a percent of the direct load moment. As discussed in the first chapter, the direct load moment is only dependent on the spacing of the system and not dependent on any of the member properties.

## 3.2. Small Model Results

The first two properties examined, stringer spacing and floor beam spacing were varied along with girder stiffness. This was done holding all other factors constant using the small model. This model treats the floor beam as connected to the slab. The results are shown in Table 3.3. All of the models used 18WF50 stringers, 27WF94 floor beams and 66-inch plate girders on the outside. These members are in the middle range of member sizes. The stiffness of the floor beams and plate girders is about 4 times and 70 times that of the stringers, respectively. Two different loading cases were also used. Trucks were placed symmetrically side by side on the bridge and at the position that will produce the maximum moment in floor beam, which occurs one foot away from the symmetric position as discussed in Chapter 2.

Both positions were analyzed using a model with stiffer exterior girders and with girders the same size as the stringers to analyze the effect of girder stiffness. DSG (different size girders) and SSG (same size girders) represent these two cases respectively. Both of these cases as well as the lever rule are normalized by expressing them as a percentage of the direct load moment at the maximum moment position and at the symmetric load case. They can then be easily compared with the percentages from models with different stringer and floor beam spacing.

**Table 3.3 Small Model Results**

| | | | Stringer Spacing | | | | | |
|---|---|---|---|---|---|---|---|---|
| | | | **7 ft** | | **7.5 ft** | | **8 ft** | |
| | | | MAX | SYM | MAX | SYM | MAX | SYM |
| Floor Beam Spacing | **15 ft** | Direct Load | 194.0 kip-ft | 190.7 kip-ft | 219.7 kip-ft | 216.7 kip-ft | 245.6 kip-ft | 242.7 kip-ft |
| | | Lever Rule | 173.3 | 164.7 | 196.4 | 186.6 | 219.6 | 208.0 |
| | | % direct | **89.4%** | **86.4%** | **89.4%** | **86.1%** | **89.4%** | **85.7%** |
| | | SAP SSG | 181.7 | 178.4 | 206.1 | 202.8 | 230.4 | 227.2 |
| | | % direct | ***93.7%*** | ***93.6%*** | ***93.8%*** | ***93.6%*** | ***93.8%*** | ***93.6%*** |
| | | SAP DSG | 181.3 | 177.9 | 205.7 | 202.5 | 230.1 | 226.9 |
| | | % direct | ***93.5%*** | ***93.3%*** | ***93.6%*** | ***93.5%*** | ***93.7%*** | ***93.5%*** |
| | **20 ft** | Direct Load | 246.2 | 242.0 | 278.9 | 275.0 | 311.7 | 308.0 |
| | | Lever Rule | 220.0 | 209.0 | 249.3 | 236.9 | 278.7 | 264.0 |
| | | % direct | **89.4%** | **86.4%** | **89.4%** | **86.1%** | **89.4%** | **85.7%** |
| | | SAP SSG | 217 | 214.1 | 245.9 | 243.1 | 274.8 | 272.0 |
| | | % direct | ***88.1%*** | ***88.5%*** | ***88.2%*** | ***88.4%*** | ***88.2%*** | ***88.3%*** |
| | | SAP DSG | 211.9 | 208.8 | 241.6 | 238.7 | 271.1 | 268.3 |
| | | % direct | ***86.1%*** | ***86.3%*** | ***86.6%*** | ***86.8%*** | ***87.0%*** | ***87.1%*** |
| | **22 ft** | Direct Load | 260.4 | 256.0 | 295.0 | 290.9 | 329.7 | 325.8 |
| | | Lever Rule | 232.7 | 221.1 | 263.8 | 250.6 | 294.8 | 279.3 |
| | | % direct | **89.4%** | **86.4%** | **89.4%** | **86.1%** | **89.4%** | **85.7%** |
| | | SAP SSG | 225.9 | 222.9 | 255.8 | 253.0 | 285.7 | 283.1 |
| | | % direct | ***86.7%*** | ***87.1%*** | ***86.7%*** | ***87.0%*** | ***86.7%*** | ***86.9%*** |
| | | SAP DSG | 217.8 | 214.9 | 248.9 | 246.1 | 279.8 | 277.2 |
| | | % direct | ***83.6%*** | ***83.9%*** | ***84.4%*** | ***84.6%*** | ***84.9%*** | ***85.1%*** |

The table is divided into nine boxes, with each box containing different models with the same floor beam and stringer spacing. For example, the box in the lower right hand corner corresponds to models with a 22-foot floor beam spacing and 8-foot stringer spacing. On the top of this grid are the direct load moments for the maximum and symmetric loading case, 329.7 and 325.8 kip-ft respectively. Looking at the left column of the box, shown next is the maximum floor beam moment calculated using the lever rule, 294.8 kip-ft or 89.4% of 329.7 kip-ft, the maximum direct load moment. The maximum moment calculated

using the SSG model is 285.7 kip-ft or 86.7% of 329.7. The maximum moment in the DSG model is 279.8 kip-ft or 84.9% of 329.7. The same pattern is followed on the right column of the box for the symmetric load case.

The first thing to notice in Table 3.3 is that the direct load increase as both stringer spacing and floor beam spacing increase. As stringer spacing increases, the floor beam becomes longer, causing a higher mid-span moment. As the floor beam spacing increases, the static forces from the wheel loads 14 feet away increase on the floor beam. Moments from the SAP analysis also increase as the spacing increases. However, the increase is not in proportion to the increase found in the direct load model. That is the reason that the moments are expressed as percentages of the direct load moment.

### 3.2.1. TRUCK POSITION

One factor shown in Table 3.3 is the effect of truck position on the maximum floor beam moment. The two columns under each stringer spacing give the moments for the two lateral truck positions. The moment is slightly higher with the loads placed one foot away from the symmetric position for both the SAP analysis and the direct load model. However, by normalizing the moment with respect to the direct load moment, the trends are basically the same using either loading case. Because of this, the rest of the values discussed for the finite element models will be for the symmetric loading case. However, for the lever rule analysis, the maximum loading position produces a moment that is a little bit higher than the symmetric load case, 89% to 86%.

### 3.2.2. LEVER RULE

The lever rule only depends on geometry and not the stiffness of the members. When normalized with the direct load method, the lever rule results in the same value of 89.4% regardless of the floor beam spacing or stringer spacing for the max load case. For the symmetric load case, the stringer spacing makes a little difference. With a 7-foot stringer spacing the moment is about 86.4% of the direct load value and with an 8-foot spacing the value falls to about 85.7%. Using the maximum value of the lever rule or 89.4% would be a conservative estimate except at smaller floor beam spacing such as 15 feet where SAP gives a value of between 93.3 and 93.7% depending on the model.

### 3.2.3. FLOOR BEAM SPACING

From Table 3.3 it is evident that the floor beam spacing plays an important role in the distribution of the lateral load. As the floor beam spacing increases, the floor beam moment as a percentage of the direct load model decreases. Using a 15-foot floor beam spacing, the SAP analysis results in a floor beam moment about 94% of the direct load moment; whereas using 22-foot floor beam spacing the normalized moment is around 84%. This is because longer spacing causes more of the load to be carried to the floor beam from the far axles. For this reason, the wheel loads on either side of the floor beam have a greater effect on the total moment as the floor beam spacing increases. Table 3.4 shows this effect for an HS-20 loading assuming a static distribution of the wheel loads to the floor beam. This causes a greater reduction in the floor beam moment for longer floor beam spacing, also shown in Table 3.4. This table also indicates that most of the

moment is caused by the loads directly over the floor beam, 92.3% for a 15-foot spacing and 68.7% for 22-foot spacing. For an H-20 loading an even greater percentage of the moment is caused by the wheels on the floor beam, 98.3% and 91.7% for the 15-foot and 22-foot spacing respectively.

**Table 3.4 Floor beam Spacing Effects for HS-20 Loading**

| Floor Beam Spacing (ft) | % of Total Moment Caused by Wheel Loads 14 feet away from Floor Beam | % Moment Reduction From Direct Load Model |
|---|---|---|
| 15 | 7.7% | 6.5% |
| 20 | 27.3% | 12.9% |
| 22 | 31.3% | 14.9% |

This is important because the wheel loads 14 feet away from the floor beam are affected much more by changing the floor beam spacing than the wheels placed directly on the floor beam. The wheel loads on either side of the floor beam are spread out more over the floor beam, while the load placed directly on the floor beam behaves more like the direct load model. This is demonstrated in Table 3.5, which shows that the small model moments produced by the loads over the floor beam are about 90% of the direct load model regardless of the floor system geometry. The table shows floor beam moments from the symmetric loading case using models with the same frame properties as the DSG models shown in Table 3.3.

**The floor beam moments shown in**

Table 3.6, for the wheels away from the from the floor beam, in contrast to the wheels placed on the floor beam, vary greatly depending on the floor beam spacing and to a lesser extent, stringer spacing. This indicates that the loads

placed away from the floor beam cause the differences in normalized floor beam moment when the floor beam spacing is changed. However, because these wheel loads contribute a small percentage of the total moment, it takes a substantial change in the floor beam moment caused by these loads to result in a small change in the total floor beam moment.

**Table 3.5 Small Model Results with Wheels on Floor Beam Only**

| | | | Stringer Spacing | | |
|---|---|---|---|---|---|
| | | | 7 ft | 7.5 ft | 8 ft |
| Floor Beam Spacing | 15 ft | Direct Load | 176.0 | 200.0 | 224.0 |
| | | Small Model | 159.3 | 180.0 | 200.4 |
| | | % of direct | ***90.5%*** | ***90.0%*** | ***89.5%*** |
| | 20 ft | Direct Load | 176.0 | 200.0 | 224.0 |
| | | Small Model | 159.5 | 180.4 | 201.1 |
| | | % of direct | ***90.6%*** | ***90.2%*** | ***89.8%*** |
| | 22 ft | Direct Load | 176.0 | 200.0 | 224.0 |
| | | Small Model | 159.5 | 180.4 | 200.8 |
| | | % of direct | ***90.6%*** | ***90.2%*** | ***89.6%*** |

**Table 3.6 Small Model Results with Wheels away from Floor Beam Only**

| | | | Stringer Spacing | | |
|---|---|---|---|---|---|
| | | | 7 ft | 7.5 ft | 8 ft |
| Floor Beam Spacing | 15 ft | Direct Load | 14.7 | 16.7 | 18.7 |
| | | Small Model | 18.6 | 22.5 | 26.5 |
| | | % of direct | ***126.8%*** | ***135.0%*** | ***142.0%*** |
| | 20 ft | Direct Load | 66.0 | 75.0 | 84.0 |
| | | Small Model | 49.3 | 58.3 | 67.2 |
| | | % of direct | ***74.7%*** | ***77.7%*** | ***80.0%*** |
| | 22 ft | Direct Load | 80.0 | 90.9 | 101.8 |
| | | Small Model | 55.4 | 65.7 | 76.4 |
| | | % of direct | ***69.3%*** | ***72.3%*** | ***75.0%*** |

Viewing influence surfaces for a 15 and 22-foot floor beam spacing also demonstrates this effect. These influence surfaces, shown in Figure 3.1, represent

the mid-span moment in the small model as a percentage of the direct load model. Using the direct load model a load placed on the second floor beam would result in zero moment on the first floor beam. It is impossible to divide by zero, so the horizontal axis in the figure is one foot less than the floor beam spacing. The wheel loads are represented by white rectangles. First of all, the two influence surfaces have a similar shape with the minimum value occurring somewhere near the center of the model. The smallest value, 63% occurs with a 22-foot floor beam spacing. The minimum value for the 15-foot floor beam spacing is 71%. The wheel loads on the floor beam (at longitudinal position zero) generate almost the same normalized mid-span floor beam moment, though they become slightly higher as the floor beam spacing increases. However, the wheel loads positioned 14 feet away are quite different for each floor beam spacing. The model with a 22-foot spacing places the center wheel loads 14 feet away from the floor beam near the minimum value while the 15-foot spacing model places those same wheel loads at a location where the small model is greater than the direct load model.

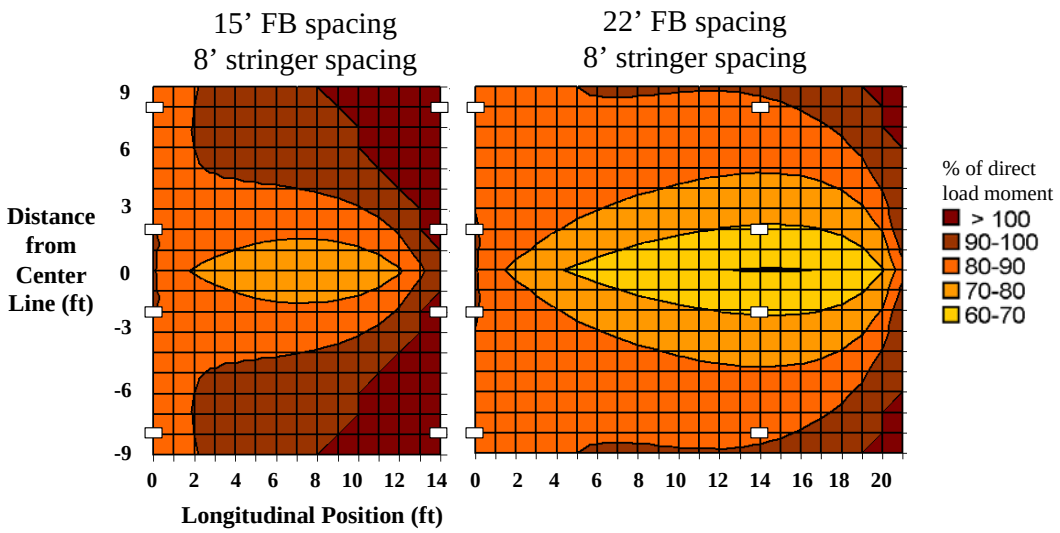


**Figure 3.1 Influence Surface Comparison of Different Floor Beam Spacing**

### 3.2.4. STRINGER SPACING

When the floor beam spacing is held constant and the stringer spacing is varied, however, there is very little difference in the normalized moment. That is partly because stringer spacing is not varied over a large range. The range of stringer spacing is only from 7 feet to 8 feet. There is virtually no difference in normalized floor beam moment varying stringer spacing using the 15-foot floor beam spacing. Using the longer 22-foot floor beam spacing there is a slight decrease from 85% to 84% in the normalized moment as the stringer spacing is decreased from 8 to 7 feet. That is because when the stringer spacing is smaller, the outside wheels are closer to the stiffer exterior girders, which attract more of the load. This phenomenon is illustrated with a comparison of influence surfaces having different stringer spacing, shown in Figure 3.2. Using the same size girders in the model results in no change due to the stringer spacing in the

normalized moment. This is because in the SSG model, girders and stringers of the same size, the girders carry less load.

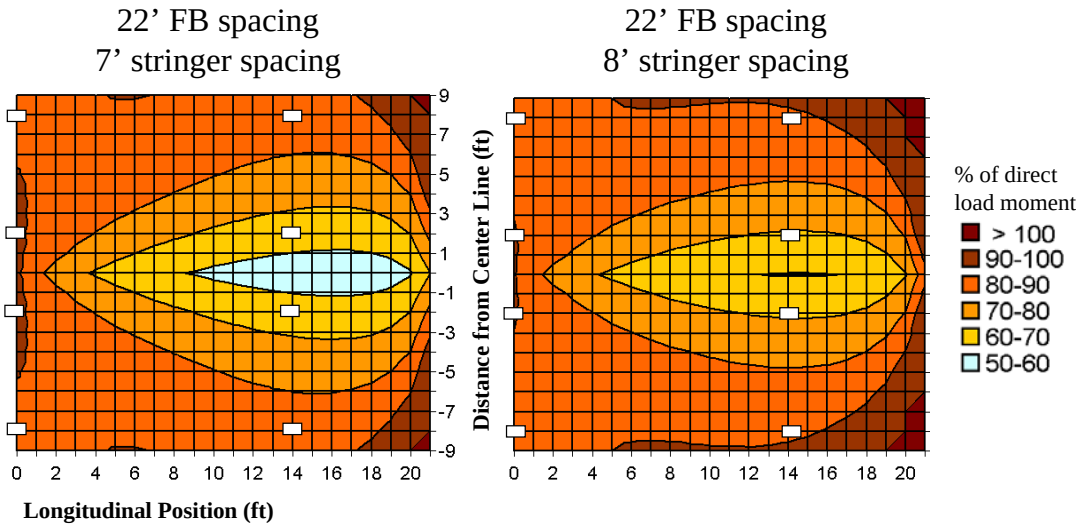


**Figure 3.2 Influence Surface Comparison of Different Stringer Spacing**

The wheels on the floor beam generate a slightly higher normalized moment with the narrower spacing because of the floor beam stiffness increases. However, that is counteracted by the decrease in normalized moment caused by the wheels away from the floor beam. For this case, the net change is almost negligible, with a decrease of 1.2% as the stringer spacing decreases.

### 3.2.5. GIRDER MOMENT OF INERTIA

Looking at the DSG and SSG models can show the effect of the moment of inertia of the exterior girders. The SSG model uses 18WF50 stringers for the outside girders, while the DSG model has 66-inch plate girders. While the plate girders have a moment of inertia 70 times that of the stringers, there is a relatively small difference in the normalized floor beam moments using the larger exterior

girders for most spacing values. The biggest difference occurs in the model with 22-foot floor beam spacing and 7-foot stringer spacing, shown in Figure 3.3. Using larger exterior girders in this model decreases the normalized moment from 87.1% to 83.9%. One would expect the maximum effect to take place in this model because with the largest floor beam spacing, the wheel loads away from the floor beam have the largest contribution to the floor beam moment. That is, the floor beam straddled by the trucks carries a greater percentage of the wheel loads away from the floor beam. Also, with the smallest stringer spacing, it places the outside wheels closest to the exterior girders, attracting the load in that direction, away from the center of the floor beam. By comparison, the 22-foot, 8-foot model goes down from 86.9% to 85.1%. Varying the girder stiffness results in virtually no change in the 15-foot floor beam spacing models.

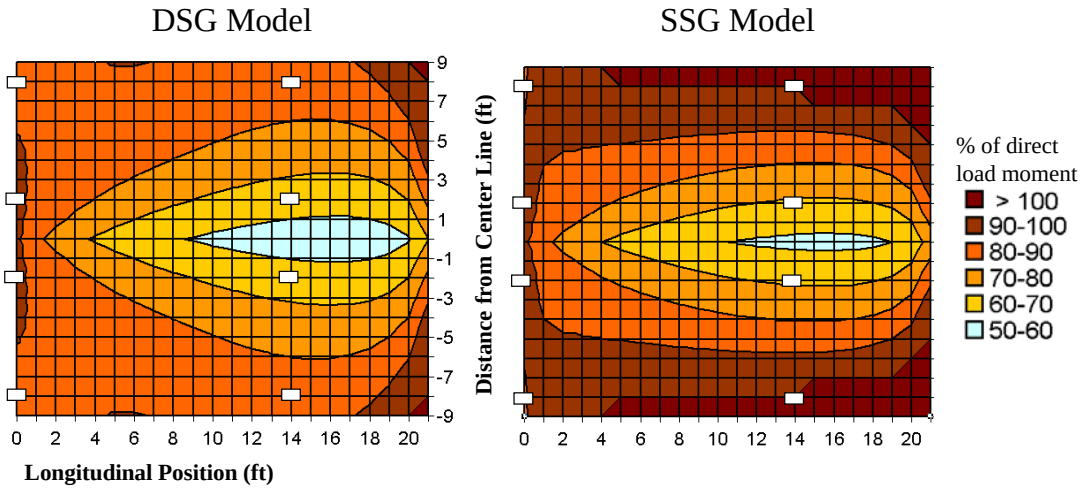


**Figure 3.3 Influence Surface Comparison of Different Size Girders**

### 3.2.6. FLOOR BEAM MOMENT OF INERTIA

The floor beam moment of inertia can also effect the floor beam moment. A stiffer floor beam will pick up more of the moment, while a floor beam with less stiffness will cause more of the moment to be carried by the slab. This is also demonstrated with the small model. The analysis was run with both 27WF94 and 30WF108 floor beams using the same stringers and girders as before in the DSG model. All values shown are for the symmetric load case. The 30WF108 section is about 35% stiffer than the 27WF94 section. A comparison of the normalized moment values for the two different floor beams with different stringer and floor beam spacing is shown in Table 3.7. This shows that for the 22-foot and 20-foot floor beam spacing models, there is an increase in normalized floor beam moment of around 2% while the increase is around 1.5% for the 15-foot models.

**Table 3.7 Effect of Floor Beam Stiffness**

| | | | Stringer Spacing | | |
|---|---|---|---|---|---|
| | | | **7 ft** | **7.5 ft** | **8 ft** |
| Floor Beam Spacing | **15 ft** | Direct Load | 190.7 | 216.7 | 242.7 |
| | | 27WF94 | 177.9 | 202.5 | 226.9 |
| | | % Direct | ***93.3%*** | ***93.5%*** | ***93.5%*** |
| | | 30WF108 | 180.7 | 205.6 | 230.4 |
| | | % Direct | ***94.8%*** | ***94.9%*** | ***94.9%*** |
| | **20 ft** | Direct Load | 242.0 | 275.0 | 308.0 |
| | | 27WF94 | 208.8 | 238.7 | 268.3 |
| | | % Direct | ***86.3%*** | ***86.8%*** | ***87.1%*** |
| | | 30WF108 | 213.5 | 244.1 | 274.6 |
| | | % Direct | ***88.2%*** | ***88.8%*** | ***89.2%*** |
| | **22 ft** | Direct Load | 256.0 | 290.9 | 325.8 |
| | | 27WF94 | 214.9 | 246.1 | 277.2 |
| | | % Direct | ***83.9%*** | ***84.6%*** | ***85.1%*** |
| | | 30WF108 | 219.9 | 252.0 | 284.1 |
| | | % Direct | ***85.9%*** | ***86.6%*** | ***87.2%*** |

The change in normalized moment caused by the floor beam stiffness is also shown in Figure 3.4. These influence surfaces are for models with 22-foot floor beam spacing and 8-foot stringer spacing. The difference in these influence surfaces is found by looking at the wheels positioned directly over the floor beam as shown in the figure. The slab and floor beam both take part of the load from these wheels. When the moment of inertia of the floor beam is increased, it carries a higher percentage of the load. That is why the influence surface for the 30WF108 floor beam has higher values near the floor beam. However, the influence surfaces look very similar away from the floor beam.

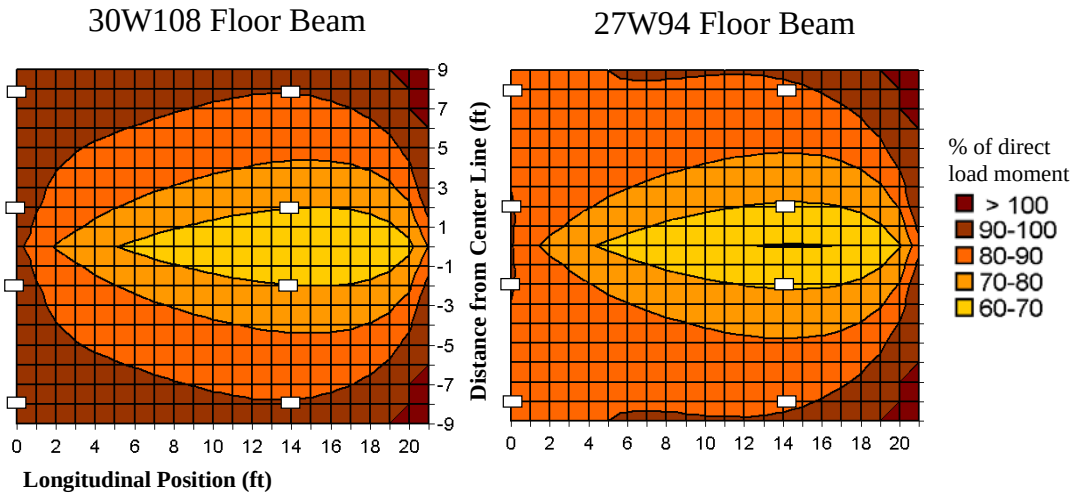


**Figure 3.4 Influence Surface Comparison of Different Floor Beam Sizes**

## 3.3. Large Model Results

When analyzing the structures with the large model the effect of different input parameters changes. An important variable becomes the overall length of

the model or number of floor beams in the model. The length is taken as 80% of the maximum span length. This value is then rounded off to give a model length that is a multiple of the floor beam spacing so the model starts and ends with a floor beam. The number of floor beams in the small model is two, one at each end of the span. The large model by definition has at least three floor beams. The floor beam being analyzed is always the floor beam in the middle of the model and the slab on either side of the middle floor beam is treated as discontinuous using the weak shell method. Table 3.8 shows the results from the large model of each bridge compared with the similar small model.

**Table 3.8 Summary of Finite Element Results**

| # | Girder height (inches) | Size | Spacing (ft) | Size | Spacing (ft) | # of Floor Beams | Direct Load (kip-ft) | SSG % of direct | DSG % of direct | Large % of direct |
|---|---|---|---|---|---|---|---|---|---|---|
| 1 | 96 | 27WF94 | 15.0 | 18WF50 | 8.0 | 11 | 242.7 | 93.5 | 93.4 | 86.5 |
| 2 | 48 | 24WF76 | 15.0 | 16WF40 | 7.3 | 9 | 208.0 | 90.6 | 90.3 | 87.5 |
| 3 | 96 | 27WF94 | 20.0 | 18WF55 | 7.5 | 7 | 275.0 | 88.3 | 86.8 | 79.3 |
| 4 | 60 | 27WF98 | 22.0 | 21WF68 | 7.3 | 7 | 279.3 | 87.3 | 85.6 | 84.7 |
| 5 | 66.5 | 27WF98 | 19.8 | 21WF63 | 7.3 | 5 | 262.7 | 88.7 | 87.5 | 81.7 |
| 5a | 66.5 | 27WF98 | 18.6 | 21WF59 | 7.3 | 7 | 251.1 | 89.6 | 88.6 | 85.6 |
| 6 | 96 | 27WF94 | 15.0 | 18WF50 | 7.3 | 11 | 208.0 | 93.5 | 93.3 | 87.2 |
| 7 | 66.5 | 30WF108 | 19.8 | S21WF68 | 8.0 | 5 | 306.5 | 90.8 | 90.1 | 85.2 |
| 7a | 66.5 | 30WF108 | 18.6 | 21WF63 | 8.0 | 7 | 292.9 | 91.6 | 91.1 | 90.1 |
| 8 | 60 | 30WF108 | 22.0 | 21WF73 | 8.0 | 7 | 325.8 | 89.5 | 88.4 | 88.5 |
| 9 | 50 | 27WF94 | 20.0 | 21WF62 | 6.9 | 3 | 242.0 | 88.6 | 87.2 | 80.5 |
| 9a | 50 | 27WF94 | 19.0 | 21WF62 | 6.9 | 7 | 233.9 | 89.4 | 88.3 | 93.0 |
| MIN | 48 | 24WF76 | 15 | 16WF40 | 7 | 3 | 208 | 87.3 | 85.6 | 79.3 |
| MAX | 96 | 30WF108 | 22 | 21WF73 | 8 | 11 | 326 | 93.5 | 93.4 | 93.0 |

As can be seen from the last column of the table, the results from the large model range from 79.3% to 93.0% of the direct load model. The floor beam

moments from the DSG and SSG models range from 85.6 to 93.4% and 87.3 to 93.5% respectively. In every case but 9a, the results from the small model are conservative with respect to the large model. In the next few sections the effect of different parameters on the large model results will be discussed.

### 3.3.1. NUMBER OF FLOOR BEAMS

The number of floor beams is a parameter that describes the overall length of the model. In the small model, there were only two floor beams so this parameter that did not exist. It will be shown here, though, that it has a significant effect on the floor beam moment. Table 3.9 shows two different bridges with the number of floor beams varied and all other parameters constant. These results show that the floor beam moment increases significantly when the number of floor beams in the model is increased.

**Table 3.9 Effect of Increasing the Number of Floor Beams**

| Floor beam spacing (ft) | Stringer spacing (ft) | Stringer Mom. of Inertia ($in^4$) | Floor Beam Mom. of Inertia ($in^4$) | Girder Mom. of Inertia ($in^4$) | # of Floor Beams | % of Direct |
|---|---|---|---|---|---|---|
| 22 | 8 | 1600 | 4470 | 42000 | 7 | 88.5 |
| 22 | 8 | 1600 | 4470 | 42000 | 9 | 90.3 |
| 19 | 7 | 1330 | 3270 | 22000 | 3 | 81.4 |
| 19 | 7 | 1330 | 3270 | 22000 | 5 | 86.3 |
| 19 | 7 | 1330 | 3270 | 22000 | 7 | 93.0 |
| 19 | 7 | 1330 | 3270 | 22000 | 9 | 99.7 |

For example, when the number of floor beams is increased from 3 to 9 the normalized moment increases from 81.4% to almost 100% of the direct load moment for the case with 19-foot floor beam spacing and 7-foot stringer spacing.

For the case with 22-foot floor beam spacing and 8-foot stringer spacing, the floor beam moment increases from 88.5% to 90.3% when the number of floor beams is increased from 7 to 9. This occurs because as the model becomes longer, the exterior girders become less stiff and therefore carry less of the load. Notice that increasing the number of floor beams has a much greater effect on models with a lower girder moment of inertia. The 22000 $in^4$ moment of inertia is the minimum moment of inertia found in any of the bridges studied. This value was calculated using the smallest section found anywhere on the bridges. Though the last row in the table shows a model that is around 100% of the direct load moment, this model geometry is unlikely. A girder size this small would not be used for a span of that length.

### 3.3.2. FLOOR BEAM MOMENT OF INERTIA

The moment of inertia of the floor beams also has an effect on the floor beam moment. As the moment of inertia of the floor beams is increased, the floor beams pick up more of the load relative to the slab, similar to the results from the small model analysis. These results shown in Table 3.10 demonstrate this effect. As the floor beams are increased from 3270 to 4470 in moment of inertia, the corresponding normalized moment increases from 85.8% to 90.3% for the model using 9 floor beams. In the model with 7 floor beams, the increase is even greater, from 82.0% to 88.5%.

**Table 3.10 Effect of Increasing the Size of Floor Beams**

| Floor beam spacing (ft) | Stringer spacing (ft) | Stringer Mom. of Inertia ($in^4$) | Floor Beam Mom. of Inertia ($in^4$) | Girder Mom. Of Inertia ($in^4$) | # of Floor Beams | % of Direct |
|---|---|---|---|---|---|---|
| 22 | 8 | 1600 | 3270 | 42000 | 9 | 85.8 |
| 22 | 8 | 1600 | 4470 | 42000 | 9 | 90.3 |
| 22 | 8 | 1600 | 3270 | 42000 | 7 | 82.0 |
| 22 | 8 | 1600 | 4470 | 42000 | 7 | 88.5 |

### 3.3.3. FLOOR BEAM SPACING

Floor beam spacing has the same effect that it had in the small model. As the spacing increases, the wheels away from the floor beam have a greater effect on the normalized floor beam moment. As the floor beam spacing decreases the normalized floor beam moment increases. This trend is shown in Table 3.11.

**Table 3.11 Effect of Decreasing the Floor Beam Spacing**

| Floor beam spacing (ft) | stringer spacing (ft) | Stringer Mom. of Inertia ($in^4$) | Floor Beam Mom. of Inertia ($in^4$) | Girder Mom. of Inertia ($in^4$) | # of Floor Beams | % of Direct | Small Model % of Direct |
|---|---|---|---|---|---|---|---|
| 22 | 8 | 1600 | 4470 | 42000 | 7 | 88.5 | |
| 19.85 | 8 | 1600 | 4470 | 42000 | 7 | 93.1 | |
| 15 | 8 | 1600 | 4470 | 42000 | 7 | 94.5 | |
| 22 | 8 | 1600 | 3270 | 61000 | 7 | 78.6 | 85.1 |
| 19.85 | 8 | 1600 | 3270 | 61000 | 7 | 83.9 | |
| 15 | 8 | 1600 | 3270 | 61000 | 7 | 87.7 | 93.5 |

This table contains three different values for floor beam spacing with all other variables held constant. Different floor beam sections and plate girders are used in the second group of three. This table also demonstrates that the normalized moment decreases as the floor beam size decreases and the girder size increases. The members used in the second group of three are the same members

used in the small model results shown earlier. The small model results shown in Table 3.3 indicate a value of 93.5% for the 15-foot floor beam spacing and 8-foot stringer spacing and a value of 85.1% for the 22-foot and 8-foot model. These values are conservative for this case compared with the large model results.

### 3.3.4. GIRDER MOMENT OF INERTIA

The moment of inertia of the girders becomes an important variable as the length of the model increases. This is demonstrated in Table 3.12. It is evident that changing the moment of inertia of the exterior girders has a significant effect on the floor beam moment in the longer models (the models using 5 and 7 floor beams). However in the model with only 3 floor beams, there is very little change in moment despite increasing the girder moment of inertia by a factor of six. This was also demonstrated using the small model when there was a relatively small difference between the SSG and DSG model despite increasing the moment of inertia by a factor of 70.

**Table 3.12 Effect of Increasing Girder Stiffness**

| Floor beam spacing (ft) | Stringer spacing (ft) | Stringer Mom. of Inertia ($in^4$) | Floor Beam Mom. of Inertia ($in^4$) | Girder Mom. Of Inertia ($in^4$) | # of Floor Beams | % of Direct |
|---|---|---|---|---|---|---|
| 19.85 | 8 | 1330 | 4470 | 22000 | 3 | 87.3 |
| 19.85 | 8 | 1330 | 4470 | 42000 | 3 | 87.0 |
| 19.85 | 8 | 1330 | 4470 | 61000 | 3 | 86.8 |
| 19.85 | 8 | 1330 | 4470 | 131000 | 3 | 86.7 |
| 19.85 | 8 | 1330 | 4470 | 22000 | 5 | 92.2 |
| 19.85 | 8 | 1330 | 4470 | 42000 | 5 | 88.3 |
| 19.85 | 8 | 1330 | 4470 | 61000 | 5 | 86.9 |
| 19.85 | 8 | 1330 | 4470 | 131000 | 5 | 85.2 |
| 19.85 | 8 | 1330 | 4470 | 22000 | 7 | 99.9 |
| 19.85 | 8 | 1330 | 4470 | 42000 | 7 | 93.1 |
| 19.85 | 8 | 1330 | 4470 | 61000 | 7 | 90.7 |
| 19.85 | 8 | 1330 | 4470 | 131000 | 7 | 87.4 |

In the longer models, as the girder moment of inertia increases, the floor beam moment decreases significantly. This is because as the moment of inertia of the girders become larger, the stiffness increases and more of the load is attracted to the outside and away from the center of the model. However, when the model is shorter, the moment of inertia of the girders has less of an effect on the floor beam moment, because the girders are already very stiff due to their smaller length. The effect of the girder stiffness is related to the effect of the stringer stiffness. The amount of load carried by the girders is also related to the stringer stiffness. With stiffer stringers, the girders carry less of the load and the resulting floor beam moment is higher. The model shown above resulting in almost 100% of the direct load moment is not a floor system used in an actual bridge. The girder moment of inertia of 21000 $in^4$ is too small to be used in a span of that length.

### 3.3.5. STRINGER SPACING

Decreasing the stringer spacing also has a minimal effect on the normalized floor beam moment. As shown in Table 3.13, when the stringer spacing decreases the normalized floor beam moment slightly increases. This is the opposite effect of what was seen using the small model. It is expected that the model with the narrower width would attract more of the load away from the center toward the outside of the bridge as was seen in the small model influence surfaces.

**Table 3.13 Effect of Decreasing the Stringer Spacing**

| Floor beam spacing (ft) | Stringer spacing (ft) | Stringer Mom. of Inertia ($in^4$) | Floor Beam Mom. of Inertia ($in^4$) | Girder Mom. of Inertia ($in^4$) | # of Floor Beams | % of Direct |
|---|---|---|---|---|---|---|
| 22 | 8 | 1600 | 4470 | 42000 | 7 | 88.5 |
| 22 | 7.33 | 1600 | 4470 | 42000 | 7 | 89.3 |
| 22 | 7 | 1600 | 4470 | 42000 | 7 | 90.2 |
| **22** | **8** | **1600** | **4470** | **131000** | **7** | **81.9** |
| 22 | 7.33 | 1600 | 4470 | 131000 | 7 | 82.4 |
| **22** | **7** | **1600** | **4470** | **131000** | **7** | **82.6** |
| 20 | 8 | 1330 | 3270 | 22000 | 7 | 89.5 |
| 20 | 7.5 | 1330 | 3270 | 22000 | 7 | 90.4 |
| 20 | 7 | 1330 | 3270 | 22000 | 7 | 92.8 |

Influence surfaces for the two entries in bold in Table 3.13 are shown in Figure 3.5. These influence surfaces demonstrate that there is little difference in normalized floor beam moment caused by a change in stringer spacing. As the spacing decreases, the slight normalized moment increase caused by the wheels directly over the floor beam is counteracted by the slight decrease caused by the wheels away from the floor beam. This results in a slight increase in overall normalized moment from 81.9% to 82.6%. The other models in the table had a slightly larger increase, but probably not enough to be significant.

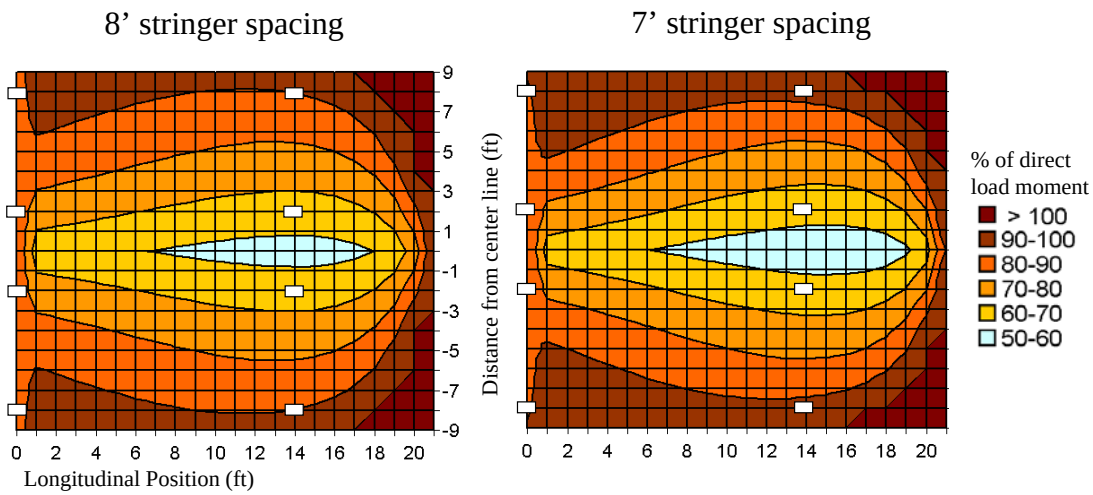


**Figure 3.5 Influence Surface Comparison for Large Model Stringer Spacing**

## 3.4. Summary of Finite Element Results

When interpreting these results, it is important to remember that the results from these finite element studies are for the case that there is contact between the floor beam and the slab, because the shell elements and frame elements share the same node. For the case when the slab does not rest on the floor beams, the lever rule is an appropriate method to use to model the floor system.

### 3.4.1. HS-20 LOAD CASE

Table 3.14 shows a summary of the effects of the various parameters studied in this chapter for the HS-20 loading. As is evident from the table, the large model shows the effects of more of the parameters. Only the floor beam spacing and floor beam moment of inertia have much effect on the normalized floor beam moment in the small model. The large model also captures the

exterior girder effects. Changing the number of floor beams and the girder moment of inertia both cause a change of stiffness in the girder.

**Table 3.14 Summary of Effects of Various Parameters on HS-20 Loading**

| Increasing this Parameter | Causes this Change in Normalized Floor Beam Moment | |
|---|---|---|
| | Small Model | Large Model |
| Floor Beam Spacing | Decrease | Decrease |
| Floor Beam Moment of Inertia | Increase | Increase |
| Girder Moment of Inertia | Slight Decrease | Decrease |
| Number of Floor Beams | X | Increase |
| Stringer Spacing | Slight Decrease | Slight Increase |

Unless a small girder size is used over a long span with relatively large stringers and floor beams, as was the case in bridge 9a, the results for the small model will be conservative compared with the large model. In bridge 9a, the plate girder moment of inertia was 21000 $in^4$ over a span of 114 ft. The floor beams and stringer had moments of inertia of 3270 $in^4$ and 1330 $in^4$ respectively. Using the small model, for all other cases would be a reasonable method for evaluating the floor beam moment. However, a better method is to come up with an equation that includes the different parameters shown in the above table.

### 3.4.2. H-20 LOAD CASE

Though the majority of the discussion in the chapter focused on the HS-20 load case, it is also important to consider the effect of the H-20 load case. It has the same wheel loads as the HS-20 load case minus the second rear axle. Because of this there is a 4-kip wheel load away from the floor beam compared with a 16-

kip wheel load on the floor beam, the effects of the 4-kip load are minimal. Almost all of the floor beam moment comes from the wheels directly over the floor beam. Figure 3.6 shows the position of the longitudinal position of the H-20 truck to produce the maximum moment.

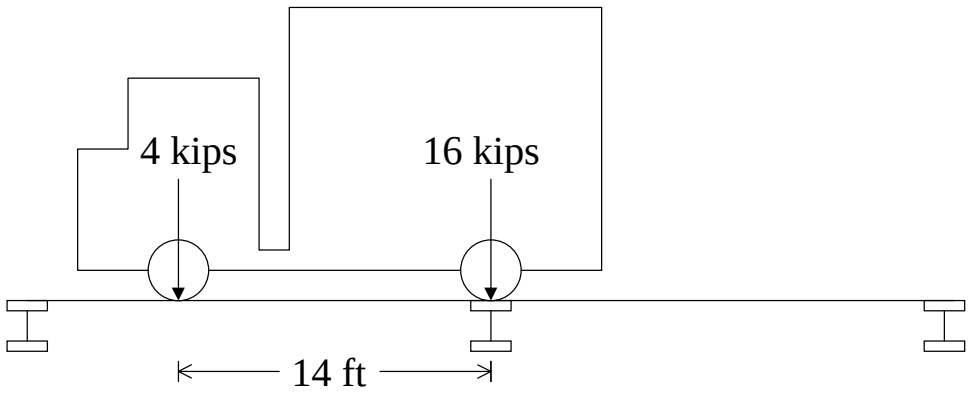


**Figure 3.6 Longitudinal Position of H-20 Truck**

Looking back at Table 3.5 shows that the stringer and floor beam spacing have almost no effect on the load placed directly on the floor beam. Intuitively that makes sense as well. The entire load is already on the floor beam, so there can be little effect due to load distribution. The only parameter that has an effect on the floor beam moment for this load case is the floor beam moment of inertia compared to that of the concrete slab. A higher floor beam moment of inertia causes the floor beam to carry more of the moment and a lower floor beam moment of inertia causes the slab to carry more of the moment. Table 3.15 shows the effect this ratio on the floor beam moment.

**Table 3.15 Effect of Floor Beam Moment of Inertia on H-20 Load Case**

| Floor Beam | | Slab | | $EI_{FB} / EI_{slab}$ | % of |
|---|---|---|---|---|---|
| I ($in^4$) | EI | I ($in^4$) | EI | | Direct |
| 2100 | 60900000 | 275 | 856830 | 71 | 85.5 |
| 3270 | 94830000 | 275 | 856830 | 111 | 89.8 |
| 4470 | 129630000 | 275 | 856830 | 151 | 92.2 |
| 6710 | 194590000 | 275 | 856830 | 227 | 94.8 |

Using this data it was possible to find a correlation between the floor beam to slab flexural stiffness (EI) ratio and the percent reduction of the floor beam moment. The moment of inertia for the slab was determined using a one-foot wide section of the slab. The modulus of elasticity of steel and concrete in the above table were 29000 ksi and 3120 ksi respectively. The moment of inertia of the slab was the same for every bridge examined since the same 6.5-inch thick slab was used. The moment due to an H-20 truck load can be predicted using the correlation shown in Equation 3.1. The correlation is a conservative estimate of the finite element results as shown in Figure 3.7.

$$M_{LL} = M_{direct} \cdot \left( 0.08 \ln\left[ \frac{EI_{FB}}{EI_{slab}} \right] + .52 \right) \tag{3.1}$$

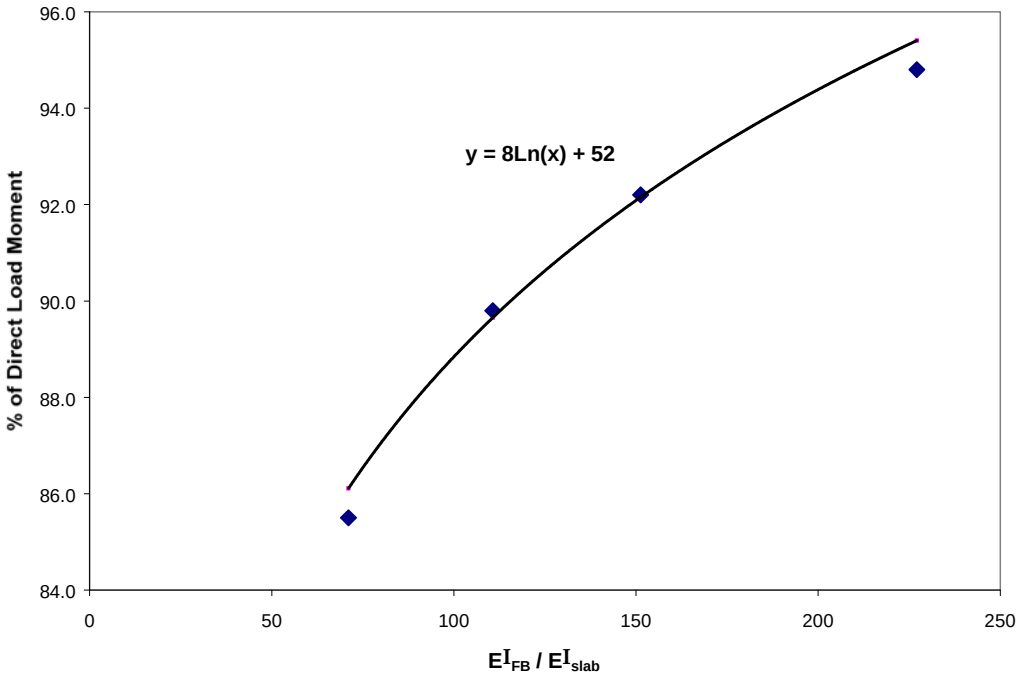


**Figure 3.7 Correlation of Floor Beam Stiffness to Moment Reduction**

# CHAPTER 4

# RESULTS OF EXPERIMENTAL TEST

## 4.1. Llano Bridge Floor System Geometry

The experiment testing was done on a bridge in Llano, TX. Charles Bowen, a Ph.D. candidate at the University of Texas, was responsible for the testing of this bridge for TxDOT's historic bridge research project, #1741. The transverse floor beams in the bridge in Llano, shown in Figure 4.1, are controlling the low load rating of the bridge. Replacement of the bridge is being considered since the floor beams have been rated deficient for the current design loads. Since this bridge was already scheduled to be tested, it was decided to use the results from this test to study of floor beam behavior and to correlate with the analytical results. The bridge was first tested on February 2nd, 1999.

**Figure 4.1 Historic Truss Bridge in Llano, TX**

Although the bridge in Llano is a truss, the floor system geometry is similar to the bridges being analyzed in this study. The bridge is made up of four identical trusses, each spanning about 200 feet. Figure 4.2 shows a plan view of a section of the floor system. This is the section adjacent to the north abutment of the bridge that was instrumented and tested. The bridge has a floor beam spacing of 22 feet, within the range of the bridges in this study. There are six identical stringers as compared to the two stringers and two girders in geometry analyzed in Chapter 3. However, the distance between the outside stringers is only 22.5 feet, the same as the distance between girders in the model with 7.5-foot stringer spacing.

Having the stringers all the same size is basically the same as the SSG model looked at earlier. One difference is that in the Llano Bridge, the floor beam does not end at the outermost stringer. It continues for another 20 inches where it connects with the truss vertical. This vertical member is then connected to the bottom chord of the truss with a gusset plate. This connection is shown in Figure 4.3. Extending the floor beam past the furthest stringer leads to a longer floor beam, which, at just under 26 feet, is about 2 feet longer than the longest floor beam from the plate girder models. In the SAP model, since only the floor system is modeled, each floor beam to truss connection was modeled as a simply supported boundary condition.

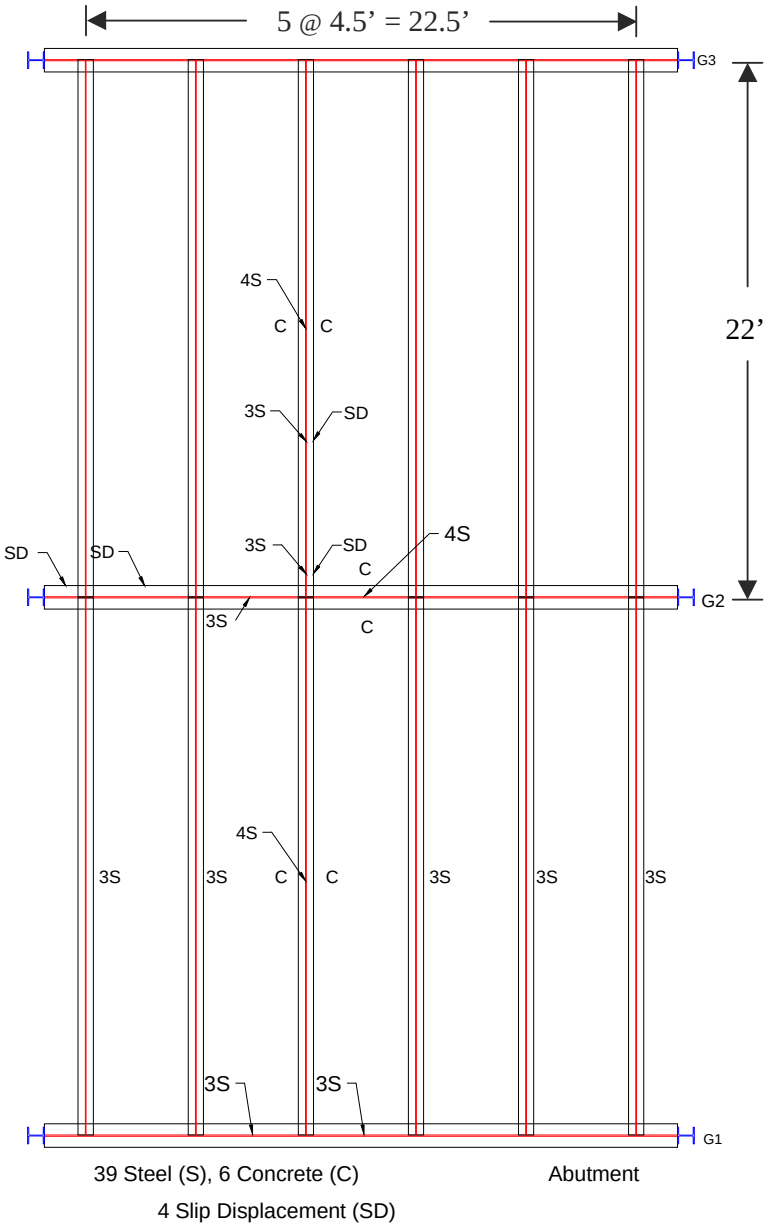


**Figure 4.2 Plan View with Strain Gage Locations**

The stringers in the Llano Bridge are 18WF50s and the floor beams are 33WF132s. However, the floor beams were modeled as W33x130s because this

was the closest section in the SAP database. These sections are in the same approximate range as the sections studied earlier, though the floor beam is a bit larger than the maximum section used in the plate girder bridges which was a 30WF108. The slab is again 6.5 inches thick, but a low modulus of elasticity of 2850 ksi is used since it has a design strength of 2500 psi. The modulus of elasticity for the bridges in Chapter 3 was 3120 ksi for a design strength of 3000 psi. A higher floor beam stiffness and a lower slab stiffness will lead to a higher normalized moment which will be shown in with the influence surfaces later.

**Figure 4.3 Connection of 2nd Floor Beam to Truss**

## 4.2. Location of Strain Gages

Gages were placed at various locations on the floor system, shown in Figure 4.2. Of primary interest, though, are the gages located on the floor beams. Both the first floor beam and second floor beam were instrumented at two

locations, at mid-span and at 4.5 feet away from mid-span. The other floor beams were not easily accessible and were not instrumented.

At each location, a gage was placed on the top flange, the bottom flange, and in the center of the web. At the mid-span location of the second floor beam there were gages placed on both sides of the top flange. The location of the strain gages on the floor beams is shown in Figure 4.4. Also shown in the figure are the dimensions of the wide flange section and the calculation for the section modulus of the floor beam. This section modulus (along with the modulus of elasticity) is used to convert strains to moments. This is assuming non-composite action with the centroid of the floor beam as the point of zero stress. The strain at the outside of the member is determined, assuming a linear strain distribution, by multiplying the correction factor with the strain from the gage.

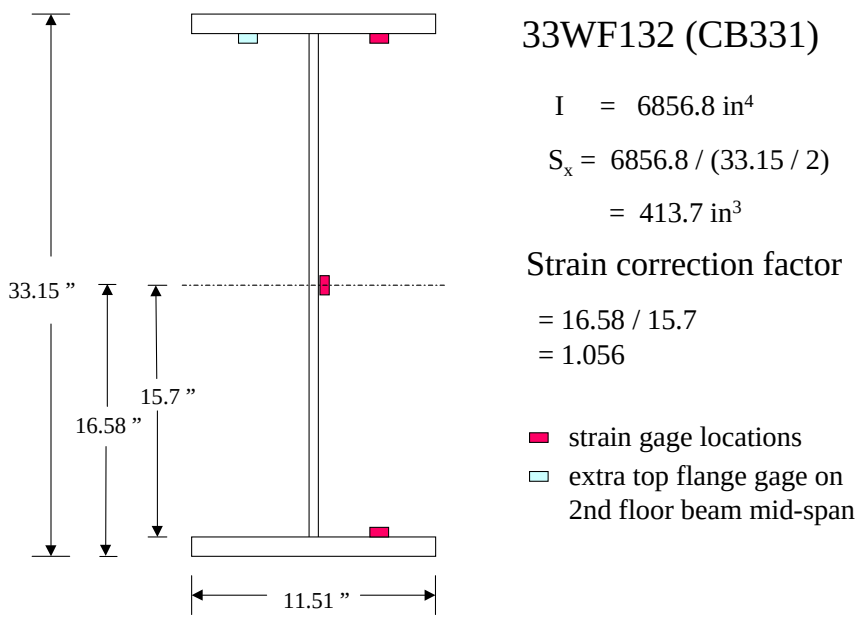


**Figure 4.4 Location of Gages on Floor Beams**

## 4.3. Truck Load

Two TxDOT dump trucks filled with sand were used in the load test of the Llano Bridge. They were almost identical in geometry and load. This made it possible to combine the trucks into one average truck for the finite element analysis. The approximate truck geometry is shown in Figure 4.5. The TxDOT vehicle is shown in Figure 4.6.

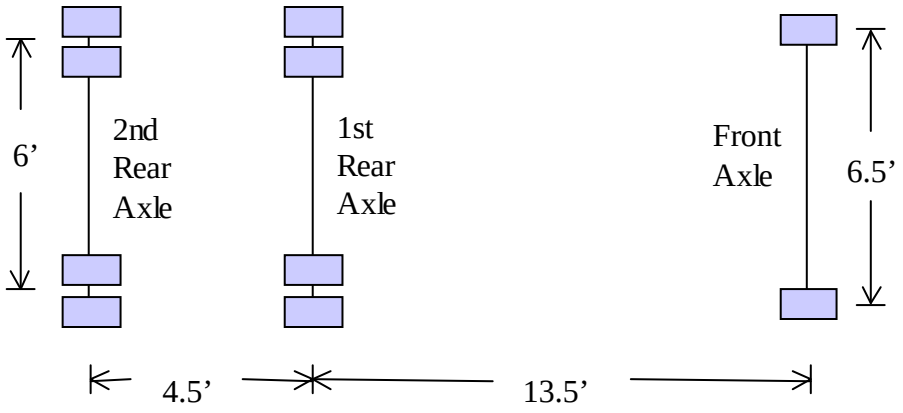


**Figure 4.5 TxDOT Truck Geometry**

**Figure 4.6 TxDOT loading vehicle**

The front axle has only two wheels, while each of the rear axles has four wheels. The total spacing of the truck is 18 feet from front to rear axle, quite a bit shorter than the 28 feet in the HS-20 model. This shorter wheel base, assuming loads of equal magnitude, would result in a higher moment in the floor beams. However, the loads are not of equal magnitude.

While there are four wheels on each of the rear axles of the loading vehicle, to simplify modeling of this truck in SAP, the pair of wheel loads on either side of the rear axles was treated as a single point loads at the centroid of the pair. These single wheel truck loads are calculated and are shown in Table 4.1. Given only the weight of the front axle and the combined weight of the two rear axles it was necessary to assume equal load distribution to the wheels. The rear tandem refers to the combined weight of the two rear axles. The final loads used in the SAP model for the Llano Bridge are shown in the final column in bold. There are two 8.66 kip loads on each rear axle spaced 6 feet apart and two 5.24 kip loads on the front axle spaced 6.5 feet apart. These trucks have a lighter load than the HS-20 trucks with a total load of approximately 45 kips as compared with 72 kips. A higher percentage of the load is also found on the front axle.

**Table 4.1 Truck Loads**

| | Truck A Weight (kips) | Truck B Weight (kips) | Average Weight (kips) | # of Wheels | Weight Per Wheel |
|---|---|---|---|---|---|
| Front Axle | 10.32 | 10.65 | 10.49 | 2 | **5.24** |
| Rear Tandem | 35.03 | 34.22 | 34.63 | 4 | **8.66** |

The trucks were run over different lateral positions on the bridge. Most of the runs had only one truck on the bridge with one of the front wheels on one of the stringer lines. Only the center run had neither front wheel on a stringer line. There were also a few runs with two trucks on the bridge. These consisted of a side by side, train, and reverse train loading cases. The side by side loading case had the trucks 4.5 feet apart, symmetric about the centerline of the bridge. This spacing was used because it puts the front center wheel of each truck on a stringer line. The train load case had the second truck following close behind the first on the center of the bridge. The reverse train run had the second truck following in reverse close behind the first in the center of the bridge. Each different run was done twice to study repeatability. The load runs of most interest in this study are the runs with two trucks on the bridge, particularly the side by side load case which is most similar to the HS-20 loading case that controls the rating of the plate girder bridges. For more detail on the load runs in the first Llano test see Appendix B.

The wheel base in the TxDOT trucks is much shorter and the front axle load is higher than in the HS-20 vehicle. Both of these facts lead to a much lower percentage of the moment coming from the wheels placed directly over the floor beam according to the direct model. Table 4.2 compares the maximum HS-20 loading case to the similar side by side loading case using TxDOT trucks using the direct load method. The wheels directly over the floor beam contribute about 50% of the total floor beam moment, while the HS-20 vehicles contribute close to

70%. Also shown in the table is that the smaller load on the bridge lead to a lower total moment despite the shorter wheel base of the TxDOT trucks.

**Table 4.2 Comparison of Moments Caused by Different Truck Types**

| Direct Load | HS-20s | | TxDOT trucks | |
|---|---|---|---|---|
| | FB Wheels | Total | FB wheels | Total |
| Moment (kip-ft) | 254.1 | 369.6 | 128.9 | 262.5 |
| % of Total | 68.8% | | 49.1% | |

## 4.4. Finite Element Model Results

The finite element models used to calculate the moments in the Llano Bridge were similar to the models used in the previous chapters. The floor system was modeled using SAP again with one-foot wide shell and frame elements. The stringers were released at the connection with the floor beams. Several different models were studied to evaluate the influence of the model size upon the results. The models analyzed were a single-span model with two floor beams, a 2-span model (3 floor beams), and a 4-span model (5 floor beams). The two-span and four-span models were modeled with the slab continuous and cracked over the floor beam.

Figure 4.7 shows the 4-span model used to calculate the moment in the floor beam due to the load applied by the TxDOT vehicle. It also shows the location of the floor beam strain gages in the finite element model. Each truss actually consists of 10 floor beams, but using more than 4 spans did not produce a difference in the models. No difference was found when the slab was modeled as cracked when more than 2 spans were used in the model. The results from the

gages located in the mid-span of the second floor beam, shown as a star in the figure are the results that will be compared with the results from the finite element models. The strains measured in the bottom flange there are converted to moment and compared with the moments predicted using finite element models. The earlier models assumed that the highest floor beam moment would occur on the middle floor beam. However, since only the first two floor beams in Llano were instrumented, these are the locations in the SAP model that were studied.

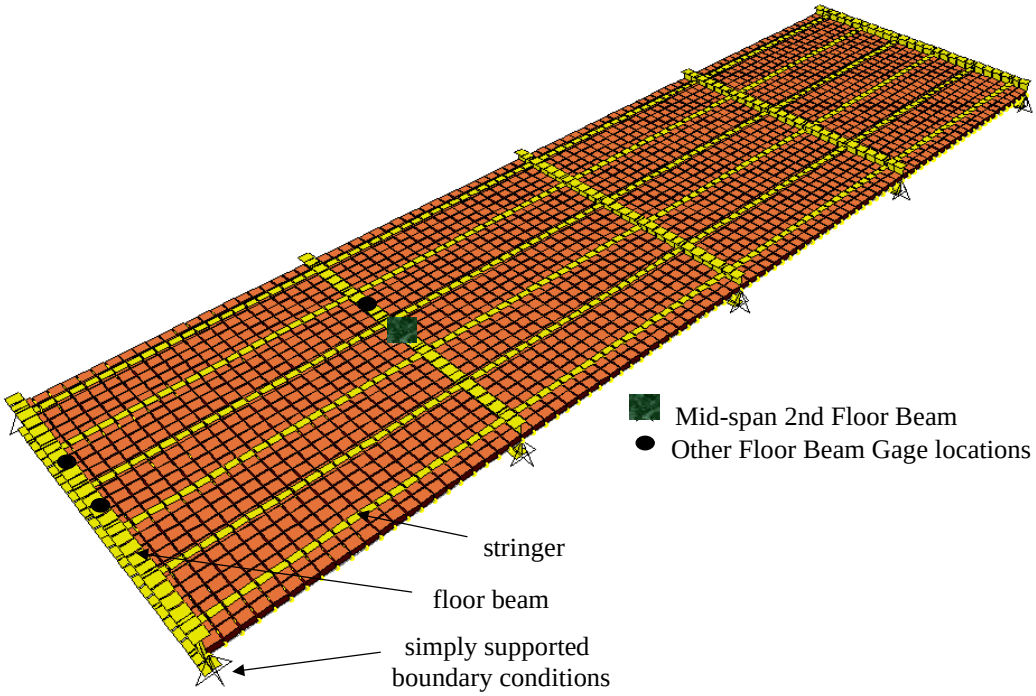


**Figure 4.7 Llano Bridge 4-span Finite Element Model**

As mentioned before, the Llano small model should be fairly similar to the previous small models that were analyzed. This is shown in Figure 4.8, which compares the influence surface of the Llano small model to a small model with

22-foot floor beam spacing and 8-foot stringer spacing. The wheels shown in the figure represent the wheels from the TxDOT vehicles used in the Llano test. The middle group of 4 wheels shown in the figure would actually be on the left side of the floor beam, but is placed on the right side in this model using symmetry. Both influence surfaces showing normalized floor beam moment have the same trends and shape. However, the Llano model has a larger value for normalized moment. That is because it has a higher floor beam moment of inertia and a lower slab modulus of elasticity. The Llano model has 33WF130 floor beams compared with 30WF108 in the plate girder model. The slab modulus of elasticity is 2850 and 3120 ksi respectively.

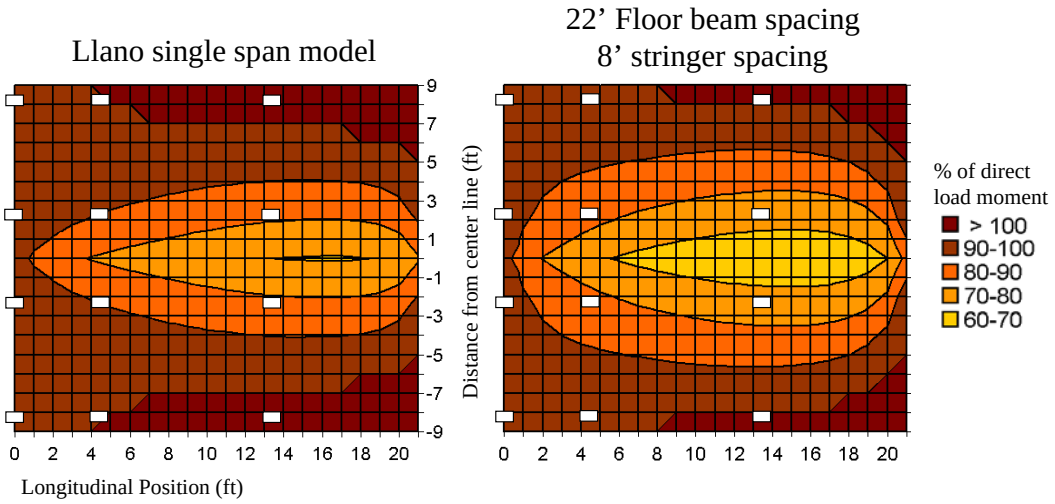


**Figure 4.8 Comparison of Llano Small Model with Plate-Girder Model**

A comparison of the different Llano model results for the side by side load case is shown in Table 4.3. The first column for each truck type is the ratio of the calculated moment divided by the direct load moment for only the truck axles

placed directly over the floor beam. The second column is the total moment of all the truck axles in the position of maximum floor beam moment. The direct load moments are shown back in Table 4.2 The axle loading is slightly smaller in the TxDOT loading model because the trucks are placed 4.5 feet apart instead of 4 feet apart. The small model has the largest prediction of total floor beam moment at almost 94% of the direct load for the TxDOT loading vehicles. The other models predict a floor beam moment in the high 80% range. The one span model has a larger moment because even though slab may be modeled as cracked over the floor beam, it still has to bend transversely as the floor beam deflects and therefore will pick up some of the moment. For the single span model, there only exists a slab on one side of the floor beam so the slab picks up less of the moment.

| Model | % of Direct Load | | | |
|---|---|---|---|---|
| | HS-20s | | TxDOT Trucks | |
| | Axle | Total | Axle | Total |
| Small model | 95.2% | 93.2% | 95.1% | 93.9% |
| 2-span continuous | 79.5% | 85.9% | 79.3% | 85.4% |
| 2-span cracked | 90.8% | 88.7% | 90.7% | 89.2% |
| 4-span continuous | 83.3% | 87.9% | 83.1% | 88.1% |
| 4-span cracked | 90.8% | 88.8% | 90.7% | 89.3% |

**Table 4.3 Comparison of Finite Element Models**

As the length of the model increases, the moment stays the same in the model with a cracked slab over the floor beam. This is different than what was shown in the plate girder models. This is because in the Llano models with a cracked slab, there is no continuity at the floor beam. In the other models, the plate-girders were continuous over the length of the bridge and there were only supports at corners of the model. When using more than two spans in the Llano

model with the cracked slab, there is no change at all in the influence surface generated. This is shown in the almost identical influence surfaces in Figure 4.9. In the other models, though, with continuous girders supported only at their ends, the girder stiffness decreased as the length increased. This led to a higher mid-span floor beam moment.

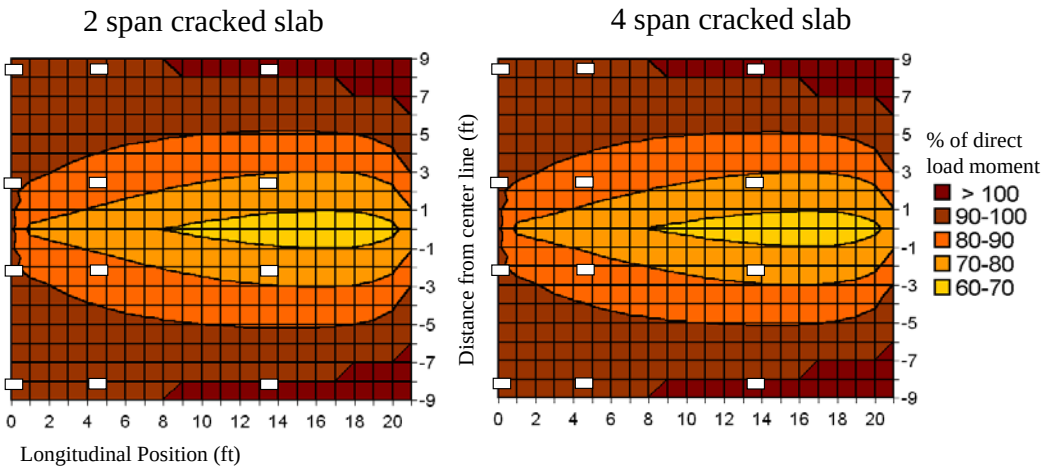


**Figure 4.9 Comparison of 2 and 4 Span Cracked Slab Models**

However, in the model with a continuous slab, the moments increase slightly as the length of the model increases. This is also different from the effect found in the earlier analysis. This effect is shown in Figure 4.10.

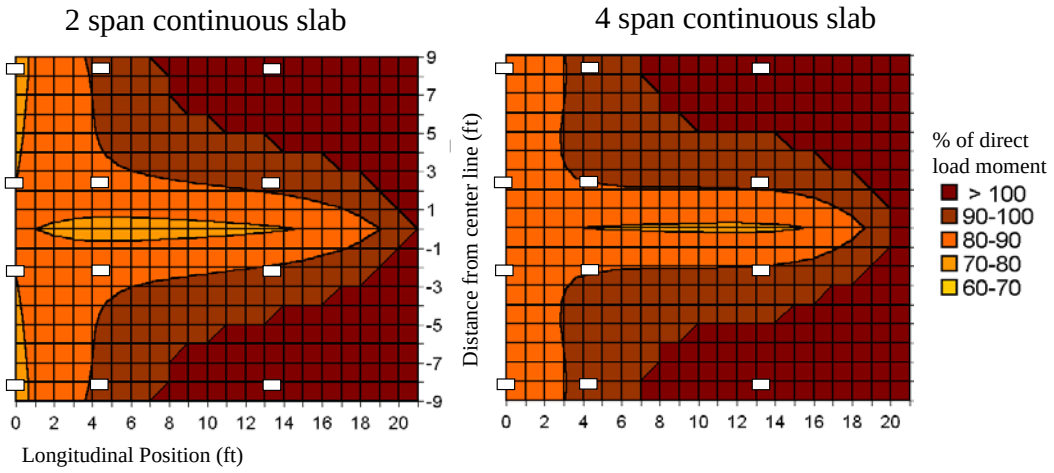


**Figure 4.10 Comparison of 2 and 4 Span Continuous Slab Models**

## 4.5. Experimental Results

The experimental results that were analyzed were from the four gage locations shown earlier. The results showed little to no composite behavior between the floor beam and the slab since the bottom flange and top flange stresses were of similar magnitude and the gage at mid-depth of the web had almost zero strain. The results from the strain gages on the first floor beam are shown for the side by side load case in Figure 4.11. This load case was repeated three times with the results shown here from Run 1b, the second run.

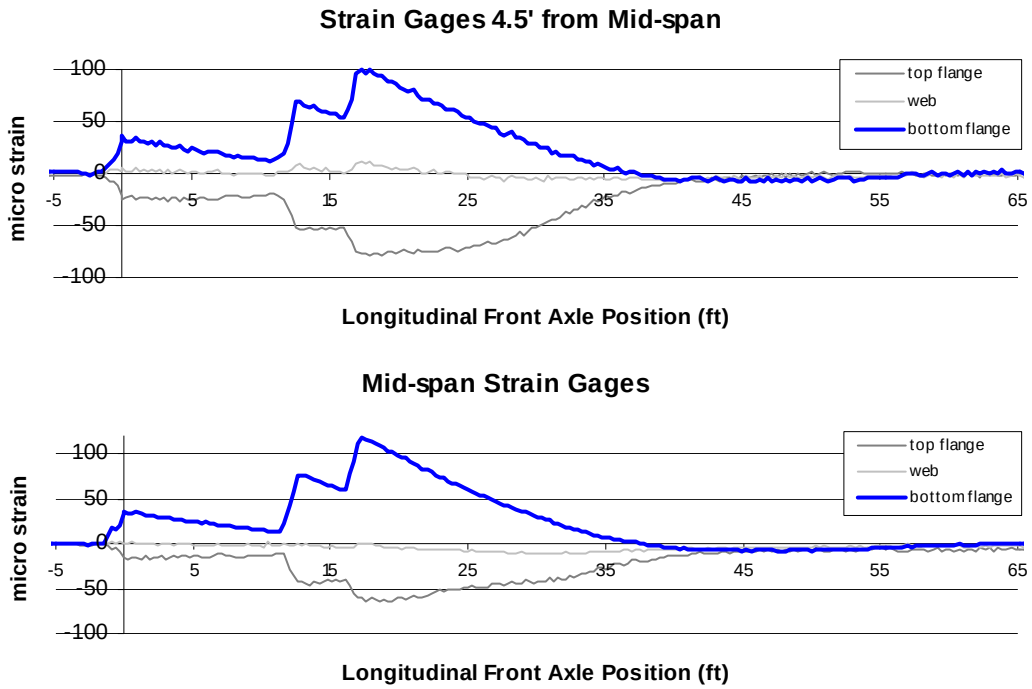


**Figure 4.11 Results from 1st Floor Beam for Side by Side Load Case**

These results show that the strain in the first floor beam has three peaks. Each peak occurs when an axle of each truck is positioned over the floor beam. The highest peak occurs when the third axle is positioned over the floor beam and the other two axles of each truck are on the same span. The plots also show that the magnitude of the bottom flange strain is slightly higher for the mid-span gage. A comparison of the top and bottom flanges of the mid-span gage would indicate some composite action, but the mid-depth gage on the web does not. However, the other location indicates almost no composite action. The results do seem to indicate that there is some continuity between spans, because the moment reverses sign as the truck moves to the next span. However, the negative moment values

as the truck moves to the next span are very small. These results can be compared with the results from the gages found on the second floor beam for the same load case, shown in Figure 4.12.

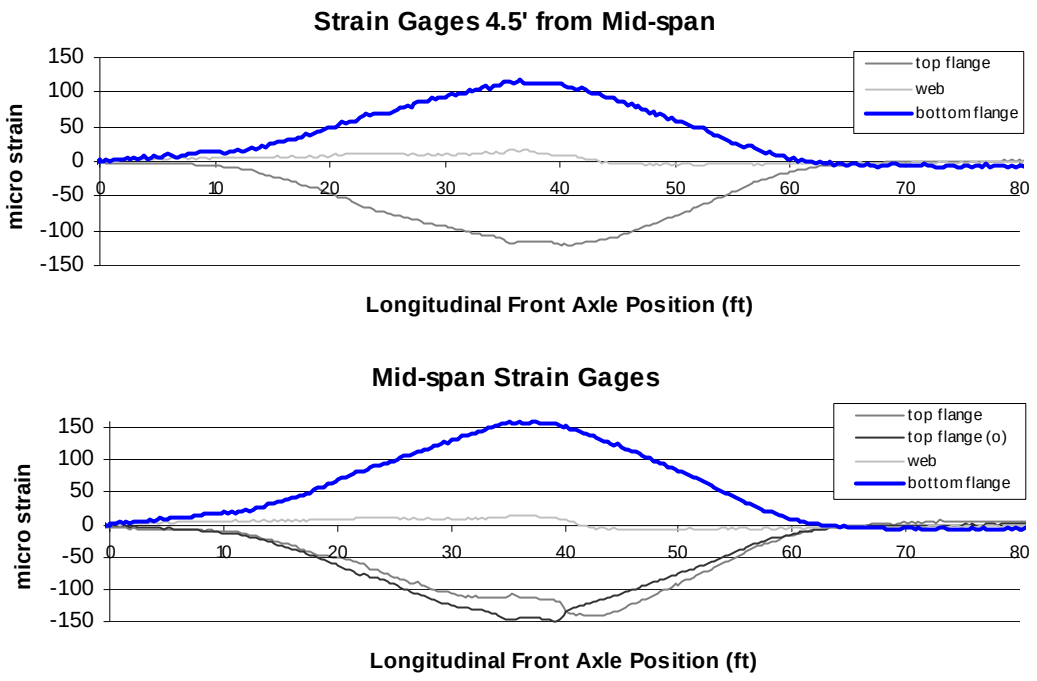


**Figure 4.12 Results from 2nd Floor Beam Gages for Side by Side Load Case**

The top flange (o) gage refers to the gage on the opposite side of the web from the other gages. However, this gage seems to give better readings than the top flange gage on the same side. The two gages gave about the same maximum strains, but the gage on the same side as the bottom gage reads a maximum strain about ten feet later than expected. This trend was repeated on every single load run. The gages on the second floor beam show a higher value for maximum strain than the same gages on the first floor beam. This trend is the same for all of the

load runs, shown in Appendix E. This is predicted by the finite element analysis as well, however this difference is larger than expected. The results from the finite element model would predict only a 6% decrease at mid-span and a 4% decrease 4.5' away. The much lower moments are in the first floor beam are probably caused by the greater amount of restraint in the 1st floor beam connection than 2nd floor beam. The two connections are shown in Figure 4.13.

**Figure 4.13 Floor Beam to Truss Connections**

These gages also show very little composite action with the top and bottom flange maximum stresses being approximately equal. The neutral axis for this floor beam was calculated and is shown in Figure 4.14. The axis is calculated from the top and bottom flange strains for the middle portion of the run where the strains are highest and the calculation is less affected by noise. The calculation was done using the top flange gage on the opposite side of the bottom flange gage because of the problem with the other top flange gage. The predicted neutral axis is located at mid-depth of the floor beam indicating non-composite action.

Appendix C shows neutral axis calculations for other load runs. In Appendix D the percent difference between the bottom flange and top flange gages is shown.

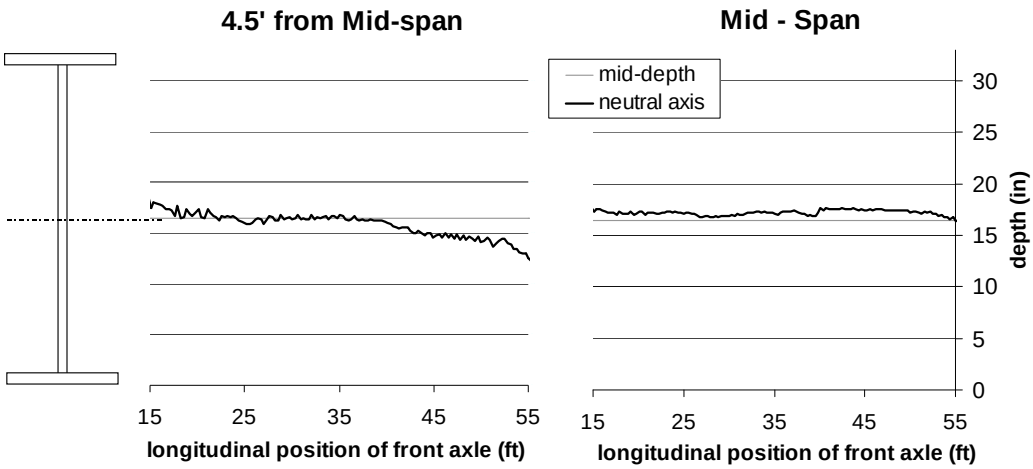


**Figure 4.14 Neutral Axis Calculation for Second Floor Beam**

## 4.6. Comparison of Results

The goal of this experimental test in this study was a comparison with the results from the finite element analysis. The comparison that is most useful is the comparison of the mid-span floor beam moment in the second floor beam. This comparison is shown in Figure 4.15. The three side by side runs are shown compared to the different models for predicting the floor beam moment.

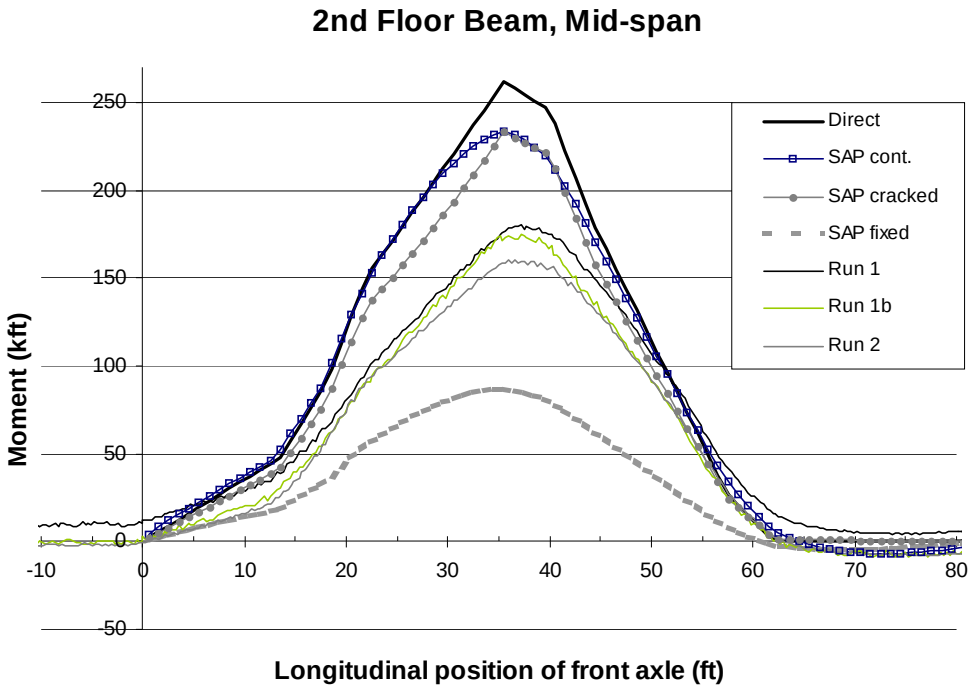


**Figure 4.15 Comparison of 2nd Floor Beam Moments**

The direct load model predicts the highest results as was shown earlier. The model identified as the SAP continuous model is a four-span model that models the slab as continuous over the floor beams. The next model, the SAP cracked model, is a four-span model with the slab modeled as cracked over every floor beam. It is evident that this model is not as smooth as the continuous model, as would be expected. These two models, however, have a similar value for maximum moment, with the continuous model only slightly higher. The fourth analytical model, called SAP fixed, is a model that treats the floor beam to truss connection as a fixed support instead of a pinned support. This moment is significantly less than the models with pinned supports.

On these three experimental runs, the agreement between the runs was not as good as it was for the other load runs. The other runs are shown in Appendix F. Run 1 did not start at or return to zero. This would indicate that the gage was not properly zeroed before the run began. In Run 2, one of the trucks was about a foot and a half in front of the other, which produced the additional peaks in the data taken at the first floor beam shown in Figure 4.16. Instead of three peaks, there were six. Run 1b gives the best estimate for floor beam moment due to two trucks placed side by side.

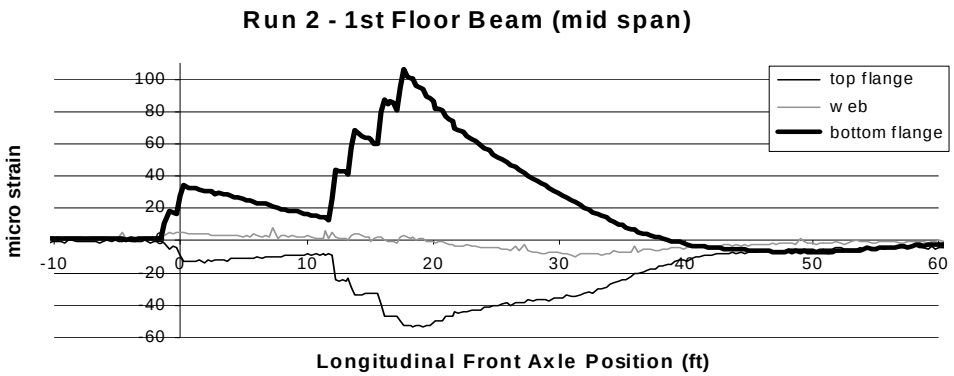


**Figure 4.16 Two Trucks out of Alignment in Run 2**

The experimental runs have the same general shape as the analytical models, although they seem to follow the smoother pattern of the continuous model. This and the fact that there is a slight sign reversal as the load passes over the floor beam indicates that there is some continuity over the floor beam. However, from inspection of the Llano bridge it was evident the there were cracks over the floor beams as shown in Figure 4.13. The cracks may not go to full

depth of the concrete and the stringer to floor beam connections may have some fixity as well.

**Figure 4.17 Cracked Slab over Floor Beam**

Table 4.4 shows the comparison of the different models for each load case. It compares the calculated moments from the experimental test with both the SAP cracked model and to the direct load model. Shown in the third column is the transverse position of the center of the truck load on the bridges (zero for a symmetrical load). Shown in the fifth column of the table is the longitudinal location of the truck in each experimental run that produced the maximum moment in the floor beam. The load cases with 1 truck or the two trucks side by side should have the maximum moment occur when the middle axle is on the floor. This means that the front axle is 35.5 feet onto the bridge. The average occurrence of the maximum value for the experimental runs is about 1 foot later at 36.6 feet. What this value may mean is that the rear axles of the truck are actually a little bit heavier than the middle axle, so the maximum moment actually occurs slightly after the middle axle crosses the floor beam, when the rear axle is closer.

**Table 4.4 Comparison of Analytical and Experiment Results**

Also, the method in which truck position is estimated on the experimental run has an error of +/- 0.3 feet. Truck position is estimated by manually closing a switch as the truck passes over a known location. This interrupts the excitation making it possible to determine when the truck is located in a known location. In the Llano test, these "clicks" were spaced 11 feet apart. Interpolation is used to determine the truck position between these various locations. This interpolation assumes a constant truck speed. There can be a slight error in manually closing the switch or in the interpolation due to a changing truck speed. Each data point represented about 0.3 ft of truck movement.

Another trend noticed both in Table 4.4 and in Figure 4.15 is that the moments from the experimental runs were significantly lower than the first three analytical models, but higher than the SAP model with using fixed boundary conditions. These experimental values for the second floor beam mid-span location were between 65% and 80% of the values predicted by the SAP cracked model. This indicates that the floor beam connection with the truss is somewhere between fixed and pinned. All connections are somewhere between perfectly fixed and perfectly pinned, but the degree of fixity is hard to determine. Unfortunately the floor beam was not instrumented more thoroughly in this first test to have a better understanding of the moment diagram of the floor beam.

Also, if the concrete has a modulus of elasticity higher than the value of 2850 ksi that was assumed for the analysis, this also would lead to a lower floor beam moment. That is because the slab would carry more of the moment. The

value of 2850 ksi assumes of compressive strength of 2500 psi. The concrete is probably much stronger than this estimated value.

## 4.7. Second Experimental Test

The second load test of the Llano bridge took place about 2 months later on the 15th of April 1999. The goals of this test were to demonstrate repeatability and to come to a better understanding of why the forces in the members were significantly lower than the finite element results indicated. In this test, the second floor beam would be more fully instrumented to get a better understanding of the fixity of the connections.

### 4.7.1. REPEATABILITY OF TEST

To determine if the test demonstrates repeatable results every effort was made to keep all field conditions the same for both tests. Gages were placed in many of the same locations as the first test and the same runs were repeated. For both tests to have the same results, the loading vehicles would have to be the same as well.

The trucks used in the second experimental test had the same geometry as the trucks from the first test, but the weights were not the same. The difference in truck weights is noticeable in the experimental results. The truck weights used in the second test are shown in Table 4.5. The weight of the rear tandem of Truck B is about 5% less than Truck A. The weight of Truck A is almost exactly the same as the weight of the average vehicle from the first run. Therefore, the maximum

floor beam values predicted by the first test should coincide with the values from Truck A. The values from the Truck B should be about 5% lower.

**Table 4.5 Comparing Truck Weights From Both Tests**

| | 1st Test Avg. | Truck A | Truck B | % less than A |
|---|---|---|---|---|
| Front Axle | 10.49 | 10.46 | 10.22 | 2.3% |
| Rear Tandem | 34.63 | 34.44 | 32.78 | 4.8% |
| Total | 45.11 | 44.90 | 43.00 | 4.2% |

The results from both tests were very similar, as shown in Table 4.6 and Table 4.7. These tables compare the maximum calculated moments from the same load runs on both tests. The load runs that are compared are the side by side load run and the load run with a single truck on the center of the bridge. Both runs being examined are symmetric about the center of the bridge in order to check lateral symmetry. The first column in both tables tells which floor beam the gage is mounted on and the distance the gage is from the mid-span of the floor beam.

**Table 4.6 Maximum Moment Comparison for Side by Side Load Case**

| Gage Location | Maximum Moments (kip-ft) | | |
|---|---|---|---|
| Floor Beam # | 1st Test | 2nd Test | |
| (distance from mid-span) | Run 1b | Run 0 | Run 1 |
| 2nd (0) | 174.5 | 176.7 | 181.6 |
| 2nd (4.5) | 128.8 | 140.0 | 141.2 |
| 1st (0) | 127.9 | 118.9 | 124.74 |
| 1st (4.5) | 110.3 | 102.9 | 113.94 |

**Table 4.7 Maximum Moment Comparison for Single Truck in Center**

| Gage Location | Maximum Moments (kip-ft) | | |
|---|---|---|---|
| Floor Beam # | 1st Test | 2nd Test | |
| (distance from mid-span) | Average | Truck A | Truck B |
| 2nd (0) | 111.7 | 124.3 | 116.3 |
| 2nd (4.5) | 80.3 | 94.7 | 91.9 |
| 1st (0) | 86.9 | 86.1 | 82.0 |
| 1st (4.5) | 76.3 | 77.3 | 72.3 |

The moment comparisons of the two tests demonstrate the repeatability of the moments. The values for floor beam moment from the two tests are fairly consistent. Run 0 and Run 1 in Table 4.6 should be the same as each other and slightly less than the values from the first test. However, the noise level of the second floor beam, mid-span gage caused the slight increase in the calculated moment from the first test to the second test at that location. Also, the gage located 4.5 feet away from the center of the second floor beam gave a moment that was 10 to 15% higher in the second test for some unknown reason. Also, in Table 4.7, moment values for Truck B are around 5% less than for the Truck A run, consistent with the decrease in the weights of the rear axles.

### 4.7.2. FLOOR BEAM MOMENT DIAGRAM

To have a better understanding of the floor beam moment diagram, the floor beams were more thoroughly instrumented in the second test than in the first test. Figure 4.18 shows the SAP model of two stringer spans of the bridge with the gage locations employed in the both load tests. In the first test the floor beams were instrumented in four locations as shown by the stars in the figure. Four locations were added in the second test to determine the moment diagram of the

floor beam and to check on the symmetry about its centerline. All gages are located mid-way between the stringer connections, 4.5 feet apart. All locations have gages at the top flange, mid-depth of the web, and at the bottom flange, the same as the first test. Other gages were placed at other depths, but many were very noisy and the results were not useful.

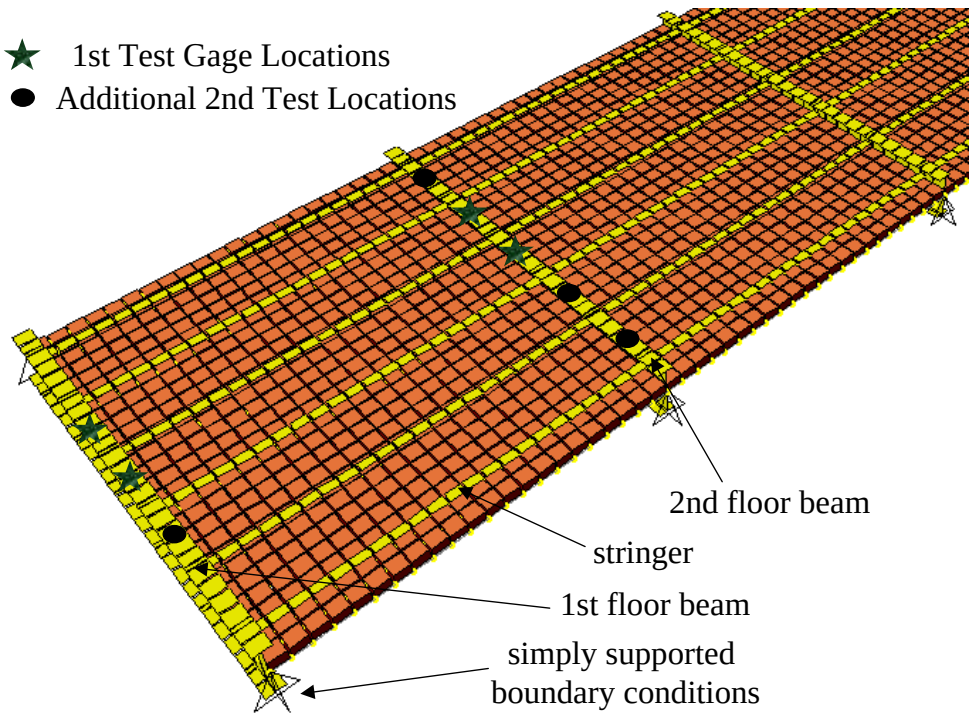


**Figure 4.18 Location of Gages in Both Load Tests**

In the first test, only two locations along each floor beam were instrumented so it was impossible to generate an accurate picture of the moment diagram from two points. The second floor beam was instrumented in 5 different locations to get a more accurate representation of the moment diagram. That moment diagram for the load case with Truck A running over the transverse

center of the bridge is shown in Figure 4.19. Also shown in the figure are the moment diagrams for the direct load moment diagram and the moment diagram from a SAP analysis. Moment diagrams for other load runs are shown in Appendix H. The moment diagrams shown occur when the truck is positioned with its center axle over the second floor beam. The x-axis in the figure shows the distance from the center of the floor beam. As was mentioned previously, the values for the bending moment in the floor beam in the SAP model are around 85 to 90% of the direct load moment values. It is also evident that there is more lateral load distribution in the SAP model, because the moment diagram is more rounded than the moment diagram for the direct load model. At mid span of the floor beam, the experimental value for moment 76% of the SAP value and 67% of the direct load value.

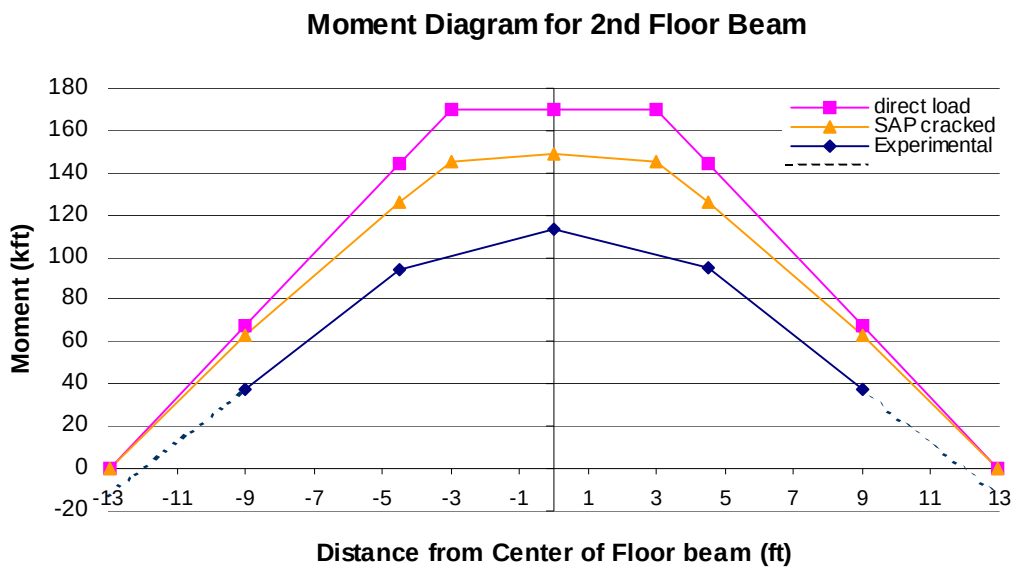


**Figure 4.19 Moment Diagram for 2nd Floor Beam, Center Run, Truck A**

It is hard to determine the amount of fixity in the connections from this moment diagram. However, it is possible to get an idea as to whether there is some fixity or not. In Figure 4.19, a straight line is drawn between the points at 4.5 feet and 9 feet and extended to the location of the connection at 12.94 feet. The same thing is done on the other side. The extensions are shown as broken lines in the figure. If there were no restraint provided by the connection, the line would terminate at zero moment at the location of the connection. However, from the figure, it is evident that there may be restraint in the connections. Using the extended line, the predicted moment at the connections is approximately -13 kip-ft, about 10% of the maximum moment.

Figure 4.20 illustrates what the moment diagram would look like if the average amount of these two values were added to the entire moment diagram. The moment diagram is still only 85% of the moment diagram for the SAP model. The remaining 15% difference between the experimental model and the SAP model is probably caused by underestimating the stiffness of the slab in the SAP model. The slab is probably thicker than the 6.5 inches due to overlays and the modulus of elasticity is probably higher than 2850 ksi based on the compressive strength specified in the plans. Both factors would cause the slab to carry a higher percentage of the moment, thereby reducing moment in the floor beam.

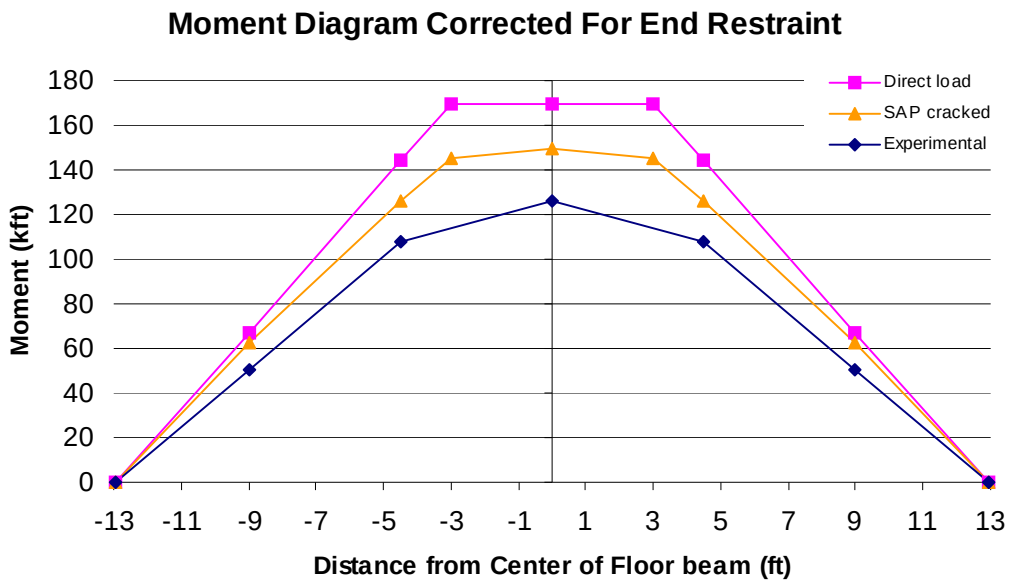


**Figure 4.20 Moment Diagram Without Restraint for Center Run, Truck A**

## 4.8. Conclusions from the Experimental Test

The experimental test of the bridge located in Llano demonstrated that the floor beam moments due to a truck load on the bridge are much smaller than the moments predicted by the direct load method. The moments are also significantly smaller even than the moments predicted by the finite element models. This can likely be attributed to the fixity of the floor beam to truss connections and underestimation of slab stiffness in the finite element model.

The experimental test does demonstrate that the moment values predicted by the finite element model are conservative compared with the actual moments seen in the bridge. This means that even though the moments from the finite element models may not match the experimental values, they give a better

estimate of the actual forces in the floor beam than the direct load model. The dissertation of Charles Bowen, a work in progress will contain much more information about the Llano bridge tests. The dissertation of David Jauregui, also a work in progress, will describe the data acquisition system and instrumentation procedures in detail.

# CHAPTER 5

# DETERMINING FLOOR BEAM REQUIREMENTS

## 5.1. Limit State Design

The rating system used to determine the capacity of bridges has changed since AASHTO moved from Allowable Stress Design in favor of Limit State Design. Limit State Design includes both Load Factor Design (LFD) and Load and Resistance Factor Design (LRFD). In both specifications, to determine if the floor beam meets the necessary requirement for moment, the allowable moment, $M_n$ (multiplied by a resistance factor in LRFD), must be greater than or equal to the required moment, $M_u$ as shown in Equation 5.1. The required moment is determined for a number of different limit states, which require different load factors.

$$\phi M_n \geq M_u \tag{5.1}$$

## 5.2. Required Moment

The right side of Equation 5.1 is the required moment. It is the sum of the moments caused by each type of load on the bridge multiplied by a load factor unique to that type of load. The required moment is computed from one of two provisions discussed in the following section.

### 5.2.1. LOAD & RESISTANCE FACTOR DESIGN

Load & Resistance Factor Design, or LRFD, is the most recent provision to determine the required moment for a bridge member.[5] There are many different limit states that must be checked to determine the required moment. However, only the Strength I Limit State, shown in Equation 5.2, will be examined. Strength I, the "basic load combination relating to the normal vehicular use of the bridge without wind", most often determines the required strength of the floor beam.

$$M_u = 1.75(LL + IM) + 1.5DW + 1.25DC \tag{5.2}$$

The live load in LRFD includes both the lane loading and the truck loading. The lane loading used by LRFD consists of a uniform load of 0.064 ksf distributed over the length of the bridge longitudinally and over a ten foot width transversely. This lane load does not include any concentrated loads and must correspond in lateral position with the truck load. That is, if the trucks are off center by one foot, the lane loads must be as well. There should always be a two foot space between the lane loads. The impact factor of 1.33 is applied to the truck load but not the lane load. The dead load is divided into the load from the wearing surface and utilities, DW, and the load from the components and attachments, DC. For the floor beam analysis, DC would is the load from the stringers and floor beams, while DW would is the load from the 6.5 inch concrete slab.

### 5.2.2. LOAD FACTOR DESIGN

Load Factor Design, the specification prior to the introduction of AASHTO-LRFD, is also still used today.[6] The LFD provision for required strength is shown in Equation 5.3. In this specification, either the lane load or the truck load is used as live load, but not both. Because of this fact there is a larger factor, about 2.17, on the live load in the LFD equation. For the bridges in this study, the truck load will always control the floor beam rating. Only for longitudinal members in longer span bridges will the lane load control. Also, the same load factor of 1.3 is applied to all dead load moments regardless of whether the moments are caused by the wearing surface or steel components in the LFD equation.

$$M_u = 1.3(DL + 1.67(LL + IM) \tag{5.3}$$

## 5.3. Allowable Moment

The left side of Equation 5.1 is the allowable moment. This determines the resistance of the floor beam to moment. The equation to determine the allowable moment in the LRFD specification is shown in Equation 5.4. This equation is 6.10.4.2.6a-1 from the AASHTO-LRFD manual.[5] Since the floor beams in this study are not hybrid girders, the factor $R_h$ is 1. A conservative estimate of $C_b$=1 is used in this study. $I_{yc}$ is the moment of inertia of the compression flange about the vertical axis in the plane of the web and "d" represents the depth of the floor beam. The unbraced length of the compression flange, $L_b$, in this case is the stringer spacing. That is because the stringers brace the compression flange, which in this case is the top flange. Because of the

relatively small unbraced length, this equation is governed by yield moment, $M_y$. The resistance factor used in the LRFD specifications for yield moment is 1.

$$M_n = 3.14EC_bR_h\left(\frac{I_{yc}}{L_b}\right)\sqrt{0.772\left(\frac{J}{I_{yc}}\right)+9.87\left(\frac{d}{L_b}\right)^2} \le R_hM_y \qquad (5.4)$$

## 5.4. Bridge Rating Example

To demonstrate the use of these equations, a bridge from the study will be examined in detail. The bridge under consideration is located in Polk County. It carries US Highway 59 over the Trinity River and is Bridge 8 from Chapter 3. The cross section of the bridge is shown in Figure 5.1. Shown in the figure are the dimensions of the floor system. The stringers are spaced 8 feet apart and the floor beams are spaced 22 feet on center. Also notice that there is a two inch gap between the floor beam and the slab indicating that the all of the load transferred from the slab to the floor beam must go through the stringers. The floor beam on this bridge did not rate sufficiently according to the current LRFD provisions. We will look at these provisions in relation to this bridge in more detail in this chapter. The bridge, designed for an H-20 loading, will be analyzed for the same loading.

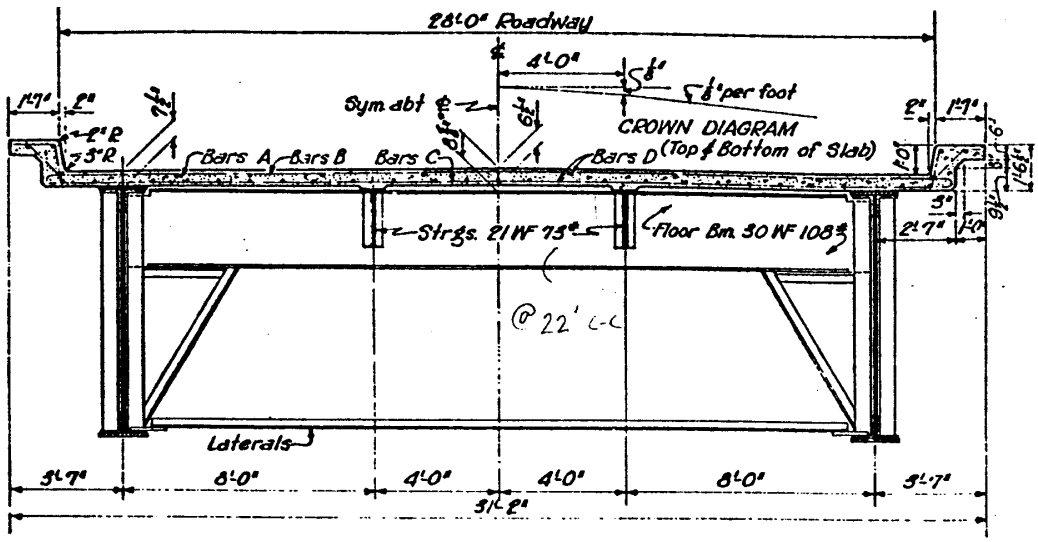


**Figure 5.1 Cross Section of Trinity River Bridge**

### 5.4.1. RATING FOR LRFD AND LFD

#### 5.4.1.1. Allowable Moment

The first step is to compute the allowable moment of the floor beam. The properties of the 30WF108 section along with the properties of the other floor beam sections are shown in Table 5.1.

**Table 5.1 Properties of Floor Beam Sections**

| Section | D (in) | $I_{yc}$ ($in^4$) | $B_f$ | $S_x$ ($in^3$) | J ($in^4$) | $M_y$ kip-ft |
|---|---|---|---|---|---|---|
| 24W76 | 23.91 | 41.22 | 8.99 | 175.4 | 2.68 | 526.2 |
| 27W94 | 26.91 | 62.06 | 9.99 | 242.8 | 4.03 | 728.4 |
| 27W98 | 27 | 66 | 10.00 | 255.3 | 4.6 | 765.9 |
| **30W108** | **29.82** | **72.98** | **10.48** | **299.2** | **4.99** | **897.6** |

The calculation for allowable moment according to the LRFD specification is shown in Equation 5.5. Because the unbraced length of the compression flange is small, the allowable moment is actually equal to the yield moment. The yield moment is calculated assuming a steel yield strength of 36 ksi. Since the resistance factor for flexure is equal to 1.0, the resulting $M_n$ from the equation is the allowable moment.

$$M_n = 3.14 * 29000 * 1 * 1 * \left(\frac{72.98}{96}\right) * \sqrt{0.772\left(\frac{4.99}{72.98}\right) + 9.87\left(\frac{29.82}{96}\right)^2}$$

$$= 69580\, k \cdot in = 5800\, k \cdot ft \geq 897.6\, k \cdot ft \quad \therefore Mn = 897.6\, k \cdot ft \qquad (5.5)$$

#### 5.4.1.2. Required Moment

To determine the required moment of the floor beam it was necessary to find the moment due to each type of load and apply a load factor for each different type of load. Figure 5.2 shows the floor beam moment caused by a pair of H-20 trucks according to the direct load method. The 16-kip loads directly over the floor beam are added to the percentage of the 4-kip loads that are longitudinally distributed to the floor beam using statics. H-20 trucks are used because that is the load that the bridge was rated for originally. The lanes are offset by one foot to produce the maximum moment. The trucks are always positioned two feet away from the edge of the lane as shown in the figure. Results for the HS-20 loading are shown later in the chapter.

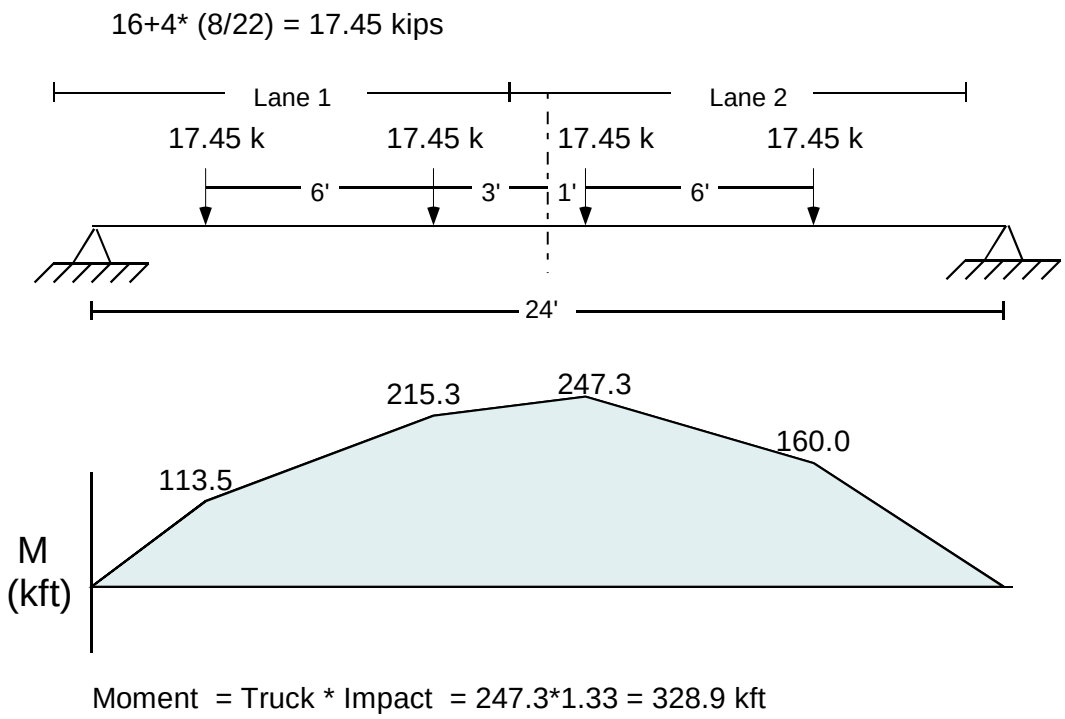


Moment = Truck * Impact = 247.3*1.33 = 328.9 kft

**Figure 5.2 H-20Truck Moment Calculation Using Direct Load**

The lane load moment is calculated using the same 12-foot lanes as the truck load. There is a minimum of one foot between the edge of the lane and the distributed lane load. This results in the two 10-foot lanes spaced 2 feet apart. The calculation for the moment caused by lane load is shown in Figure 5.3. The distributed load on the floor beam from the lane load is calculated by multiplying the 0.064 ksf lane by the tributary width of 22 ft.

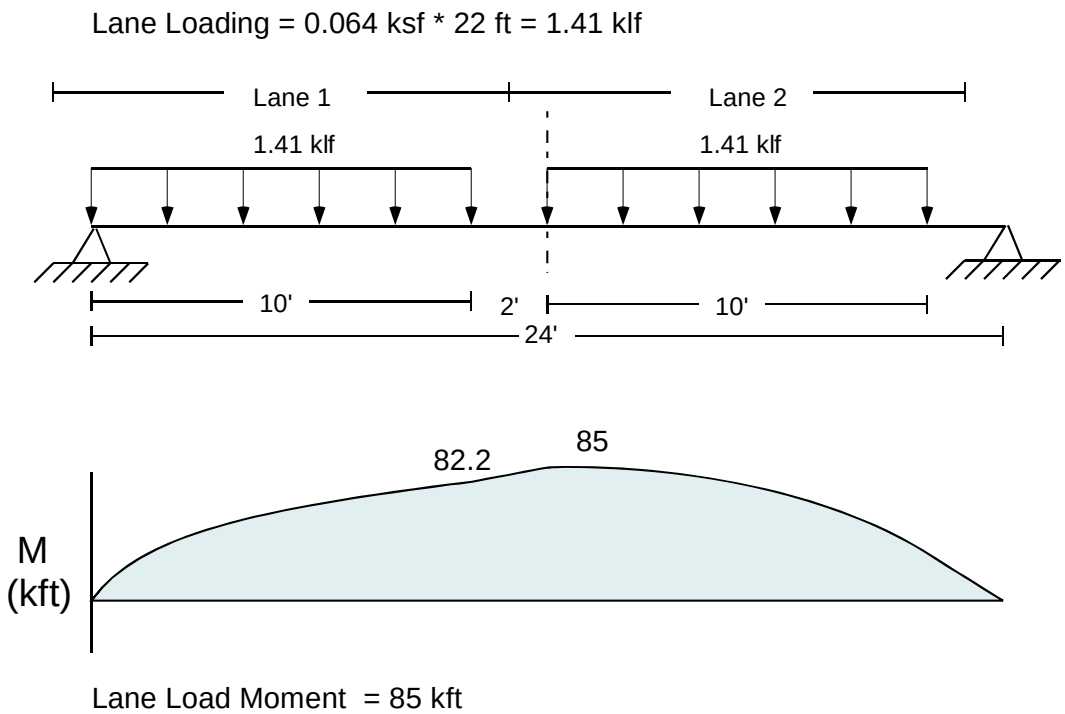


**Figure 5.3 H-20 Lane Loading Moment Using Direct Load**

The loads from the slab, stringers, and floor beam can easily be calculated using statics. The load from the slab is treated as a distributed load on the floor beam. The moment values from the different loads are shown in Table 5.2. The load factors for both LFD and LRFD are then used to calculate the total required moment for each specification. Notice the high percentage of the moment supplied by the truck loading in both specifications. This is the reason most of this research has gone into determining if the method for distributing the truck load is accurate. With an allowable moment of 897.6 kft, this floor beam does not meet the specifications using either design method. The under-strength is around 1% for the LFD method and 5% for the LRFD method.

| | $M_i$ (kft) | LFD | | LRFD | |
|---|---|---|---|---|---|
| | | $\gamma_i$ | $\gamma_i M_I$ | $\gamma_i$ | $\gamma_i M_I$ |
| Slab | 128.7 | 1.3 | 167.3 | 1.5 | 193.1 |
| Stringers | 12.8 | 1.3 | 16.7 | 1.25 | 16.1 |
| Floor beams | 7.8 | 1.3 | 10.11 | 1.25 | 9.7 |
| Lane | 85 | 0 | 0 | 1.75 | 148.8 |
| Truck + IM | 328.9 | 2.171 | 714 | 1.75 | 575.5 |
| Sum | | | **908** | | **943.2** |

**Table 5.2 Calculation of Required Moment**

### 5.4.2. RATING USING ALLOWABLE STRESS DESIGN

The TxDOT approach is taken from the 1988 TxDOT bridge rating manual.[4] The basic rating equation, shown below follows an allowable stress approach. The allowable load is determined by using 55% of the yield stress as the allowable stress in the member for the inventory rating and 75% of the yield stress for the operating rating. In this study, only the inventory rating will be examined.

$$H - Rating = H - \left[ 20 * \frac{M_{all} - M_{DL}}{M_{LL}\,(H - 20\,Vehicle)} \right] \tag{5.6}$$

TxDOT uses the information shown in Table 5.3 to compute the allowable moment, $M_{all}$. To determine the load rating allowable stress is rounded to a value and a correction is made with respect to the unbraced length. The rounded value of allowable stress is represented by A while the correction for unbraced length is represented by B in Table 5.3 and in Equation 5.7. The allowable moment is then

calculated by multiplying the allowable stress in the floor beam, $F_b$, by the section modulus, $S_x$.

**Table 5.3 TxDOT Table to Compute Allowable Stress for Inventory Rating**

| $F_y$ (ksi) | 0.55 $F_y$ (ksi) | Rounded Allowable A | Bracing Factor B |
|---|---|---|---|
| 26 | 14.3 | 14.0 | 0.0039 |
| 30 | 16.5 | 16.0 | 0.0052 |
| 33 | 18.1 | 18.0 | 0.0063 |
| **36** | **19.8** | **20.0** | **0.0075** |
| 45 | 24.7 | 24.0 | 0.0117 |
| 50 | 27.5 | 27.0 | 0.0144 |
| 55 | 30.3 | 30.0 | 0.0174 |

$$F_b\,(Inventory) = A - B\left(\frac{L_b}{b_f}\right)^2 \quad \rightarrow \quad M_{all} = F_b \cdot S_x \tag{5.7a}$$

$$F_b\,(Inventory) = 20 - 0.0075 \cdot \left(\frac{8 \cdot 12}{10.48}\right)^2 = 19.3\ ksi \tag{5.7b}$$

$$M_{all} = \frac{19.3 \cdot 299.2}{12} = 481.2\ k\ ft \tag{5.7c}$$

The live load moment is determined using the direct load method for an H-20 or HS-20 loading vehicle. The live load used in this equation is also multiplied by a smaller impact factor that has a maximum value of 1.3. The dead load is also determined using the direct load method. However, all dead load is treated as a distributed load over the length of the floor beam. This is appropriate for the self-weight of the floor beam. However, the weight from the stringers should be treated as concentrated loads at the connection to the floor beam. If the slab were in contact with the floor beam, it would be appropriate to treat the weight of the slab as a distributed load over the floor beam. However, if the slab weight is all transferred through the stringers, it should be included in the stringer

reactions on the floor beam. Using the moment values determined previously, and shown in Table 5.2, the calculation of dead load moment is shown in Equation 5.8a. Equation 5.8b shows the calculation of the live load moment and Equation 5.8c shows the final rating value for the floor beam using allowable stress design.

$$M_{DL} = M_{slab} + M_{st}r + M_{FB} = 128.7+12.8+7.8 = 149.3\ kft \tag{5.8a}$$

$$M_{LL} = H\text{-}20\ Load * Impact\ Factor = 247.3*1.3 = 321.5\ kft \tag{5.8b}$$

$$H - Rating = H - \left[20 \cdot \frac{481.2 - 149.3}{321.5}\right] = \boldsymbol{H - 20.6} \tag{5.8c}$$

Because the rating is greater than H-20, the floor beam meets the requirements for an H-20 loading. Therefore, if the live load from the direct load model were used, the floor beam would meet the specifications following the ASD provisions, but not the provisions from LFD or LRFD.

### 5.4.3. RATING USING THE LEVER RULE

If there is no contact between the floor beam and the slab, the lever rule is a more appropriate way to rate the floor beam. It is still a conservative estimate, though, because a higher percentage of the load is attracted to the stiffer outside girder, thereby causing less moment in the mid-span of the floor beam. This was demonstrated using finite element modeling.

The lever rule affects the way both live load and dead load moments are calculated. The dead load affected is the load from the slab. Instead of

calculating the dead load from the slab as a uniformly distributed load along the floor beam, the dead load from the slab can be treated as point loads at the location of the stringer connections. Moving the load away from the mid-span of the floor beam toward the stringer connections reduces the moment due to the slab weight.

Both the lane load and truck load moment are affected by using the lever rule. The lever rule actually slightly increases the value of the lane moment because instead of being uniformly distributed along 2 ten-foot widths, it is transmitted through point loads at the stringer connections. The difference between the lane loading and slab dead load is that the lane loads do not occur over the entire 24 feet and are placed eccentrically on the bridge to match the truck loads. The lane load has no effect on the LFD method or ASD method because truck loading controls those specifications.

Using the lever rule instead of the direct load model significantly reduces the moments from the design truck, which make up the largest percentage of the total moment. The lever rule, as shown in Chapter 3, reduces the maximum moment, independent of the floor beam spacing, to 89.4% of the direct load moment. This same value was calculated with the floor beam spacing anywhere from 6 feet to 12 feet. The range of floor beam spacing in Texas is from 7 to 8 feet. The 0.894 factor then could be applied to all bridges with this geometry rather than recalculating the lever rule moment. Using the new moment values for the slab, lane, and truck loads, the calculations for required moment are shown in Table 5.4. Notice that using the lever rule, the allowable moment of 897.6 kip-ft

is now greater than the required moment using both the LRFD and LFD specification.

**Table 5.4 Calculation of Required Moment Using Lever Rule**

| | $M_i$ (kft) | LFD | | LRFD | |
|---|---|---|---|---|---|
| | | $\gamma_I$ | $\gamma_i M_I$ | $\gamma_I$ | $\gamma_i M_i$ |
| Slab | 114.4 | 1.3 | 148.7 | 1.5 | 171.6 |
| Stringers | 12.8 | 1.3 | 16.7 | 1.25 | 16.06 |
| Floor beams | 7.8 | 1.3 | 10.1 | 1.25 | 9.72 |
| Lane | 89.2 | 0 | 0.0 | 1.75 | 156 |
| Truck + IM | 294.0 | 2.17 | 638.0 | 1.75 | 514.5 |
| Sum | | | **813.5** | | **868** |

### 5.4.4. RATING USING FINITE ELEMENT RESULTS

If the slab is in contact with the floor beam, the simple lever rule could not be applied as easily. The floor beam moment diagram would have to include the effects from load transmitted directly to the floor beam. Because the truck used to rate this bridge is an H-20 and not an HS-20, most of the load is positioned directly over the floor beam. Because of this there is not as much distribution of the H-20 truck load. However, the slab does take some of the moment. Using the small model, which is conservative in most cases, the reduction would depend only on the floor beam to slab ratio. The calculation for live load is shown in Equation 5.9. Using the trend developed in Chapter 3 for a 6.5-inch slab the live load is then multiplied by the factor determined from the equation.

$$M_{LL} = M_{direct} \cdot \left( 0.08 \ln(\frac{EI_{FB}}{EI_{slab}}) + .52 \right) \tag{5.9a}$$

$$M_{LL} + IM = 1.33 \cdot \left[ 247.3 \cdot \left( 0.08 \ln\left( \frac{4470 \cdot 29000}{275 \cdot 3120} \right) + 0.52 \right) \right] = 303.1\, kft \tag{5.9b}$$

Table 5.5 shows the how this factor affects the overall rating of the bridge. Both of these values are slightly larger than the lever rule but smaller than the direct load method. Notice that the LFD required moment is well under the allowable moment using this provision and the LRFD required moment is now less than 0.1% too high. A more detailed finite element model could be used in this case to get a more exact value for the floor beam moment.

**Table 5.5 Calculation of Required Moment Using Equation 5.9**

| | $M_i$ (kft) | LFD | | LRFD | |
|---|---|---|---|---|---|
| | | $\gamma_I$ | $\gamma_i M_I$ | $\gamma_I$ | $\gamma_i M_i$ |
| Slab | 128.7 | 1.3 | 167.3 | 1.5 | 193.05 |
| Stringers | 12.8 | 1.3 | 16.7 | 1.25 | 16.06 |
| Floor beams | 7.8 | 1.3 | 10.1 | 1.25 | 9.72 |
| Lane | 85.0 | 0 | 0.0 | 1.75 | 148.75 |
| Truck + IM | 303.1 | 2.17 | 657.7 | 1.75 | 530.43 |
| Sum | | | **851.8** | | **898.0** |

## 5.5. Bridge Ratings with H-20 Loading

Using the methods outlined above, all of twelve bridge sections were examined for the H-20 truck load, except for one bridge, Brazos 2, which was designed for the H-15 truck loading. The results are shown in Table 5.6. The bridges italicized in the table were designed for two HS-20 trucks, but were rated here for H-20 vehicles. The percentages show the amount of over-strength using each different design method. Negative percentages, shown in bold, represent floor beams that have insufficient strength. Notice that using the direct load

method, there are four floor beams that are do not meet the LRFD specification and three that do not meet LFD. Using the lever rule, all of the bridges have sufficient strength. Using the Equation 5.9 to factor in slab moment, only two floor beams have insufficient strength, though not by much, according to LRFD and none for LFD. Trinity 8 was the bridge used in the example calculations earlier in the chapter.

**Table 5.6 Over-Strength Factors for the 12 Cross Sections for H-20 Trucks Using LRFD and LFD Specifications**

| | | Mn | Direct | | Lever Rule | | Equation 5.9 | |
|---|---|---|---|---|---|---|---|---|
| | | (kft) | LRFD | LFD | LRFD | LFD | LRFD | LFD |
| 1 | Brazos | 728.4 | **-7.3%** | **-8.5%** | 1.3% | 2.2% | **-0.3%** | 0.1% |
| 2 | Brazos* | 526.2 | **-0.8%** | **-1.7%** | 8.5% | 9.8% | 9.0% | 10.5% |
| 3 | Colorado | 728.4 | **-2.4%** | 1.5% | 6.0% | 13.3% | 4.1% | 10.4% |
| *4* | *N Llano* | *765.9* | *1.9%* | *7.4%* | *10.4%* | *19.8%* | *8.2%* | *16.2%* |
| *5* | *N Llano* | *765.9* | *0.4%* | *2.3%* | *9.2%* | *14.2%* | *7.1%* | *11.1%* |
| *5a* | *N Llano* | *765.9* | *3.6%* | *4.6%* | *12.8%* | *16.7%* | *10.6%* | *13.7%* |
| 6 | Red | 728.4 | 8.9% | 7.0% | 18.8% | 19.5% | 17.1% | 17.1% |
| 7 | Sabine | 897.6 | 0.0% | 2.3% | 8.8% | 14.1% | 5.1% | 9.0% |
| 7a | Sabine | 897.6 | 3.2% | 4.6% | 12.4% | 16.7% | 8.6% | 11.6% |
| 8 | Trinity | 897.6 | **-4.8%** | **-1.2%** | 3.4% | 10.3% | **-0.1%** | 5.3% |
| *9* | *Trinity* | *728.4* | *6.7%* | *8.4%* | *15.9%* | *21.0%* | *14.1%* | *18.2%* |
| *9a* | *Trinity* | *728.4* | *9.2%* | *10.2%* | *18.7%* | *23.0%* | *17.0%* | *20.2%* |

* This bridge was rated for H-15 loading instead of H-20

It is evident that even though the reductions from the lever rule and slab moment are small, around 10%, it can have a critical effect on whether a bridge meets the rating standards. Note that all calculations from the table above were based on a yield stress of 36 ksi. Calculations using 33 ksi steel, the expected yield strength for bridges built during this time period according to the TxDOT Bridge Rating Manual, are shown in Table 5.7.

**Table 5.7 Over-Strength Factors with 33 ksi Steel using H-20 Trucks**

| | | Mn | Direct | | Lever Rule | | Equation 5.9 | |
|---|---|---|---|---|---|---|---|---|
| | | (kft) | LRFD | LFD | LRFD | LFD | LRFD | LFD |
| 1 | Brazos | 667.7 | **-15.0%** | **-16.1%** | **-7.1%** | **-6.3%** | **-8.6%** | **-8.3%** |
| 2 | Brazos | 482.4 | **-9.0%** | **-9.9%** | **-0.5%** | 0.6% | **-0.1%** | 1.3% |
| 3 | Colorado | 667.7 | **-10.5%** | **-6.9%** | **-2.9%** | 3.9% | **-4.5%** | 1.2% |
| *4* | *N Llano* | *702.1* | ***-6.6%*** | ***-1.6%*** | *1.2%* | *9.8%* | ***-0.8%*** | *6.5%* |
| *5* | *N Llano* | *702.1* | ***-8.0%*** | ***-6.2%*** | *0.1%* | *4.7%* | ***-1.8%*** | *1.8%* |
| *5a* | *N Llano* | *702.1* | ***-5.0%*** | ***-4.1%*** | *3.4%* | *7.0%* | *1.4%* | *4.2%* |
| 6 | Red | 667.7 | **-0.2%** | **-1.9%** | 8.9% | 9.5% | 7.4% | 7.3% |
| 7 | Sabine | 822.8 | **-8.4%** | **-6.3%** | **-0.3%** | 4.6% | **-3.7%** | **-0.1%** |
| 7a | Sabine | 822.8 | **-5.4%** | **-4.1%** | 3.0% | 7.0% | **-0.5%** | 2.3% |
| 8 | Trinity | 822.8 | **-12.8%** | **-9.4%** | **-5.2%** | 1.1% | **-8.4%** | **-3.5%** |
| *9* | *Trinity* | *667.7* | ***-2.2%*** | ***-0.6%*** | *6.2%* | *11.0%* | *4.6%* | *8.4%* |
| *9a* | *Trinity* | *667.7* | *0.1%* | *1.0%* | *8.8%* | *12.8%* | *7.2%* | *10.2%* |

The over-strength factors using allowable stress design are shown in Table 5.8 for both 33 and 36 ksi yield stress. Using 36 ksi steel, all but one floor beam rates sufficiently, even with the direct load method. However, using 33 ksi steel, only three of the floor beams rate sufficiently with the direct load method. Using the lever rule and Equation 5.9 with a 33 ksi yield stress, almost all of the floor beams rate satisfactorily. These tables demonstrated that a small difference in the yield strength of steel can make a significant difference to the rating of a bridge. By determining the actual yield stress of the steel could determine whether a bridge is rated acceptable or unacceptable.

**Table 5.8 Over-Strength Factors for ASD using H-20 Trucks**

| | | 36 ksi | | | | 33 ksi | | | |
|---|---|---|---|---|---|---|---|---|---|
| | | $M_{all}$ (kft) | Direct | Lever | Eq. 5.9 | $M_{all}$ (kft) | Direct | Lever | Eq. 5.9 |
| 1 | Brazos | 390.7 | **-3.2%** | 12% | 8% | 352.4 | **-15.9%** | **-2%** | **-6%** |
| 2 | Brazos | 281.8 | 3.4% | 20% | 20% | 254.3 | **-10.9%** | 4% | 3% |
| 3 | Colorado | 392.4 | 8.2% | 26% | 21% | 353.9 | **-7.0%** | 9% | 4% |
| *4* | *N Llano* | *413.1* | *16.2%* | *35%* | *29%* | *372.6* | ***-0.2%*** | *17%* | *11%* |
| *5* | *N Llano* | *413.1* | *10.8%* | *28%* | *23%* | *372.6* | ***-4.2%*** | *12%* | *6%* |
| *5a* | *N Llano* | *413.1* | *14.8%* | *33%* | *27%* | *372.6* | ***-0.3%*** | *16%* | *11%* |
| 6 | Red | 392.9 | 19.9% | 38% | 34% | 354.3 | 4.9% | 21% | 17% |
| 7 | Sabine | 483.0 | 10.1% | 28% | 19% | 435.6 | **-4.9%** | 11% | 3% |
| 7a | Sabine | 483.0 | 14.2% | 32% | 24% | 435.6 | **-0.9%** | 15% | 7% |
| 8 | Trinity | 483.0 | 3.8% | 21% | 13% | 435.6 | **-10.9%** | 5% | **-3%** |
| *9* | *Trinity* | *394.2* | *20.5%* | *39%* | *34%* | *355.4* | *4.6%* | *21%* | *17%* |
| *9a* | *Trinity* | *394.2* | *23.5%* | *42%* | *38%* | *355.4* | *7.4%* | *24%* | *20%* |

As is evident from the results in the preceding tables, a better understanding of the forces actually on a system can cause a floor beam member previously rated deficient to have enough strength to meet the design requirements. Also evident from the tables is the difference in the different specifications. As you move from ASD to LFD to LRFD, the requirements become harder to meet. Floor beams that meet requirements for ASD do not necessarily meet the requirements of the other specifications.

## 5.6. Bridge Rating Using HS-20 Loading

Though the bridges were designed for H-20 design trucks, the same procedure can be followed to examine the floor beam for an HS-20 truck load. The lever rule would apply exactly the same way for a slab not in contact with the floor beam. However, a different equation would have to be used to determine

the moment reduction when the slab sits directly on the floor beam. This equation would take into account more factors than only the floor beam and slab stiffness. According to the direct load method, the HS-20 truck loading causes a moment that is up to 33% higher than the moment caused by the H-20 loading. With a larger floor beam spacing, the extra axle will have a greater effect on the floor beam moment. The over-strength factors are shown for LRFD and LFD in Table 5.9 for the HS-20 loading. Table 5.10 shows the over-strength factors for Allowable Stress Design using the HS-20 loading. Both tables show the results from the direct load and lever rule only.

**Table 5.9 Over-Strength for HS-20 Loading, 36 ksi Steel**

| | | | Direct Load | | Lever Rule | |
|---|---|---|---|---|---|---|
| | | Mn | LRFD | LFD | LRFD | LFD |
| 1 | Brazos | 728.4 | **-11.2%** | **-13.3%** | **-2.9%** | **-3.1%** |
| 2 | Brazos | 526.2 | **-5.0%** | **-6.8%** | 3.9% | 4.1% |
| 3 | Colorado | 728.4 | **-22.5%** | **-23.9%** | **-15.3%** | **-15.0%** |
| *4* | *N Llano* | *765.9* | ***-20.8%*** | ***-21.9%*** | ***-13.6%*** | ***-12.8%*** |
| *5* | *N Llano* | *765.9* | ***-14.7%*** | ***-16.4%*** | ***-6.9%*** | ***-6.7%*** |
| *5a* | *N Llano* | *765.9* | ***-10.2%*** | ***-12.2%*** | ***-1.9%*** | ***-2.0%*** |
| 6 | Red | 728.4 | 3.9% | 1.2% | 13.6% | 13.0% |
| 7 | Sabine | 897.6 | **-14.8%** | **-16.2%** | **-6.9%** | **-6.4%** |
| 7a | Sabine | 897.6 | **-10.2%** | **-11.9%** | **-1.9%** | **-1.7%** |
| 8 | Trinity | 897.6 | **-20.9%** | **-21.7%** | **-13.6%** | **-12.6%** |
| *9* | *Trinity* | *728.4* | ***-9.8%*** | ***-11.9%*** | ***-1.6%*** | ***-1.6%*** |
| *9a* | *Trinity* | *728.4* | ***-6.2%*** | ***-8.6%*** | *2.3%* | *2.0%* |

**Table 5.10 ASD Over-Strength Factors for HS-20 Loading**

| | | 36 ksi | | | 33 ksi | | |
|---|---|---|---|---|---|---|---|
| | | $M_{all}$ (kft) | Direct | Lever | $M_{all}$ (kft) | Direct | Lever |
| 1 | Brazos | 390.7 | **-9.1%** | 5% | 352.4 | **-21.1%** | **-8%** |
| 2 | Brazos | 281.8 | **-3.3%** | 13% | 254.3 | **-16.7%** | **-2%** |
| 3 | Colorado | 392.4 | **-24.1%** | **-12%** | 353.9 | **-34.7%** | **-23%** |
| *4* | *N Llano* | *413.1* | ***-21.8%*** | ***-9%*** | *372.6* | ***-32.8%*** | ***-21%*** |
| *5* | *N Llano* | *413.1* | ***-13.3%*** | *0.4%* | *372.6* | ***-25.0%*** | ***-13%*** |
| *5a* | *N Llano* | *413.1* | ***-7.1%*** | *7%* | *372.6* | ***-19.3%*** | ***-6%*** |
| 6 | Red | 392.9 | 12.2% | 29% | 354.3 | **-1.9%** | 13% |
| 7 | Sabine | 483.0 | **-13.6%** | 0.2% | 435.6 | **-25.4%** | **-13%** |
| 7a | Sabine | 483.0 | **-7.3%** | 7% | 435.6 | **-19.6%** | **-7%** |
| 8 | Trinity | 483.0 | **-22.2%** | **-9%** | 435.6 | **-33.2%** | **-22%** |
| *9* | *Trinity* | *394.2* | ***-6.4%*** | *8%* | *355.4* | ***-18.7%*** | ***-6%*** |
| *9a* | *Trinity* | *394.2* | ***-1.5%*** | *14%* | *355.4* | ***-14.3%*** | ***-1%*** |

# CHAPTER 6

# CONCLUSIONS

## 6.1. Purpose of Research

The main goal of the research was to more accurately determine the moments in the transverse floor beams in twin girder steel bridges. This was accomplished by modeling actual bridge geometries with the SAP2000 finite element program. These results from this analysis were then compared with the moment resulting from the current provisions and with the moments from experimental results. Using these results it was possible to quantify the force experienced by the floor beam for a given loading condition.

## 6.2. Overview of Findings

### 6.2.1. CURRENT ANALYSIS METHODS ARE OVER-CONSERVATIVE

Using finite element modeling as well as simple statics, it was determined that the floor beams in the bridge do not experience the amount of force estimated by the current rating procedures. The amount of reduction due to the lateral load distribution and moment carried by the slab is about 10%. Though 10% may not seem like much, it often makes the difference between rating the member as adequate of inadequate, as was shown in Chapter 5.

### 6.2.2. SUGGESTED CHANGES IN LOAD DISTRIBUTION METHODS

If the floor beam does not come into contact with the slab, the lever rule should be used to determine the moment in the floor beam. This is a relatively simple calculation. In fact, if the system has only two stringers spaced from 6 to 12 feet, the value for the maximum moment using the lever rule is determined by simply multiplying the direct load moment by 0.894. This is still conservative with respect to moment values in the floor beam predicted by finite element analysis.

If the floor beam does come into contact with the slab, that way that the load is transferred in a bit more complicated manner. To avoid having to take the time to use a finite element model for each bridge, it was necessary to come up with an equation that gives a moment value closer to the actual value, yet still conservative. The equation shown in chapter 3 accomplishes this for the H-20 load case. This specification uses the ratio of floor beam stiffness to slab stiffness to predict the percentage of moment taken by the floor beam and slab. A correlation predicted moments from an HS-20 truck loading is not yet available at this time.

### 6.2.3. COMPARISON OF EXPERIMENTAL AND ANALYTICAL RESULTS

The experimental test of the Llano bridge confirmed what was demonstrated using finite element modeling, that the direct load model results in moments that are much higher than those actually experienced. Even the results from the SAP analyses are quite a bit higher than the moments calculated using the experimental results. The reason for this could be attributed to the fixity of

the connections and the higher stiffness of the concrete deck. However, it is not known with certainty why the experimental moments were lower. It does imply, though, that using a finite element model with simply supported floor beams is still a conservative approach.

## 6.3. Practical Results of Research

The result of the research was not the development of a new design method. In fact, new bridge construction rarely includes the type of bridges analyzed in this study. The research looks primarily at existing structures to determine if they are being rated properly. The result of this research is a more realistic assessment of the floor beam moment, which will lead to a more rational rating of the bridge. Bridges that are functioning at an acceptable level should be rated accordingly. This would make available both time and money to use on structures that should demand more attention. Another result of this research should be a new interest in transverse load distribution. This has been a subject that has been long overlooked by the codes and it is the hope of this author that more work will be done to determine exactly how load is distributed transversely. There is still much that can be done in this area.

# APPENDIX A

# BRIDGE CROSS SECTIONS

## Brazos 1

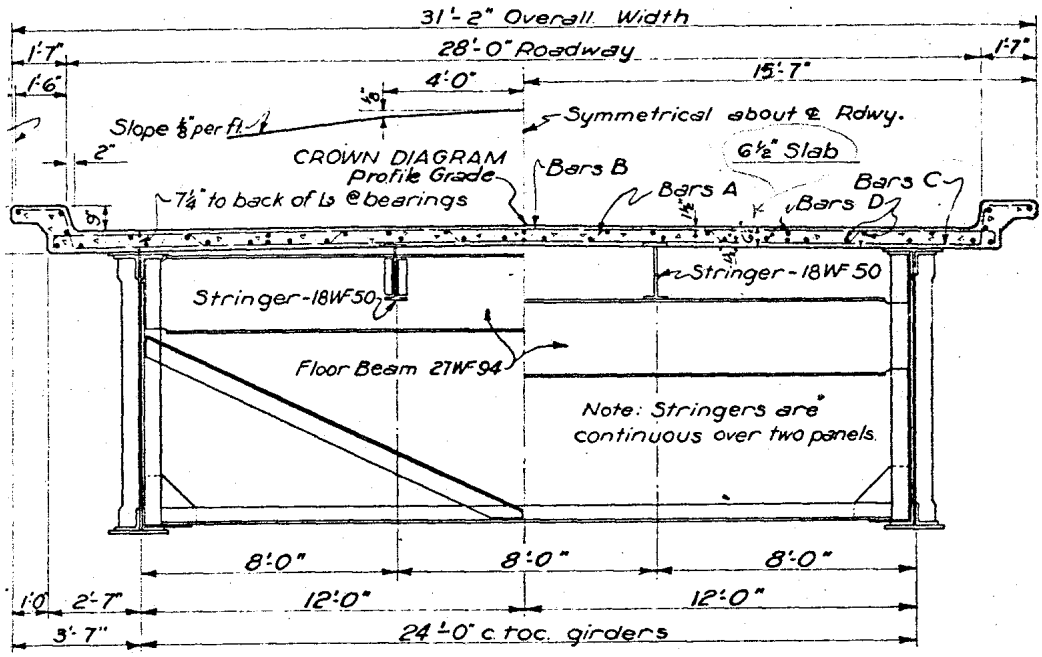

## Brazos 2

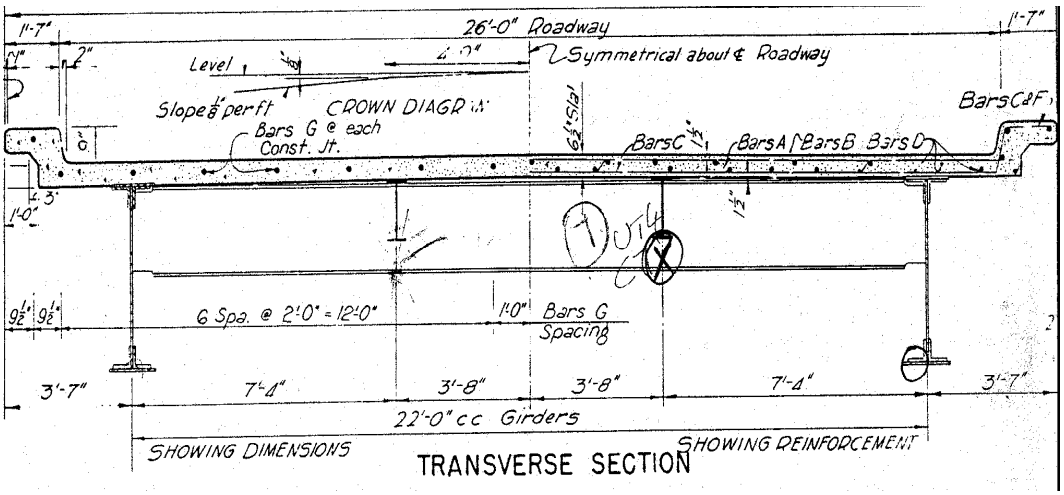


## Colorado 3

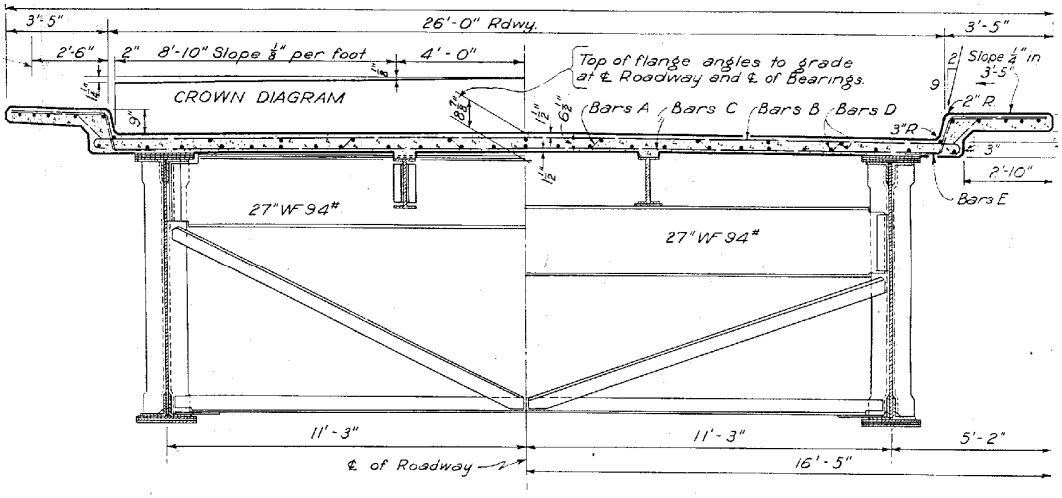

## N. Llano 4

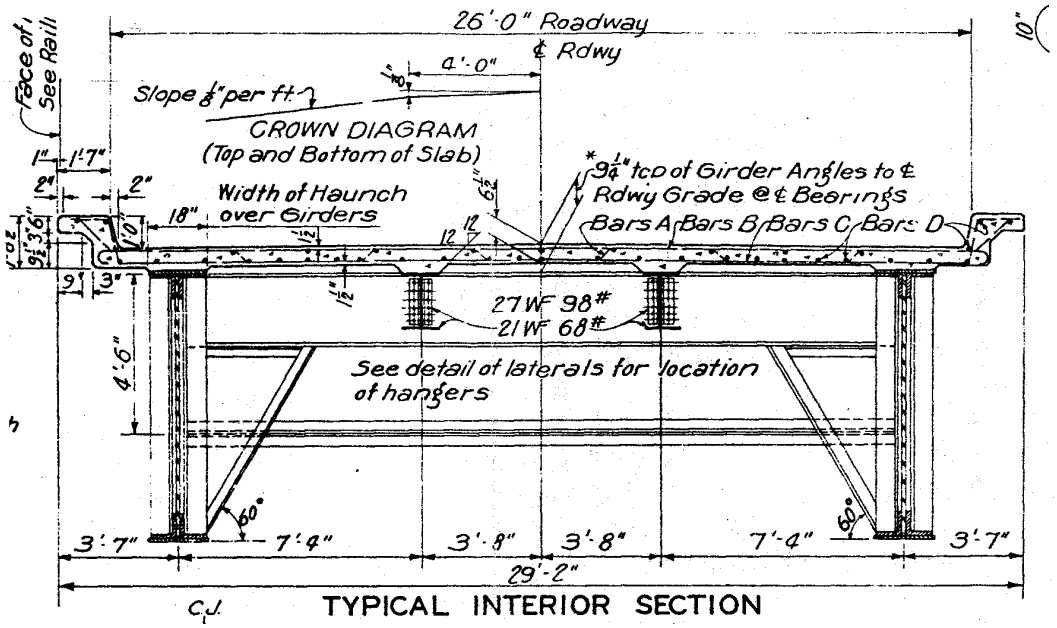


## N. Llano 5 & 5a

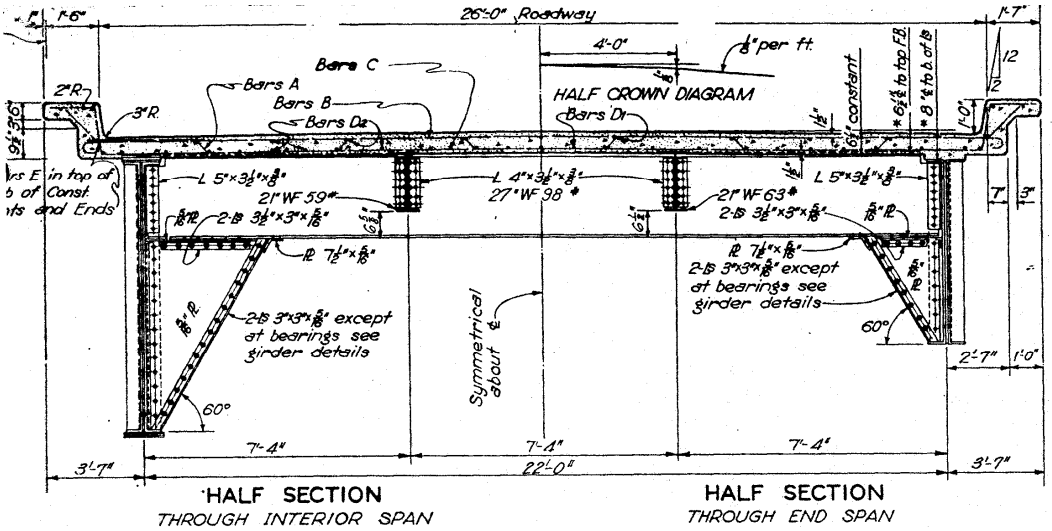

## Red 6

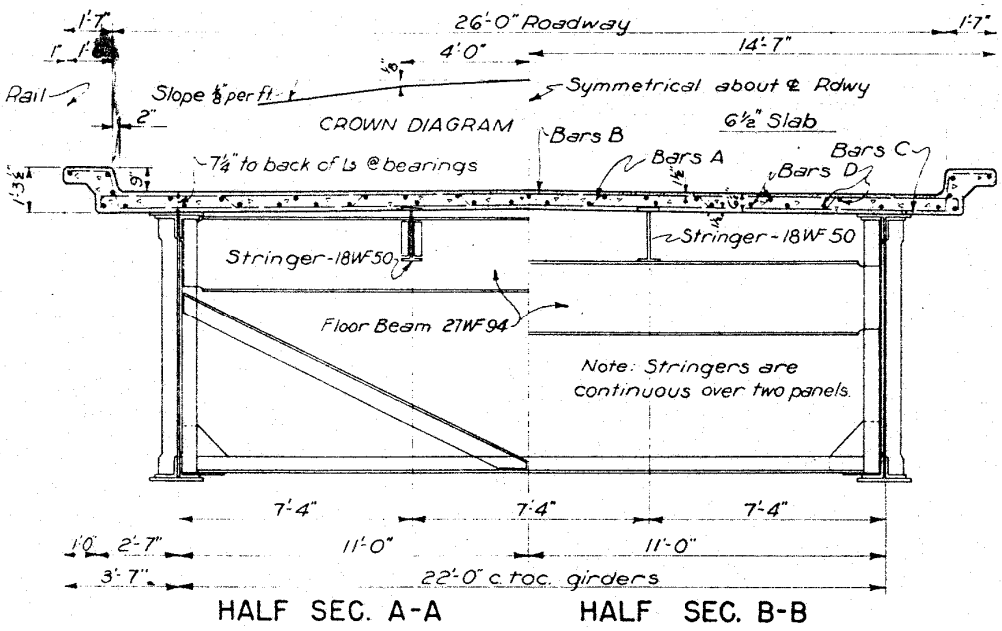


## Sabine 7 & 7a

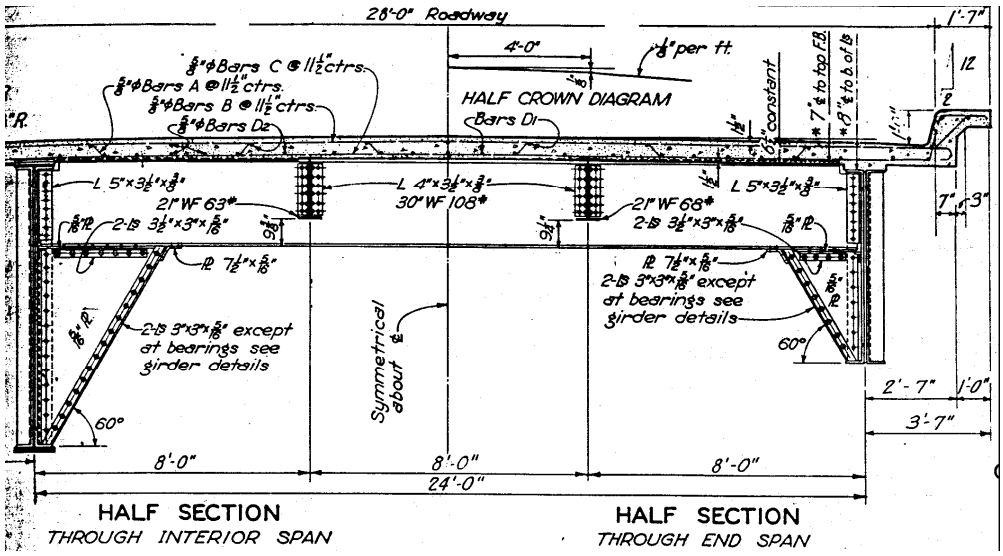

## Trinity 8

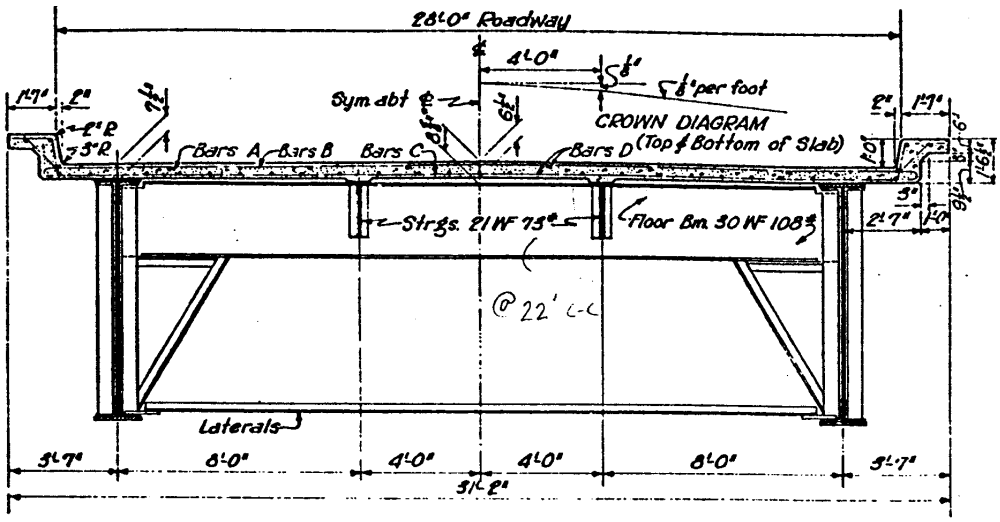


TYPICAL INTERIOR SECTION

## Trinity 9 & 9a

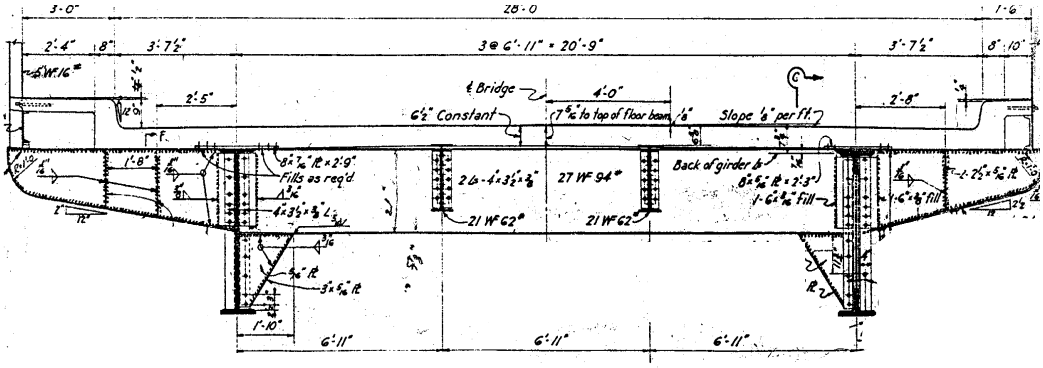


SECTION A-A

# APPENDIX B

## LOAD RUN DESCRIPTIONS FOR 1ST LLANO TEST

| Run | Truck | Description of Run (Transverse Location of Center of Load, ft) |
|---|---|---|
| 1 | A & B | Two Trucks, Side by Side (0) |
| 1B | A & B | Two Trucks, Side by Side (0) |
| 2 | A & B | Two Trucks, Side by Side (0) |
| 3 | A & B | Two Trucks, Train (0) |
| 4 | A & B | Two Trucks, Train (0) |
| 5 | A | One Truck, Center (0) |
| 6 | B | One Truck, Center (0) |
| 7 | A | One Truck (-5.5) |
| 8 | B | One Truck (-5.5) |
| 9 | A | One Truck (-3.5) |
| 10 | B | One Truck (-3.5) |
| 11 | A | One Truck (1) |
| 12 | B | One Truck (1) |
| 13 | A | One Truck (5.5) |
| 14 | B | One Truck (5.5) |
| 15 | A | One Truck (3.5) |
| 16 | B | One Truck (3.5) |
| 17 | A | One Truck (-1) |
| 18 | B | One Truck (-1) |
| 19 | A & B | Two Trucks, Reverse Train (0) |
| 20 | A & B | Two Trucks, Reverse Train (0) |
| 21 | A & B | Two Trucks, Reverse Train (0) |

# APPENDIX C

## SELECTED NEUTRAL AXIS CALCULATIONS FOR 1ST LLANO TEST

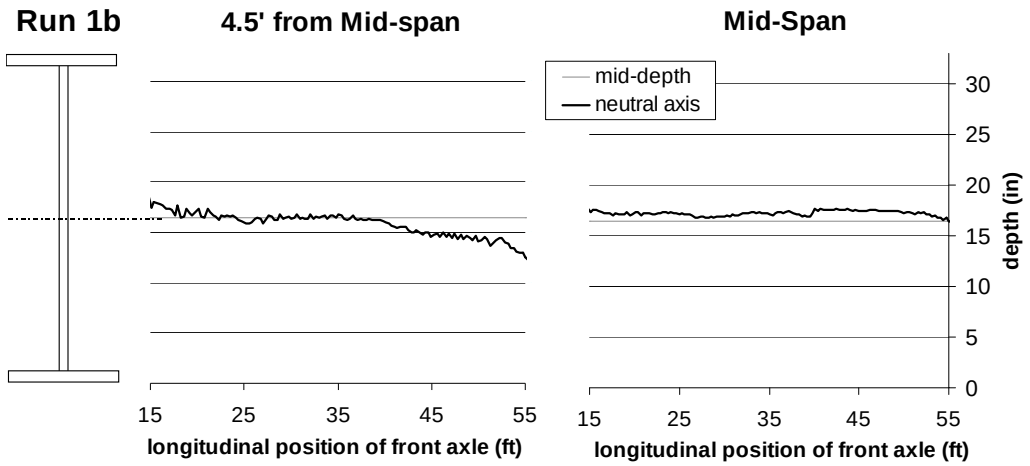


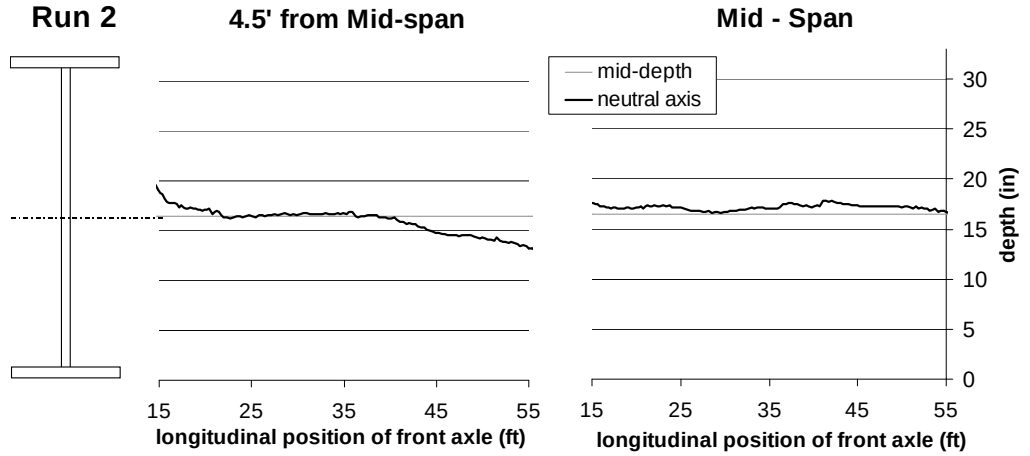

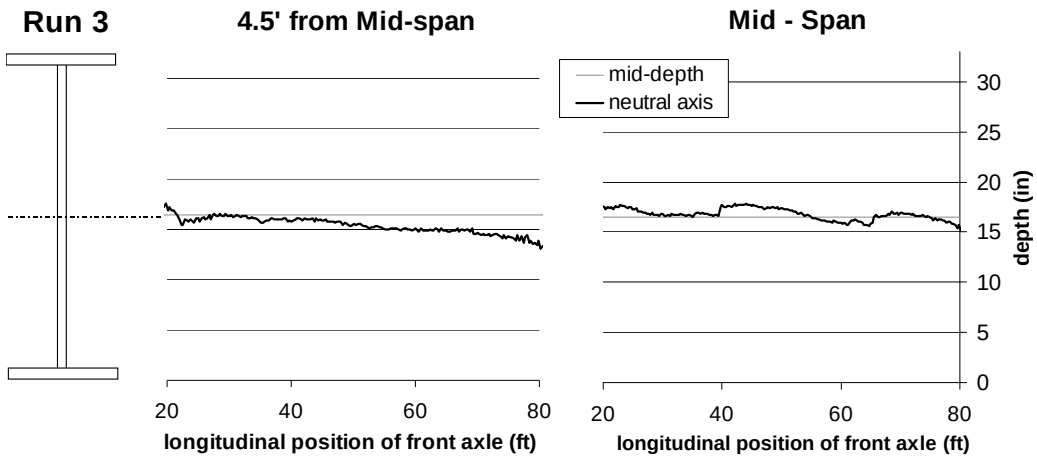
Run 3
4.5' from Mid-span
Mid - Span
mid-depth
neutral axis
30
25
20
15
10
5
0
depth (in)
20
40
60
80
longitudinal position of front axle (ft)
20
40
60
80
longitudinal position of front axle (ft)

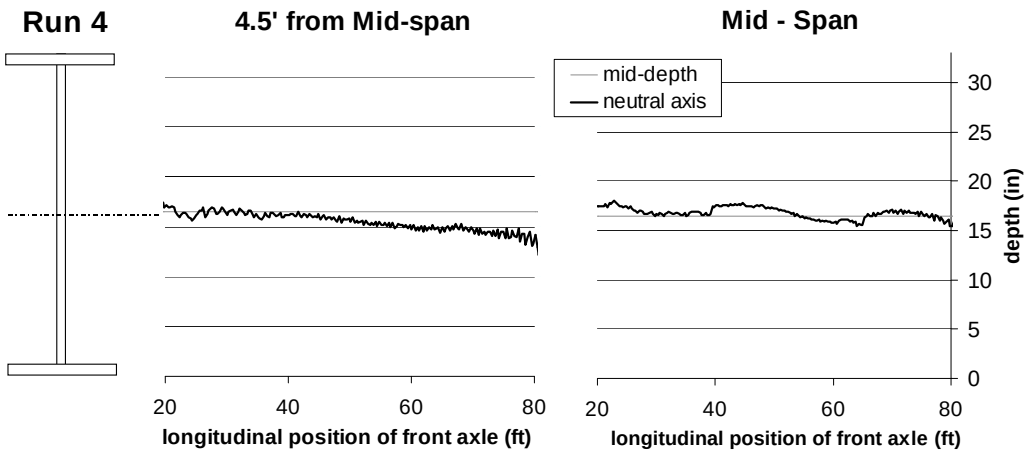
Run 4
4.5' from Mid-span
Mid - Span
mid-depth
neutral axis
30
25
20
15
10
5
0
depth (in)
20
40
60
80
longitudinal position of front axle (ft)
20
40
60
80
longitudinal position of front axle (ft)

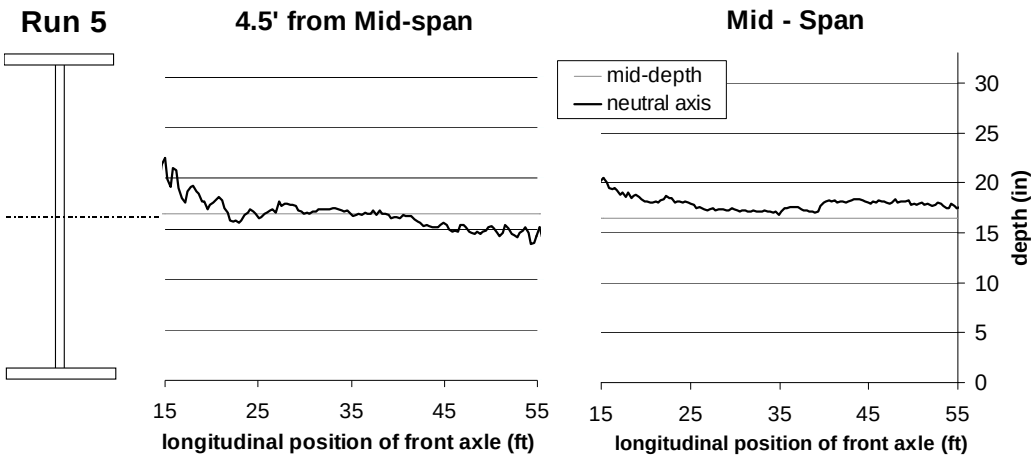
Run 5
4.5' from Mid-span
Mid - Span
mid-depth
neutral axis
30
25
20
15
10
5
0
depth (in)
15
25
35
45
55
longitudinal position of front axle (ft)
15
25
35
45
55
longitudinal position of front axle (ft)

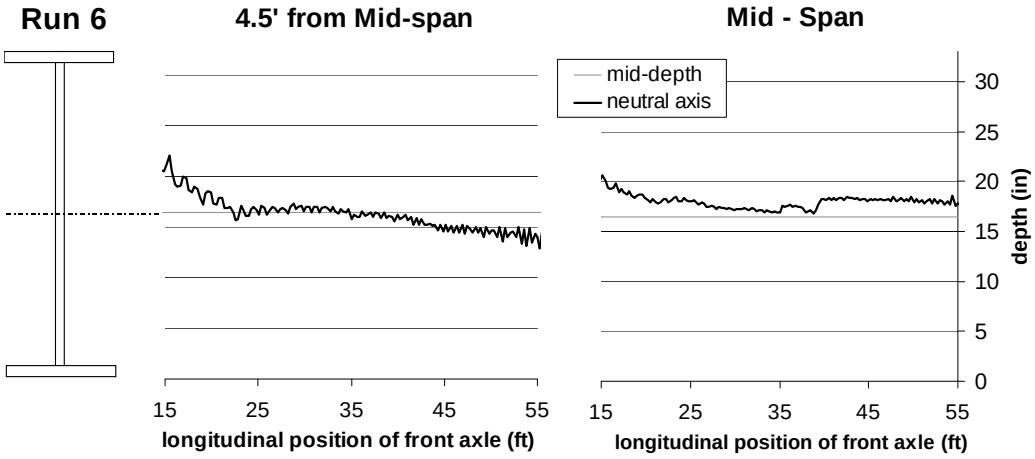
Run 6
4.5' from Mid-span
Mid - Span
mid-depth
neutral axis
30
25
20
15
10
5
0
depth (in)
15
25
35
45
55
longitudinal position of front axle (ft)
15
25
35
45
55
longitudinal position of front axle (ft)

# APPENDIX D

## COMPARISON OF TOP TO BOTTOM FLANGE STRAINS IN FIRST LLANO TEST

| Run | % top flange max is less than bottom flange max | | | |
|---|---|---|---|---|
| | FB1 -mid | FB2-mid | FB1-4.5' | FB2-4.5' |
| 1 | 48% | 19% | 18% | -6% |
| 1b | 44% | 7% | 22% | -2% |
| 2 | 50% | 7% | 19% | -4% |
| 3 | 40% | 1% | -1% | -11% |
| 4 | 41% | 0% | -3% | -8% |
| 5 | 38% | 5% | 1% | -1% |
| 6 | 46% | 7% | -2% | -3% |
| 7 | 54% | 28% | 23% | 5% |
| 8 | 59% | 25% | 18% | 3% |
| 9 | 50% | -29% | 18% | 4% |
| 10 | 54% | 9% | 20% | 6% |
| 11 | 40% | -1% | 2% | -4% |
| 12 | 49% | 1% | -2% | -3% |
| 13 | 32% | 9% | -2% | -2% |
| 14 | 42% | 14% | -2% | -2% |
| 15 | 39% | 5% | 5% | -3% |
| 16 | 42% | 3% | 3% | -9% |
| 17 | 43% | 6% | 3% | -7% |
| 18 | 48% | 14% | 4% | -2% |
| 20 | 45% | 7% | -10% | -11% |
| 21 | 46% | 8% | -3% | -4% |
| Avg. | 45% | 7% | 6% | -3% |

# APPENDIX E

## COMPARISON OF 2ND FLOOR BEAM TO 1ST FLOOR BEAM STRAINS

| Run | Mid-Span | | | 4.5' Away | | |
|---|---|---|---|---|---|---|
| | FB2 (με) | FB1 (με) | % smaller | FB2 (με) | FB1 (με) | % smaller |
| 1 | 164.6 | 108.0 | 34% | 110.6 | 94.0 | 15% |
| 1b | 159.5 | 116.9 | 27% | 117.8 | 100.8 | 14% |
| 2 | 146.6 | 106.1 | 28% | 109.3 | 95.0 | 13% |
| 3 | 118.5 | 83.1 | 30% | 83.6 | 69.7 | 17% |
| 4 | 119.9 | 84.1 | 30% | 85.4 | 69.5 | 19% |
| 5 | 103.3 | 80.1 | 22% | 73.4 | 71.1 | 3% |
| 6 | 101.0 | 78.8 | 22% | 73.4 | 68.4 | 7% |
| 7 | 72.4 | 55.5 | 23% | 72.0 | 69.9 | 3% |
| 8 | 68.8 | 54.3 | 21% | 70.1 | 65.5 | 7% |
| 9 | 75.6 | 72.8 | 4% | 80.2 | 76.8 | 4% |
| 10 | 86.3 | 67.6 | 22% | 76.9 | 73.6 | 4% |
| 11 | 102.2 | 82.3 | 19% | 68.3 | 67.2 | 2% |
| 12 | 99.5 | 81.2 | 18% | 68.5 | 63.8 | 7% |
| 13 | 73.0 | 60.1 | 18% | 38.8 | 33.6 | 13% |
| 14 | 73.2 | 57.3 | 22% | 38.8 | 33.6 | 13% |
| 15 | 91.8 | 73.2 | 20% | 53.4 | 48.8 | 9% |
| 16 | 86.0 | 70.1 | 18% | 49.5 | 42.8 | 13% |
| 17 | 102.4 | 79.6 | 22% | 75.7 | 74.5 | 2% |
| 18 | 104.4 | 77.6 | 26% | 76.5 | 73.8 | 4% |
| 20 | 147.5 | 96.5 | 35% | 102.9 | 81.5 | 21% |
| 21 | 148.8 | 94.9 | 36% | 106.2 | 79.9 | 25% |
| Avg. | | | 24% | | | 10% |
| Comparison of Experimental to SAP and Direct Load using Run 1b | | | | | | |
| Exp. | 159.5 | 116.9 | 27% | 117.8 | 100.8 | 14% |
| SAP | 233.7 | 219 | 6% | 203 | 194.7 | 4% |
| Direct | 261.4 | 237.8 | 9% | 226.3 | 205.9 | 9% |

# APPENDIX F

## RESULTS FROM LOAD RUNS IN FIRST LLANO TEST

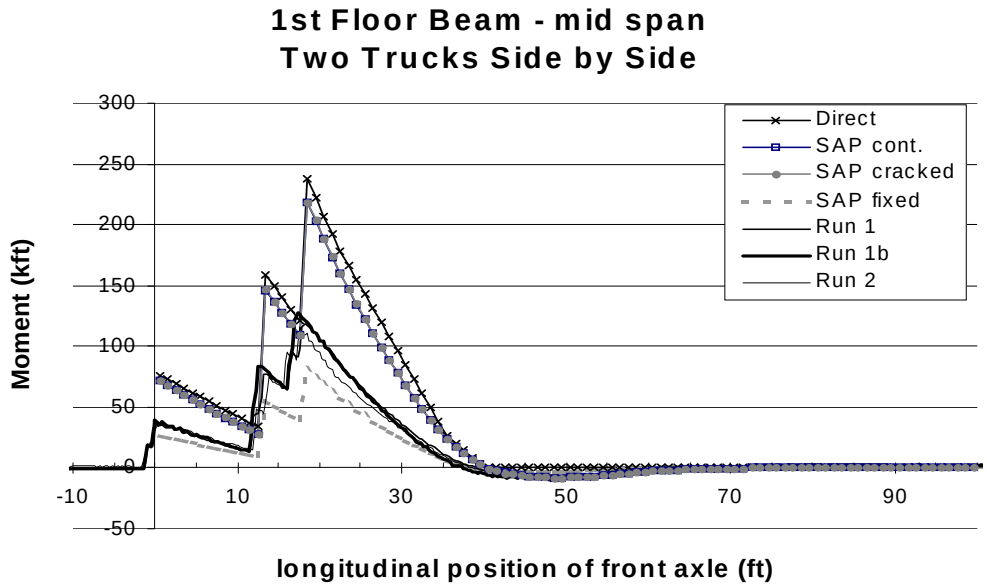


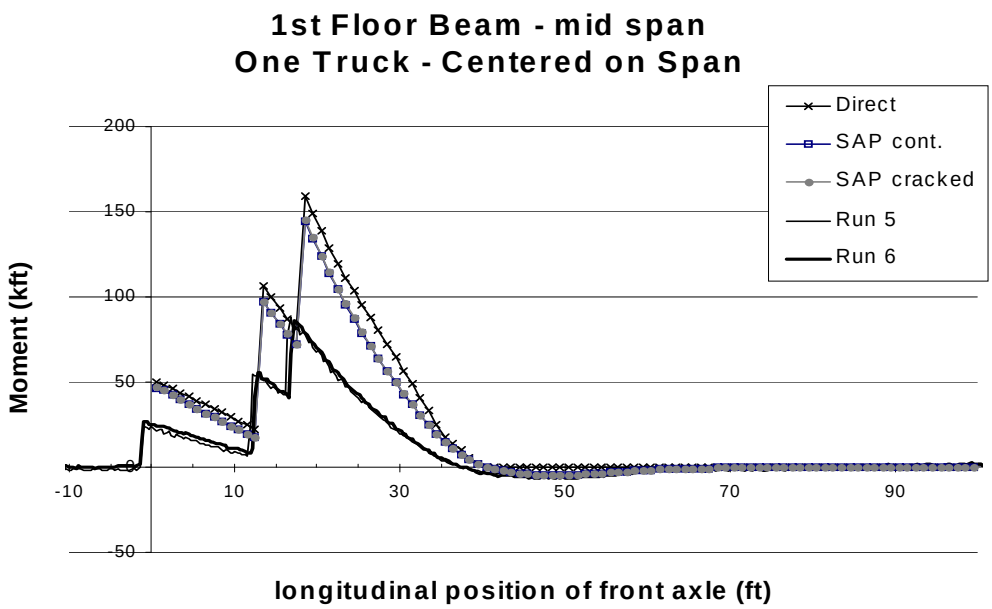

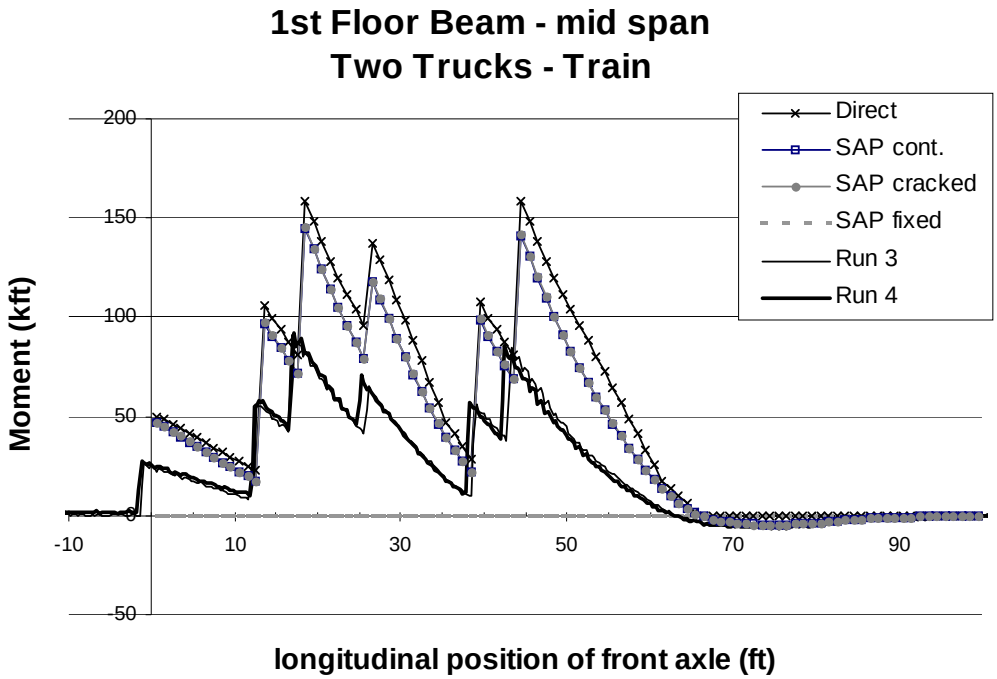
1st Floor Beam - mid span
Two Trucks - Train
Direct
SAP cont.
SAP cracked
SAP fixed
Run 3
Run 4
Moment (kft)
200
150
100
50
0
-50
-10
10
30
50
70
90
longitudinal position of front axle (ft)

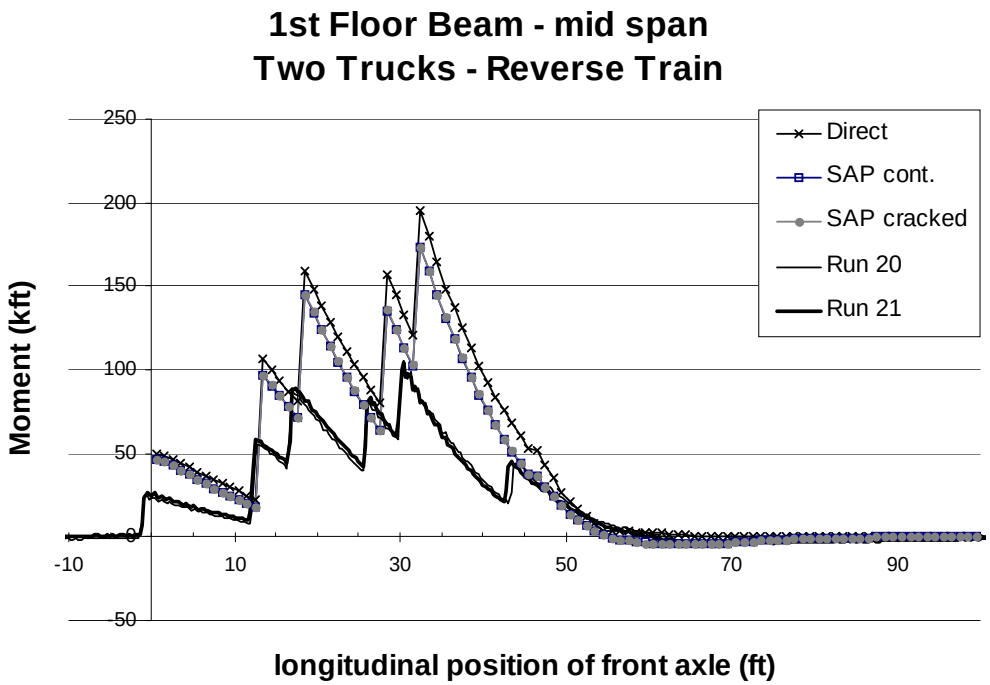
1st Floor Beam - mid span
Two Trucks - Reverse Train
Direct
SAP cont.
SAP cracked
Run 20
Run 21
Moment (kft)
250
200
150
100
50
0
-50
-10
10
30
50
70
90
longitudinal position of front axle (ft)

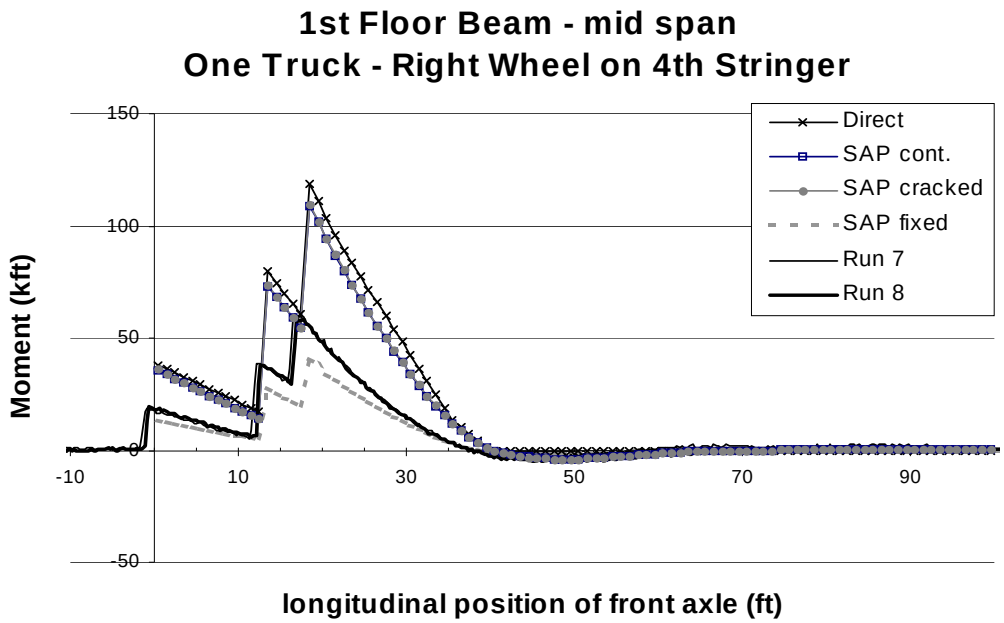
1st Floor Beam - mid span
One Truck - Right Wheel on 4th Stringer
Moment (kft)
150
100
50
0
-50
-10
10
30
50
70
90
longitudinal position of front axle (ft)
Direct
SAP cont.
SAP cracked
SAP fixed
Run 7
Run 8

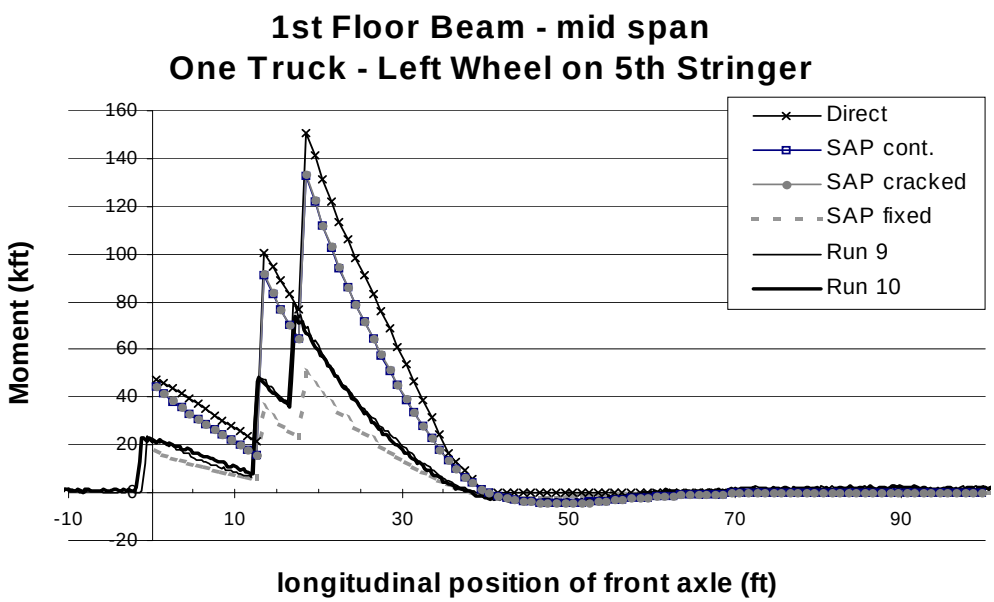
1st Floor Beam - mid span
One Truck - Left Wheel on 5th Stringer
Moment (kft)
160
140
120
100
80
60
40
20
0
-20
-10
10
30
50
70
90
longitudinal position of front axle (ft)
Direct
SAP cont.
SAP cracked
SAP fixed
Run 9
Run 10

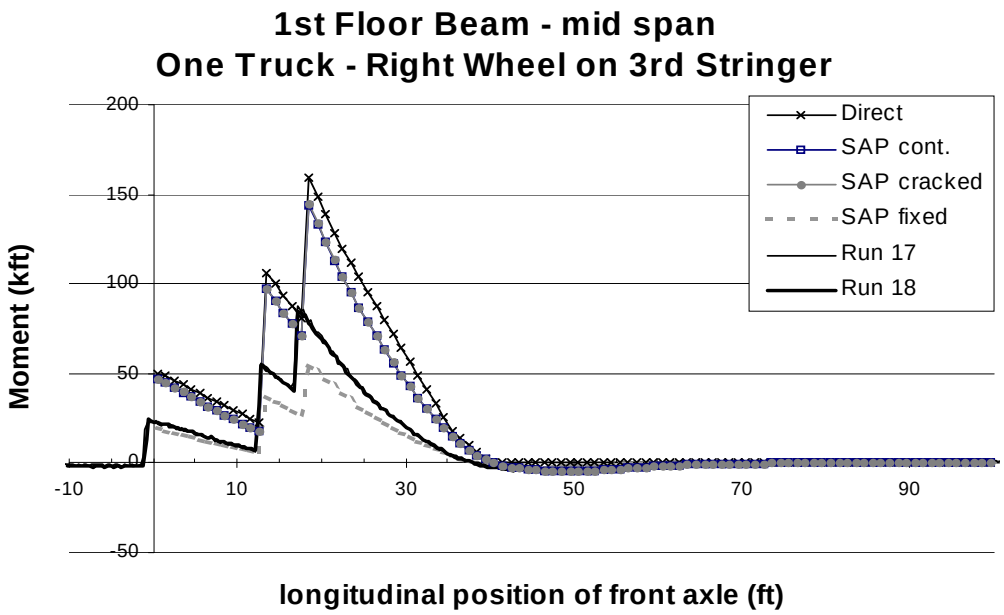
1st Floor Beam - mid span
One Truck - Right Wheel on 3rd Stringer
Moment (kft)
200
150
100
50
0
-50
-10
10
30
50
70
90
longitudinal position of front axle (ft)
Direct
SAP cont.
SAP cracked
SAP fixed
Run 17
Run 18

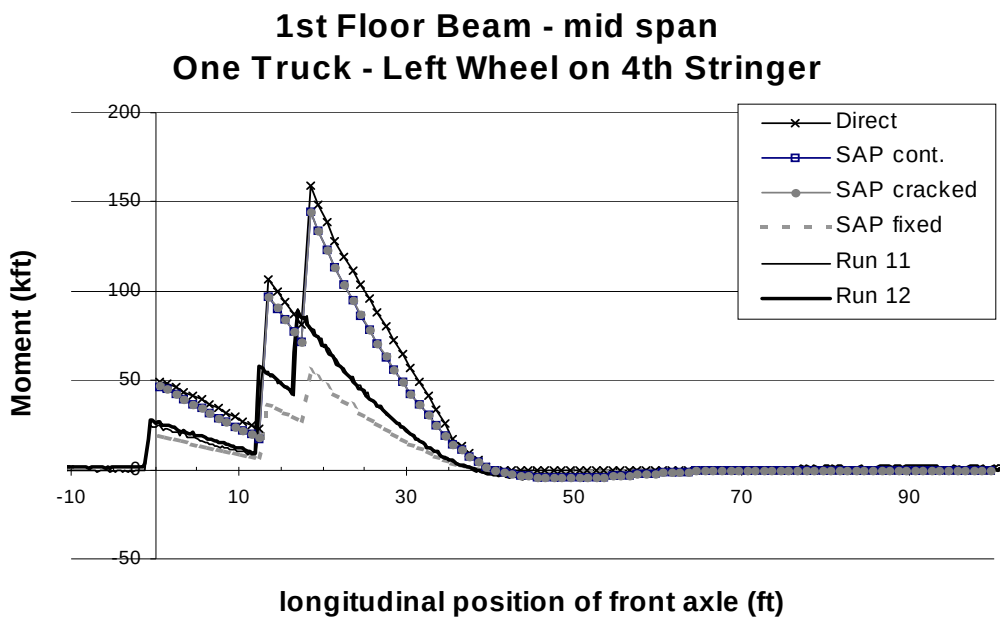
1st Floor Beam - mid span
One Truck - Left Wheel on 4th Stringer
Moment (kft)
200
150
100
50
0
-50
-10
10
30
50
70
90
longitudinal position of front axle (ft)
Direct
SAP cont.
SAP cracked
SAP fixed
Run 11
Run 12

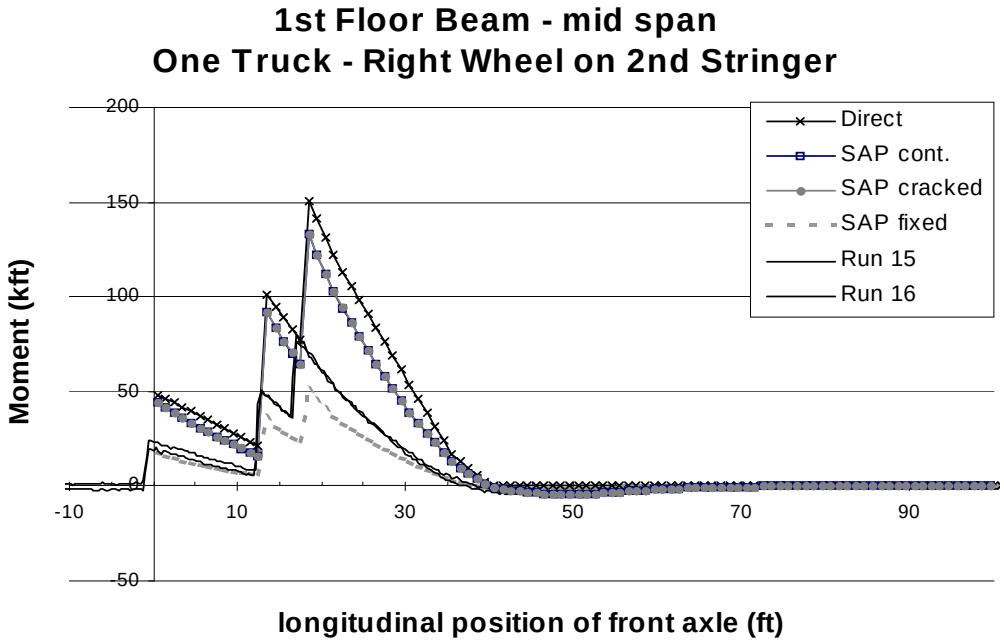
1st Floor Beam - mid span
One Truck - Right Wheel on 2nd Stringer
Moment (kft)
200
150
100
50
0
-50
-10
10
30
50
70
90
longitudinal position of front axle (ft)
Direct
SAP cont.
SAP cracked
SAP fixed
Run 15
Run 16

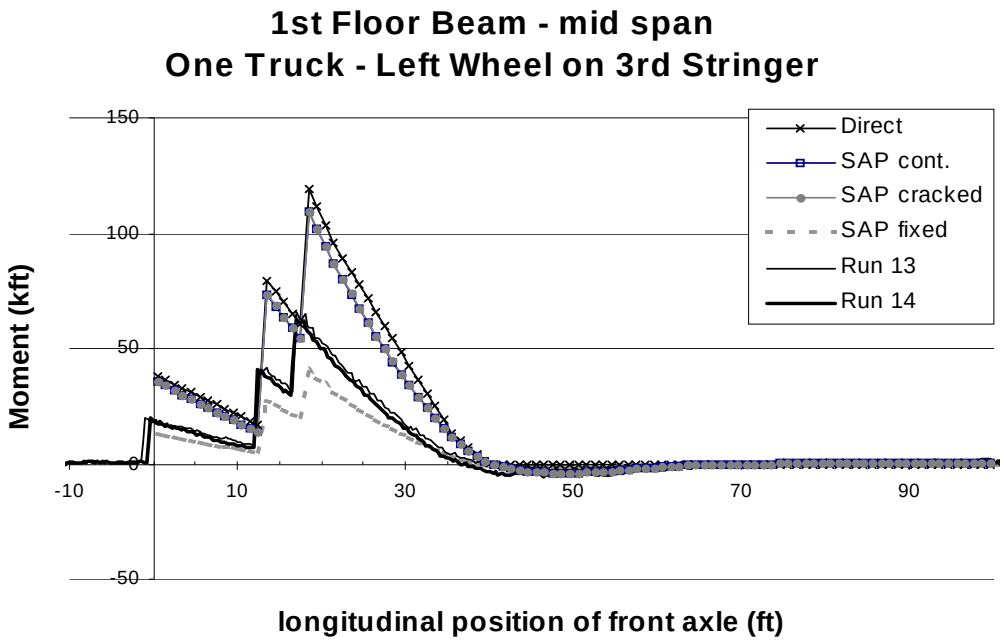
1st Floor Beam - mid span
One Truck - Left Wheel on 3rd Stringer
Moment (kft)
150
100
50
0
-50
-10
10
30
50
70
90
longitudinal position of front axle (ft)
Direct
SAP cont.
SAP cracked
SAP fixed
Run 13
Run 14

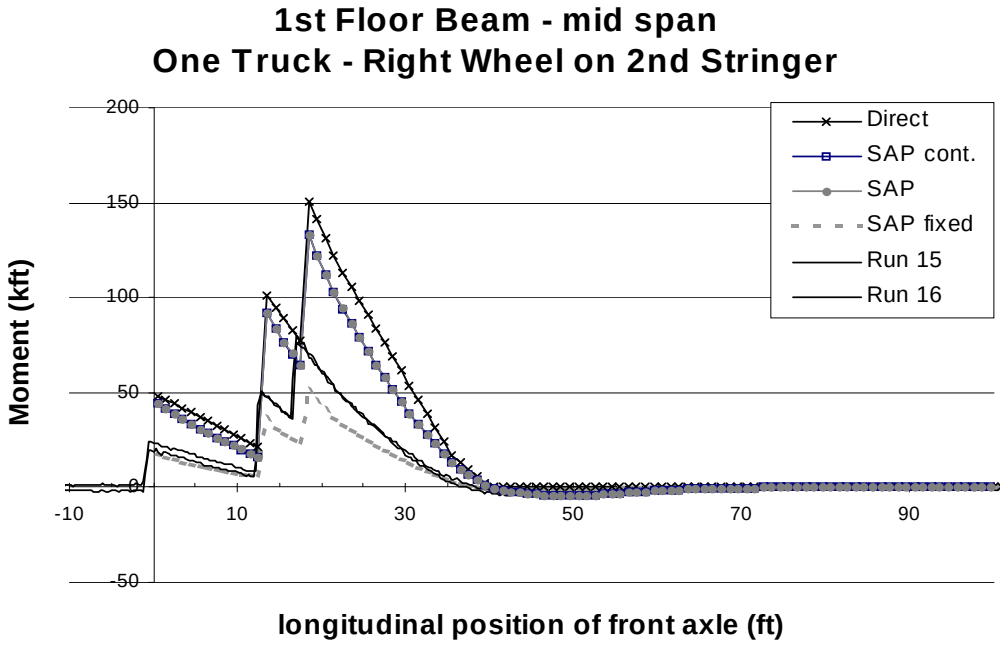
1st Floor Beam - mid span
One Truck - Right Wheel on 2nd Stringer
Moment (kft)
200
150
100
50
0
-50
-10
10
30
50
70
90
longitudinal position of front axle (ft)
Direct
SAP cont.
SAP
SAP fixed
Run 15
Run 16

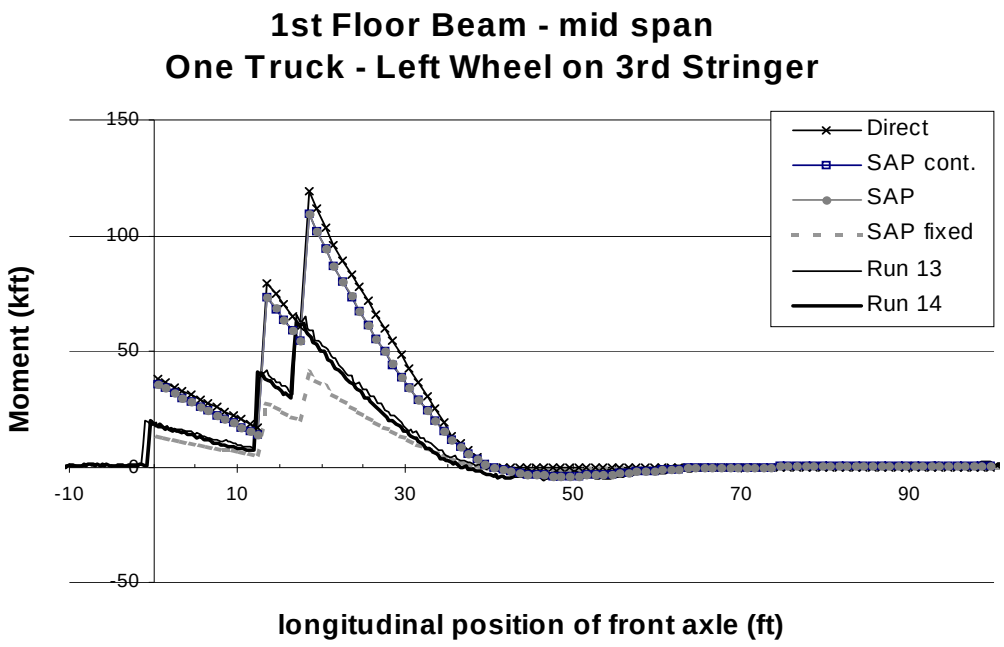
1st Floor Beam - mid span
One Truck - Left Wheel on 3rd Stringer
Moment (kft)
150
100
50
0
-50
-10
10
30
50
70
90
longitudinal position of front axle (ft)
Direct
SAP cont.
SAP
SAP fixed
Run 13
Run 14

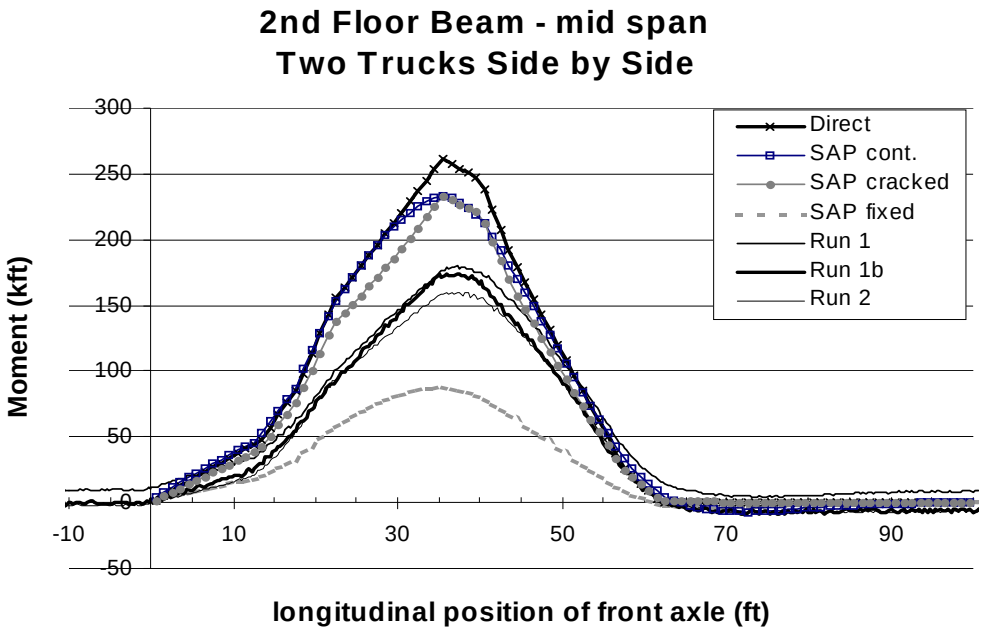
2nd Floor Beam - mid span
Two Trucks Side by Side
Moment (kft)
300
250
200
150
100
50
0
-50
-10
10
30
50
70
90
longitudinal position of front axle (ft)
Direct
SAP cont.
SAP cracked
SAP fixed
Run 1
Run 1b
Run 2

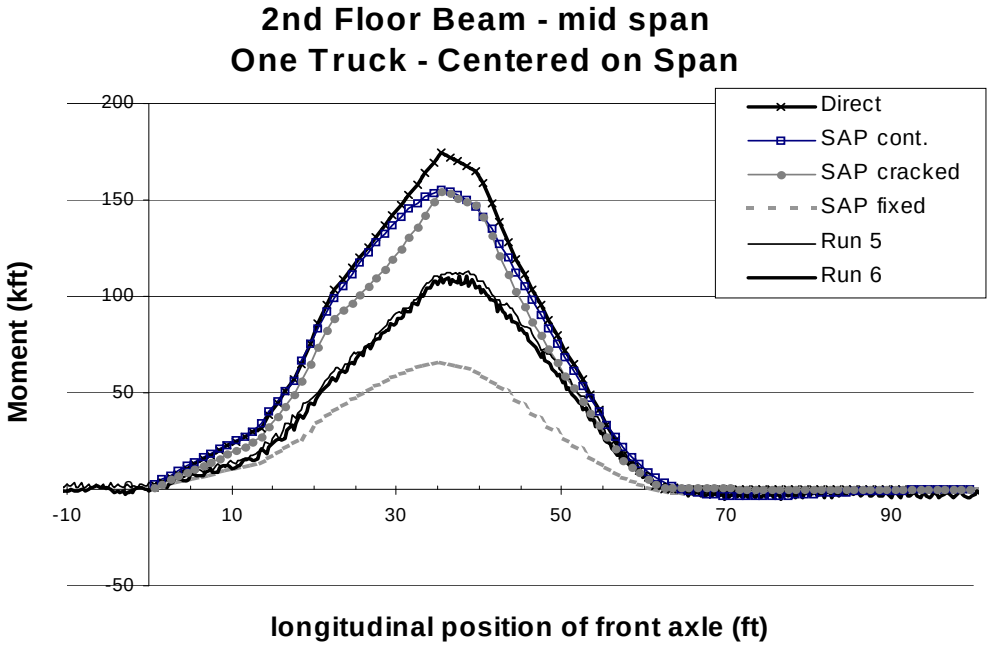
2nd Floor Beam - mid span
One Truck - Centered on Span
Moment (kft)
200
150
100
50
-50
-10
10
30
50
70
90
longitudinal position of front axle (ft)
Direct
SAP cont.
SAP cracked
SAP fixed
Run 5
Run 6

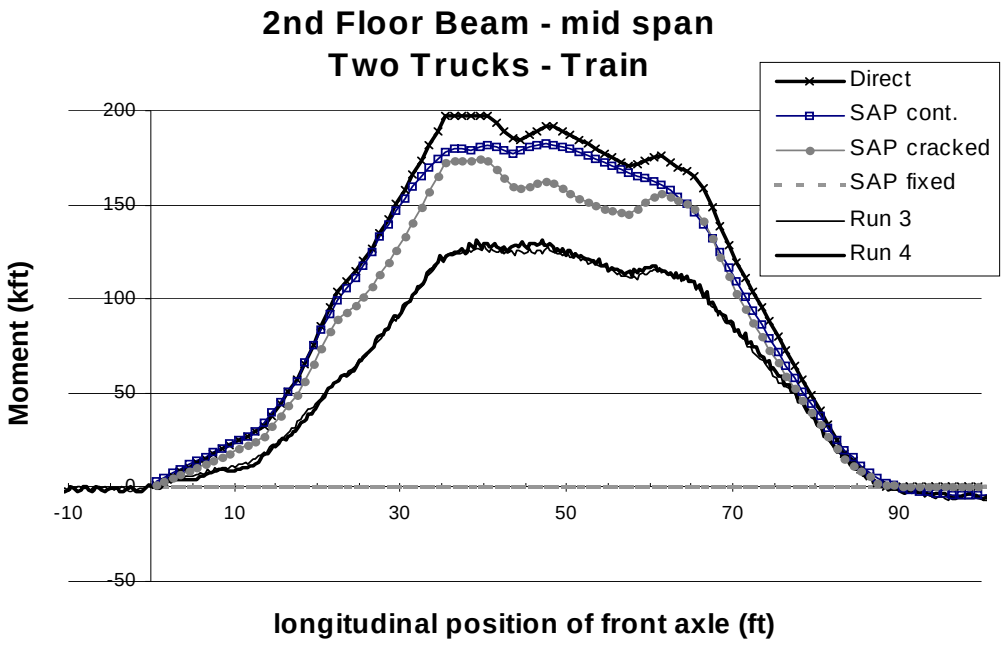
2nd Floor Beam - mid span
Two Trucks - Train
Direct
SAP cont.
SAP cracked
SAP fixed
Run 3
Run 4
Moment (kft)
200
150
100
50
0
-50
-10
10
30
50
70
90
longitudinal position of front axle (ft)

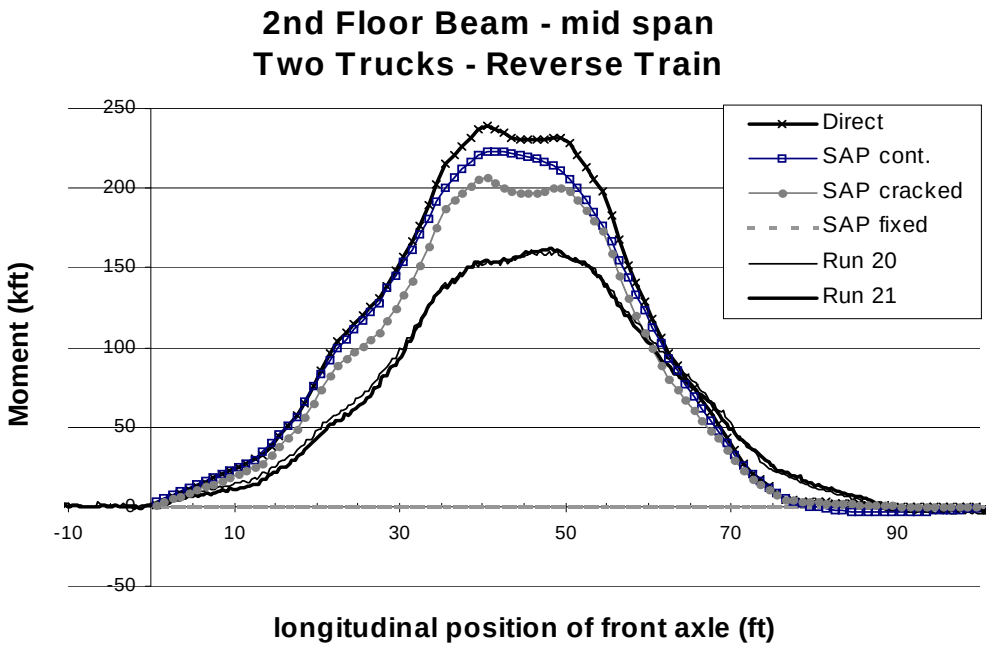
2nd Floor Beam - mid span
Two Trucks - Reverse Train
Direct
SAP cont.
SAP cracked
SAP fixed
Run 20
Run 21
Moment (kft)
250
200
150
100
50
0
-50
-10
10
30
50
70
90
longitudinal position of front axle (ft)

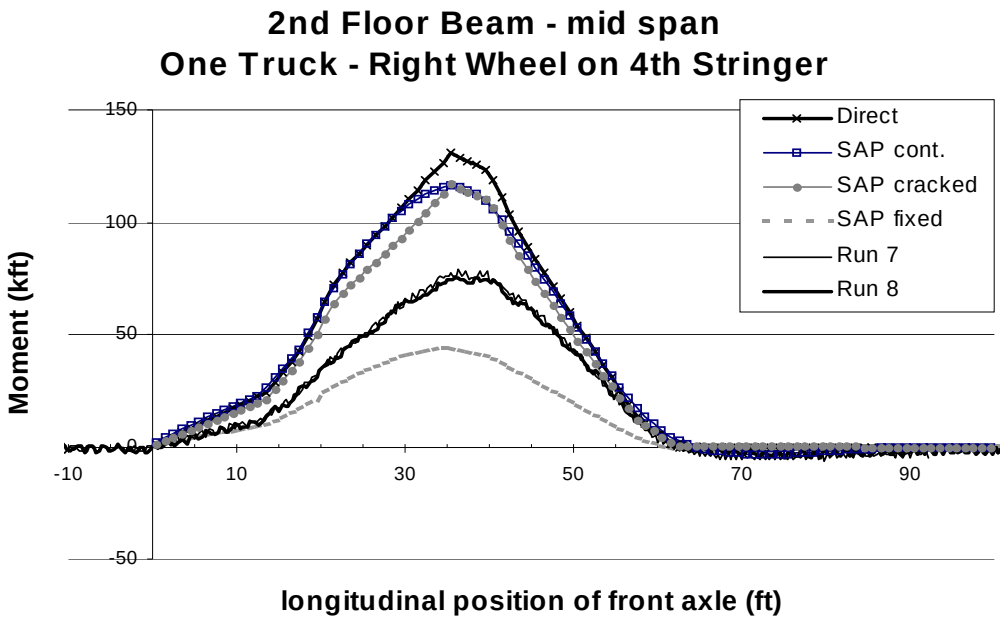
2nd Floor Beam - mid span
One Truck - Right Wheel on 4th Stringer
Moment (kft)
150
100
50
0
-50
-10
10
30
50
70
90
longitudinal position of front axle (ft)
Direct
SAP cont.
SAP cracked
SAP fixed
Run 7
Run 8

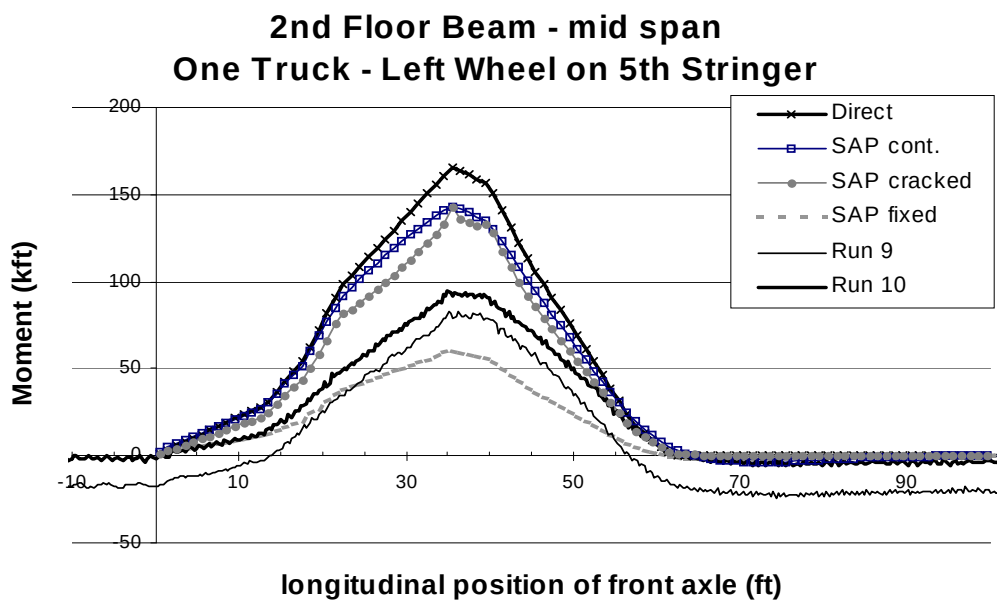
2nd Floor Beam - mid span
One Truck - Left Wheel on 5th Stringer
Moment (kft)
200
150
100
50
0
-50
-10
10
30
50
70
90
longitudinal position of front axle (ft)
Direct
SAP cont.
SAP cracked
SAP fixed
Run 9
Run 10

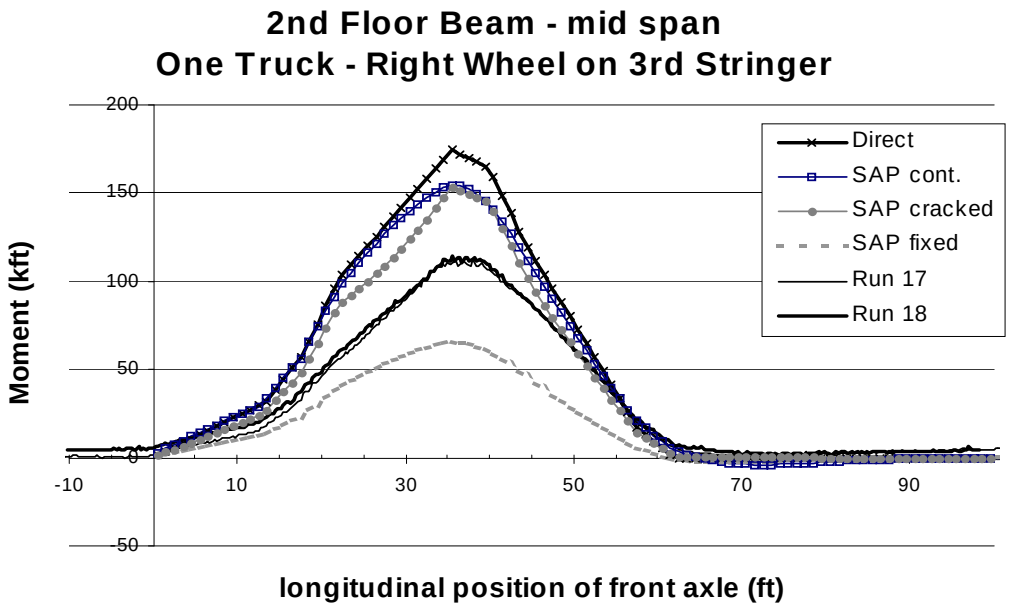
2nd Floor Beam - mid span
One Truck - Right Wheel on 3rd Stringer
Moment (kft)
200
150
100
50
0
-50
-10
10
30
50
70
90
Direct
SAP cont.
SAP cracked
SAP fixed
Run 17
Run 18
longitudinal position of front axle (ft)

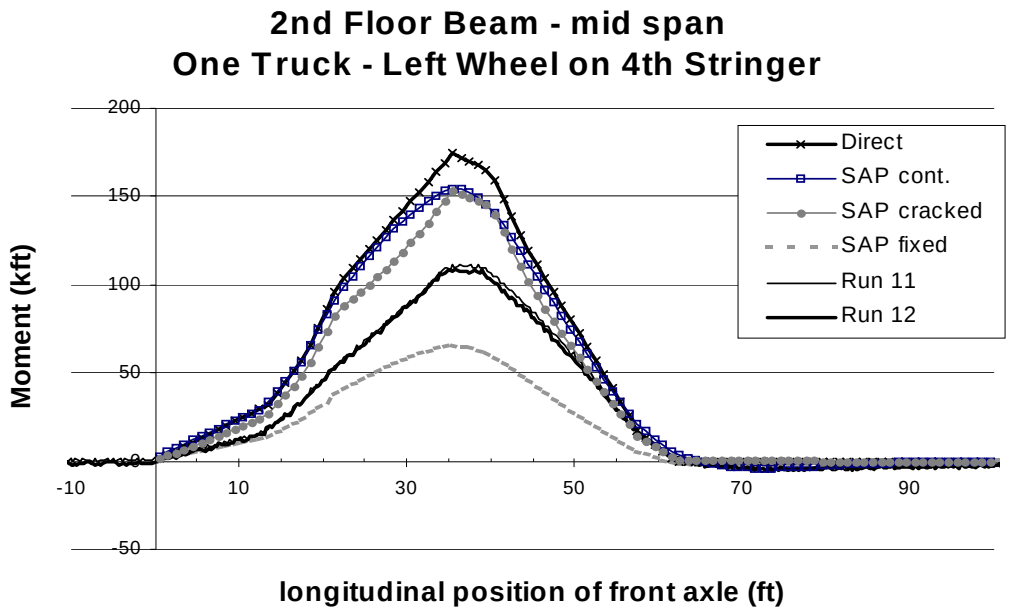
2nd Floor Beam - mid span
One Truck - Left Wheel on 4th Stringer
Moment (kft)
200
150
100
50
0
-50
-10
10
30
50
70
90
Direct
SAP cont.
SAP cracked
SAP fixed
Run 11
Run 12
longitudinal position of front axle (ft)

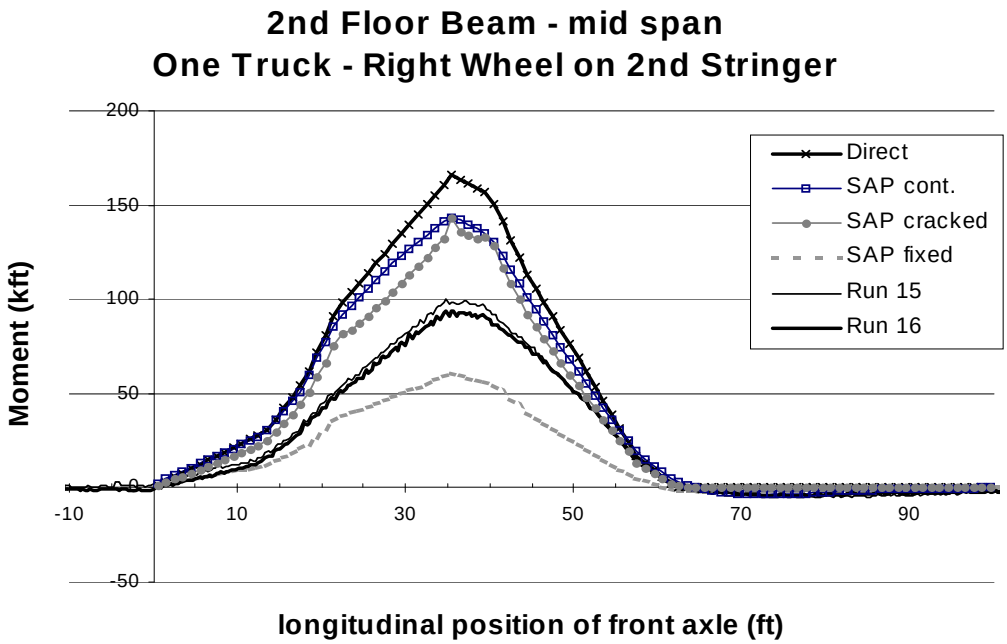
2nd Floor Beam - mid span
One Truck - Right Wheel on 2nd Stringer
Moment (kft)
200
150
100
50
0
-50
-10
10
30
50
70
90
Direct
SAP cont.
SAP cracked
SAP fixed
Run 15
Run 16
longitudinal position of front axle (ft)

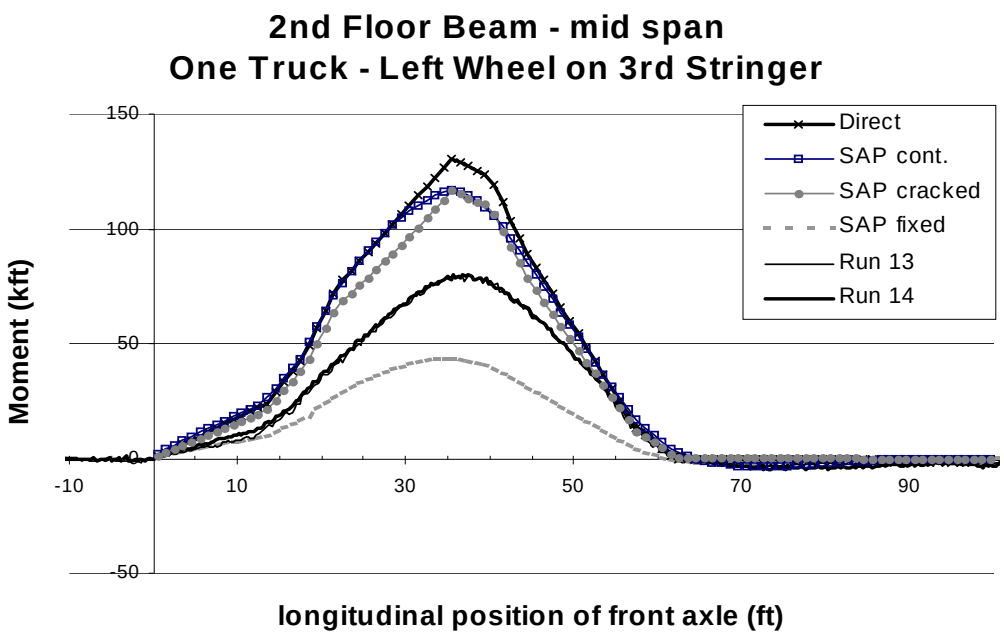
2nd Floor Beam - mid span
One Truck - Left Wheel on 3rd Stringer
Moment (kft)
150
100
50
0
-50
-10
10
30
50
70
90
Direct
SAP cont.
SAP cracked
SAP fixed
Run 13
Run 14
longitudinal position of front axle (ft)

# APPENDIX G

# COMPARISON OF MAXIMUM MOMENTS FROM 1ST LLANO TEST

# APPENDIX H

# MOMENT DIAGRAMS OF 2ND FLOOR BEAM IN 2ND LLANO BRIDGE TEST

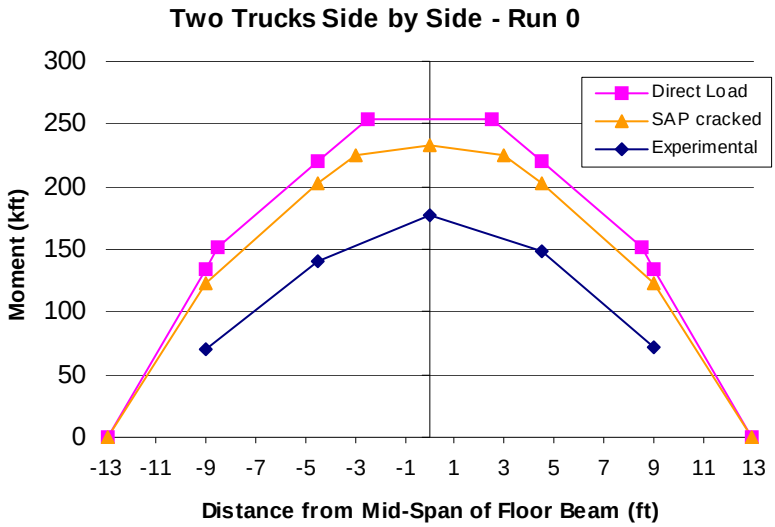


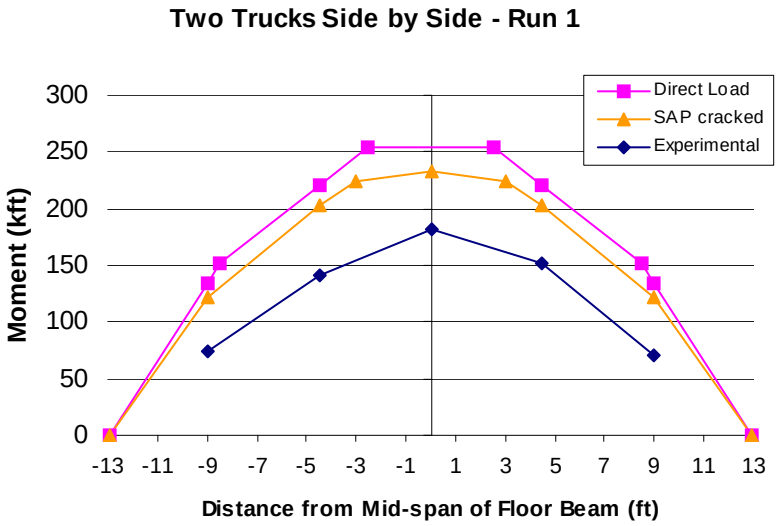

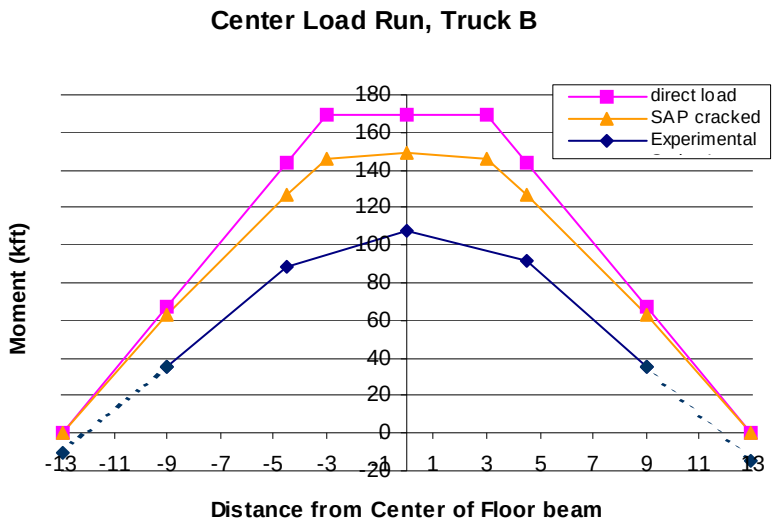
Center Load Run, Truck B
direct load
SAP cracked
Experimental
Moment (kft)
180
160
140
120
100
80
60
40
20
0
-20
-13
-11
-9
-7
-5
-3
-1
1
3
5
7
9
11
13
Distance from Center of Floor beam